Title
P. aeruginosa interactions with the ocular surface epithelia

Author
Sullivan, Aaron Barton

Publication Date
2015

Peer reviewed|Thesis/dissertation

P. aeruginosa interactions with the ocular surface epithelia

By

Aaron Barton Sullivan

A dissertation submitted in partial satisfaction of the
requirements for the degree of
Doctor of Philosophy
in
Vision Science
in the
Graduate Division
of the
University of California, Berkeley

Committee in charge:

Professor Suzanne M. J. Fleiszig

Professor Lu Chen

Professor Nancy McNamara

Professor Ellen Robey

Spring 2015

Abstract

Pseudomonas aeruginosa interactions with the ocular surface epithelia

by

Aaron Barton Sullivan

Doctor of Philosophy in Vision Science

University of California, Berkeley

Professor Suzanne M. J. Fleiszig, Chair

Microbial keratitis, a sight-destroying disease that affects wearers of contact lenses, is caused by microbes in the cornea. To succeed in causing disease, the microbe (e.g. bacteria, fungus or virus) must adhere to, penetrate, and traverse the corneal epithelium and enter the stroma. Once they are inside the stroma, the inflammatory response caused by infiltrating erythrocytes, proteins, and fluid results in opacity of the cornea. (Niederkorn, Kaplan et al. 2007) The most common strategy for researching microbial keratitis is to inject bacteria under the epithelium or to scratch the epithelium down to the stroma before application of the bacteria, because the epithelium has barrier functions that prevent both bacterial adhesion and penetration of the cornea. Therefore, the role of the corneal epithelium in this disease has been understudied. Further study of the epithelium is important to find out how bacteria attempt to exploit vulnerabilities in our protective barriers, and even more so to identify the critical barriers providing the protection we need to stay healthy and free from disease.

My research focuses on the initial stages of infection and how the bacteria cross the corneal epithelial barrier to begin the process. To that end, I have been studying two virulence systems of *Pseudomonas aeruginosa*, namely the Type II and Type III secretion systems, which are known to be involved in corneal infections (Hobden 2002, Coburn, Sekirov et al. 2007). The Type II secretion system (T2SS) is an extracellular system that secretes several proteases (including LasA, LasB and AprA) and other virulence factors outside the bacteria to interact with the surface of the host cell. The Type III secretion system (T3SS) is an injection system that uses a needle apparatus to inject virulence factors directly into the host cell. Previous research has shown that a knockout of the entire T3SS stops traversal completely, but which virulence factor is responsible has not yet been identified. Both systems have been shown to be important in bacterial virulence and are associated with severe disease. It is suspected that these systems help penetrate and traverse the corneal epithelium, which is the initial stage in microbial keratitis not caused by deep injury.

My first finding reported in this study is that LasB from the T2SS is the protease involved in bacterial traversal of the corneal epithelium. Knockout bacteria lacking the LasB protease are

unable to traverse the corneal epithelium to the basal lamina, whereas, in a rescue experiment in which LasB encoded on a plasmid is reintroduced to bacteria lacking LasA and LasB, the bacteria regain the ability to traverse. Though the T3SS is important, the role of individual secreted factors in this system remains unclear. I have used knockout bacteria for all of the secreted effectors (ExoS, ExoT, ExoU, and ExoY) but still observe epithelial disruption and bacterial traversal to the stroma. Further knockouts of the translocon (PopB, PopD) also failed to prevent this outcome. Only knockouts of the T3SS structural proteins pertaining to the needle (PscC and PscD) or to the entire secretion system (ExsA, the master regulator) were able to prevent this process. Therefore, we cannot establish whether any secreted factor is involved in this process, but it is possible that a fourth previously unknown effector is involved, or that the T3SS structural proteins are involved in virulence.

I addressed quantification of the relative position of 1µm bacteria within the corneal epithelium in order to quantify bacterial positions and epithelial damage. By means of 3D modeling of confocal microscopy images taken at increasing depths through an eye, the apical surface was reconstructed in Bitplane Imaris software. Then, using a distance transform algorithm in MatLab that I developed, both the distance of individual bacteria from the basement membrane and the epithelial thickness were measured. This allowed quantification and statistical analysis of damage to the layers of the cornea, which offers an advantage over qualitative analysis of images using pathology scoring in terms of both accuracy of object identification and flexibility of application. Pathology scores are subjective with very few criteria by which to score results; therefore, small changes are difficult to quantify in this subjective method of analysis. Using 3D reconstruction methods and advanced distance measurement algorithms, we are able to accurately describe any 3D situation in a variety of ways to suit the data. These methods can also be automated, eliminating the subjective variability provided by observational assessments and allowing both higher throughput of data analysis and replication by multiple users.

Several null infection models are discussed in this study. A null infection model is a model where the normal outcome is no disease; the initial stages of disease can be studied through interactions with these models. In addition to evaluating current null infection methods, I discovered a new approach by exposing the corneal surface to 5% FBS. (Fetal Bovine Serum, a common growth medium derived from fetal bovine blood serum) However, the null infection models differed with regard to which bacterial factors were needed for epithelial barrier disruption and bacterial traversal. These differences point to different susceptibilities caused by the models, which may relate to the barriers of infection. Thus, virulence factors used by *P. aeruginosa* to traverse the corneal epithelium depend upon how host defenses are compromised.

I also used models to investigate whether or not a stable microbiome exists on the ocular surface and therefore possibly contributes to protecting the eye, as has been found with microbiomes in other areas of the body. Microbiome analysis uses DNA evidence to identify microbes in a very sensitive assay not dependent on culture techniques that may be unable to grow bacteria with special needs. Our initial analysis of interactions between bacteria found in microbiome analysis and the ocular surface indicate that it is very difficult for bacteria to survive on the ocular surface or within the conjunctival mucosal membrane of the eye, and that this is true for both gram-positive and gram-negative ocular pathogens. Staining experiments, designed to enable a live look at bacteria in the eye, were promising in their ability to stain bacteria but, unfortunately, stained epithelial tissue as well. Human subjects whose ocular washes were collected to grow in

multiple nonstandard conditions were equally unable to produce results, indicating that the bacteria implicated in microbiome DNA analysis, some culturable even under standard conditions, may not be actually present– at least not in a live form. There still might be a stable microbiome on the ocular surface that I was unable to find, but current results suggest that this possibility is remote. Further investigation with a murine model is currently underway to determine whether the use of DNA evidence to identify living colonies of microbes can be achieved.

Taken together, the research presented in this dissertation advances our understanding of how the ocular surface remains healthy despite exposure to the barrage of potentially pathogenic microbes that exist in our environment. The data continue to support the notion that the healthy ocular surface harbors only transient microbes due to its capacity to rapidly clear even large inocula. They also show that when corneal surface defenses are compromised severely enough to allow bacteria to traverse the epithelial barrier, multiple virulence bacteria factors can contribute, with the details depending on the nature of the corneal compromise and the state of the bacteria. While implicating specific host and bacterial factors, these findings also highlight the importance of mimicking conditions allowing health or susceptibility in animal models, and the need to monitor variability among bacterial isolates from different sources, even for the same strain.

List of Abbreviations

ARVO	Association for Research in Vision and Ophthalmology
BRISK	Biome representational in silico karyotyping
CFU	Colony Forming Units (# of live bacteria found able to reproduce and form colonies)
CL	Contact Lens
DIC	Differential interference contrast
DMEM	Dulbecco's minimum Eagle's media
EDTA	Ethylenediaminetetraacetic acid
EGTA	ethylene glycol tetraacetic acid. A Calcium chelator (binds calcium to prevent its
FBS	Fetal Bovine Serum (a common cell culture additive which promotes growth)
GA	Gluteraldehyde
HBD2	Human beta defensin 2
IL-1R	Interlukin-1 Receptor
KDAMPs	Keratin derived anti-microbial peptides
KO	Knock Out. A mutant lacking a specific gene, either in its entirety or in functionality.
LB	Luteinizing Broth
LPS	Lipopolysaccharide
LSF	Line spread function
MBD3	Mouse beta defensing 3
MK	Microbial Keratitis. An infection of the cornea by microbes which can cause blindness.
MT	Mutant. An altered genetic arrangement of an organism artificially engineered.
MyD88	Myeloid Differentiation factor 88
p.i	Post inoculation
PCR	Polymerase Chain Reaction
PFA	Paraformaldehyde
PSF	Point spread function
RT-PCR	Real Time PCR
SP-D	Surfactant Protein D
T2SS	Type II Secretion System
T3SS	Type III Secretion System
TLR	Toll-Like Receptor
TSA	Tryptic soy agar
WT	Wild Type. The native genetic arrangement of an organism. Unaltered metabolism

List of Figures and Tables

Acknowledgments

First and foremost, I would like to thank my family for supporting me through the PhD process. My wife Sara has helped me in many ways, including some editing advice and giving me the time and space to get my work done. My son Gavin has helped to pick up my mood and give me energy, and my brother Michael and parents Ann, Drew and V have never let me quit.

I would also like to thank Kaylin Kim for her invaluable assistance during the many hours of ex-vivo traversal assays. Several of the figures in this paper pertaining to T3SS expression of protease knockouts were created with her assistance. Although I analyzed the data personally, Kaylin performed the RT-PCR under my supervision. I also wish to thank Stephanie Wan, Annikah McNally, and Ryan Martinez for their help with the microbiome portion of this paper. All data collection for the microbiome project was done with their help under my supervision.

I have learned so much from the Berkeley faculty and postdocs who have taught me over the years. In chronological order: Christine Wildsoet, Vivian Choh, Karsten Gronert, Alexander Leedom, Elvira Liclican, Xiaohua Gong, Connie Tam, Victoria Hritonenko, Amber Jolly, Matteo Metruccio, Abby Kroken, and Jianfang Li. And of course, special thanks to my dissertation committee: Suzanne Fleiszig, Lu Chen, Nancy McNamara and Ellen Robey.

Thank you, everyone!

Aaron Barton Sullivan PhD, MS

Contents

Chapter 1:

Introduction and Background

Chapter 1: Introduction and Background

Pseudomonas is a ubiquitous environmental opportunistic pathogen that broadly causes disease in compromised hosts, including bacteremia in severe burn victims, chronic lung infection in cystic fibrosis patients, and acute microbial keratitis (MK) in users of extended-wear soft contact lenses. MK is a sight-threatening disease, responsible for nearly one million medical office and emergency room visits every year in the United States (Collier, Gronostaj et al. 2014). Keratitis is defined by inflammation of the cornea (the transparent dome of the eye covering the iris and pupil) (Figure 1.1 A). MK is keratitis caused by microbes (i.e., bacteria, fungi, and viruses). Contact lens wearers are at least 12 times more likely to develop MK than non–contact lens wearers, and extended wear users are at least 10 times more likely to develop MK than daily wear (Musch, Sugar et al. 1983, Dart, Stapleton et al. 1991). The CDC's estimate of office and emergency room visits does not include visits to the optometrist, so it may be underrepresenting the prevalence of MK. In 2010, this disease cost the United States an estimated $175 million in direct health care expenditures, including $58 million for Medicare patients and $12 million for Medicaid patients. (Collier, Gronostaj et al. 2014). Since the invention of soft contact lenses in 1959 (Wichterle, Lim et al. 1961), the MK disease rate has remained steady despite the invention of silicone hydrogels in 1998 (Ciba Vision), which alleviated the oxygen starvation of the cornea that was thought to be causing many of the problems.

Figure 1.1: The cornea and Microbial Keratitis

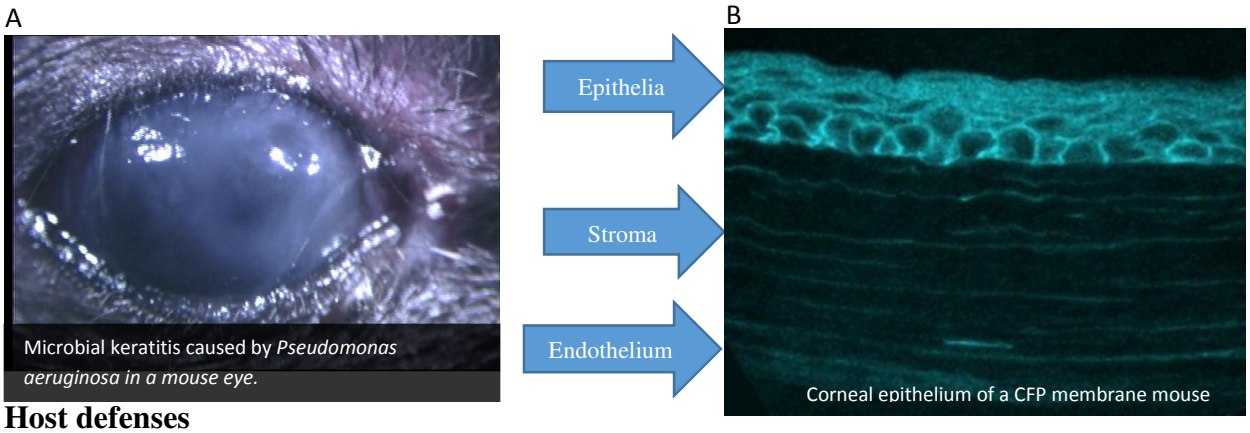

Host defenses

The ocular surface is a very inhospitable environment for microbes. The cornea is a dense protective barrier made up of three levels of tissue: the epithelium, the stroma, and the endothelium (Figure 1.1 B). The epithelium is five layers thick and constantly replenishes itself; every seven days, a completely new epithelium covers the eye. The stroma is a mostly acellular region of overlapping collagen fibers packed at 90-degree angles to one another to allow for maximum transparency. In the Bowman's layer, the upper layer of the stroma, collagen fibers form a meshwork with less than a 0.4-micron gap between fibers. The endothelium is a single layer of cells responsible for providing most of the nutrients to the cornea, as well as being the cells that regulate fluid exchange of the tissue above, maintaining a perfect balance to prevent edema.

Tears cover the surface of the eye and have a multitude of antimicrobial effects. Several glands secrete separate components, some aqueous in nature (e.g., the lacrimal glands) and others lipid

in nature (e.g., the meibomian glands). Immune cells such as neutrophils are a vital component of the tear film. They migrate into the tear film when eyes are closed and are found dried up in the corners of our eyes; we commonly refer to them as "sand" or "sleep." Combined with mucin secretions from the ocular surface and other defensive compounds like defensins, lysozyme, lactoferrin, and immunoglobulins, the tear film presents a formidable barrier to microbial invaders. Defensins are a group of antimicrobial peptides made up of three subfamilies (α, β, and θ) that are secreted as part of the innate immune response. They are non-specific in action and recognize a host of microbes including bacteria, mycobacteria, fungi, and enveloped viruses (Ganz and Lehrer 1995, Schneider, Unholzer et al. 2005). Lactoferrin, as its name suggests, was first discovered as the major iron-binding glycoprotein in milk (Sorensen 1939). It has since been found in blood plasma after neutrophil degranulation and in tears (Broekhuyse 1974, Iyer and Lonnerdal 1993). It has many activities, some of which are not iron-dependent, including iron metabolism, cell proliferation, and antibiotic, antiviral, or antiphrastic activity. Recently, Keratin-derived antimicrobial peptides (KDAMPs) within the tears were discovered to have notable antimicrobial properties (Tam, Mun et al. 2012). Much is still unknown as to the number of layers on the ocular surface and the degree of mixing that occurs between them. Currently it is believed to be made up of three layers: a lipid layer on the surface, an aqueous layer representing the majority of the tear volume, and a mucin layer on the surface of the cornea (Figure 1.2).

Figure 1.2: The tear film

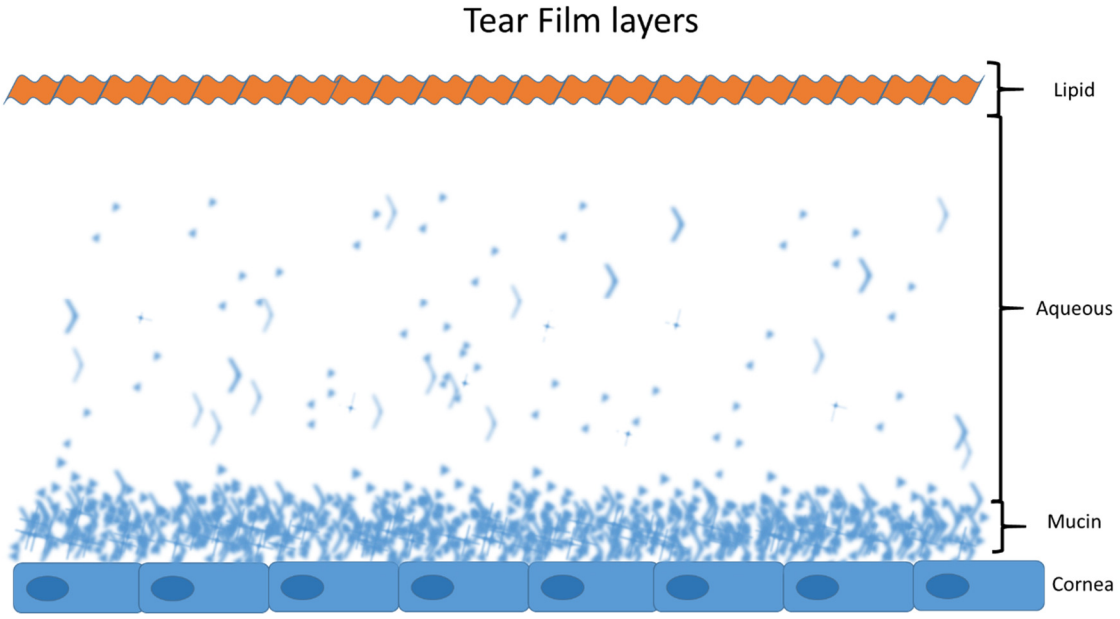

The lipid layer is believed to protect the aqueous layer from evaporation, and deficiencies in that layer are attributed to dry eye (Foulks 2007, Liu, Begley et al. 2009). The aqueous layer contains salts as well as a variety of soluble proteins and mucins. The mucin layer is a mucosal layer on the corneal surface secreted by the cornea and goblet cells of the conjunctiva. It helps to keep the other layers adherent to the corneal surface. The mucins are bound to the corneal surface and its glycocalyx (a coating on the external surface cells, consisting of several carbohydrate moieties of membrane glycolipids and glycoproteins that forms a matrix to support extracellular proteins and sugars necessary for functioning).

Figure 1.3: Schematic of the ocular surface

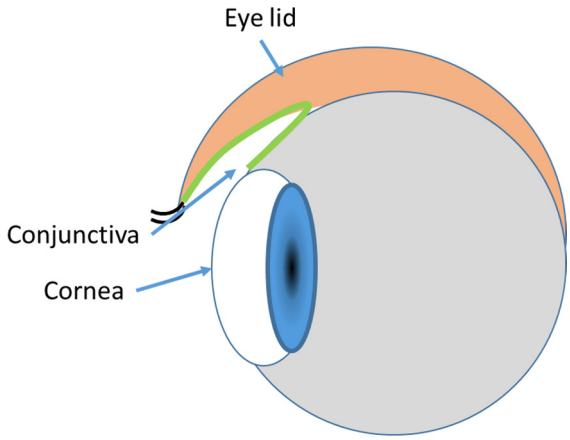

Mechanical factors help to protect the eye from microbes. Blinking generates a tremendous amount of shear stress on the surface of the cornea, wiping away anything not strongly adhered to the corneal surface. Secreted mucins bind to foreign particles, wrapping them up for disposal either by the nasal drainage ducts or mechanically by our hands when deposited in the canthus. Lastly the surface of the cornea produces a glycocalyx, which can repulse and prevent the adhesion of many microbial invaders, enabling the above-stated mechanical properties to wash away anything found in the eye. Indeed, when bacteria are put into the eye at 10^11 CFU/mL concentration, they are all removed from the surface of the eye within 12 hours (Mun, Tam et al. 2009).

The eye has an impressive array of defensive parameters in place to prevent infection, but one common defensive measure, inflammation, is absent in the cornea. The cornea is one of a small number of regions of the body that are considered "immune-privileged." This means that the normal inflammatory response, including the recruitment of T-Cells, macrophages, and neutrophils or other events that accompany inflammation do not normally occur. Even though neutrophils are a regular part of tear secretions and are present in the conjunctiva, they are not present in the cornea during normal function. Inflammation can cause significant damage to surrounding tissue, which negatively impacts corneal clarity. Yet unlike other immune-privileged sites (e.g., the brain, testis, and spinal cord) the surface of the eye is exposed to the environment and constantly awash with potential threats and infectious agents.

Other immunological differences can also cause susceptibility to infection. Surfactant protein D (SP-D) gene knockout mice also showed partial *P. aeruginosa* traversal without blotting or EGTA treatment, suggesting that SP-D also contributes toward corneal epithelial defense. (EGTA is ethylene glycol tetraacetic acid, a calcium chelator that binds calcium to prevent its metabolism.) Subsequently, my research showed that corneal epithelial defense against *P. aeruginosa* adhesion and traversal also requires myeloid differentiation factor 88 (MyD88), an essential adaptor protein for Toll-Like Receptor (TLR) and Interleukin-1 Receptor (IL-1R) mediated innate defense responses (Maresso, Baldwin et al. 2004, Sun, Maresso et al. 2004). Indeed, loss of the anti-bacterial peptide mBD3, the murine equivalent of hBD2, reduces ocular clearance of *P. aeruginosa* from the healthy cornea in vivo (Vance, Rietsch et al. 2005)representing at least one TLR- or IL-1R-dependent factor (Masters, Pederson et al. 1999, Olson, Fraylick et al. 1999) involved in defense of the healthy cornea against *P. aeruginosa*. MyD88 has also been linked to host defense from *Pseudomonas* traversal of the corneal epithelium (Sullivan, Tam et al. 2015). MyD88 KO mice were much more susceptible to traversal than their wild type (WT) counterparts. Even bacteria with the T3SS components were knocked out or expressed at a level so low that they were normally unable to traverse. This would indicate that active detection of the bacteria is needed to maintain the barrier to infection that the eye enjoys. MyD88 has also been linked to tight junctions (Clarke, Francella et al.

2011), which are important in maintaining the barrier needed to prevent infections and have been shown to tighten further with stimulation of the MyD88-dependent pathway through TLR-4 signaling.

The effect of contact lenses on the corneal surface

Extended wear is a significant risk factor increasing the risk of MK by 100 times. However, most of what we know about these bacteria has been learned through injury models of disease (Hazlett, Rosen et al. 1977, Valyi-Nagy, Deshmane et al. 1991, Lee, Evans et al. 2003, Alarcon, Kwan et al. 2009). Very little is known about the onset of disease, due to the barrier function of the corneal epithelium. The specifics of why contact lens wearers are more susceptible to infections is not well understood; however, it is clear that they are at greater risk of infection the longer they wear lenses.

Several factors need to be considered about contact lens wear. First, the contact lens is essentially an implantable device. When we blink, the contact lens is suspended within a body cavity and is no longer exposed to the outside world. The tear film is made up of several layers of lipids, aqueous secretions, and mucins. When we put a contact lens in the eye, the tear film is divided in two (Polse 1979, Nichols and King-Smith 2004). This likely separates the lipid and aqueous phases of the tear film. Tear exchange has been reported to be minimal under soft contact lenses as opposed to hard lenses(Kok, Boets et al. 1992). This finding correlates well with the increased rate of disease when comparing rigid gas permeable lenses to soft contact lenses (Dart, Stapleton et al. 1991) and may be a factor in the increased susceptibility to MK. Underneath the contact lens, where there is minimal tear exchange, bacterial biofilms (colonies of bacteria living in a protective environment made up of secretions and dead bacteria) form, and these biofilms (Sack, Jones et al. 1987), when transferred into an eye, can cause MK (Tam, Mun et al. 2010). Also, bacteria growing on the underside of the contact lens have a very close association to the surface of the eye (within less than 7 microns).

Not only do contact lenses divide the protective tear film in half and give bacteria intimate proximity to the surface of the eye, but the mere presence of a contact lens on the corneal epithelium has been shown to decrease the corneal tissue's contributions to defensive secretions. Human Beta Defensin 2 (HBD2) and the mouse analogue MBD3 have been shown to be suppressed in vitro (Maltseva, Fleiszig et al. 2007). On the whole, the contact lens has a dramatic effect on the surface of the eye and its defensive capabilities.

There are several different types of contact lens solutions, some with calcium chelators, others with peroxides, and even some with both. Every manufacturer strives to keep the contact lenses that patients are putting in their eye as clean as possible, but side effects of these harsh treatments are just beginning to be investigated. The contact lens (CL) can act like a sponge, allowing the release of any chemical or solution in which it is stored in for up to an hour (Jain 1988); this feature has recently been exploited to use CLs as drug delivery devices to the ocular surface (Gulsen and Chauhan 2004, Xinming, Yingde et al. 2008, Peng, Burke et al. 2012, Hsu, Fentzke et al. 2013). However, whatever is absorbed into the contact lens eventually leaches out onto the corneal surface, releasing all kinds of chemicals. CL solutions often contain; hydrogen peroxide, EDTA, hydroxypropyl methylcellulose, phosphate buffered saline, sodium borate, polyquarternium-1, boric acid, and many other chemicals. (Jones, Jones et al. 1997, Eiden 2011)

Pseudomonas aeruginosa

Pseudomonas aeruginosa is a rod-shaped, gram-negative bacterium that lives in soil and water and on our skin. Gram-negative bacteria are classified as such because they do not take up crystal violet in a gram stain. This is because they have a thinner peptidoglycan membrane than gram-positive bacteria and a lipopolysaccharide (LPS) outer membrane that prevents small molecules like crystal violet from entering and remaining in the bacteria. The LPS outer membrane provides structure as well as defense against a variety of chemicals, but it is also easily recognized by the immune system, causing a rapid immunological response. *Pseudomonas* is a flagellate bacteria, meaning that it has flagella, or whip-like appendages that spin and whip about, enabling rapid transportation. They also contain pili, or small, rod-shaped protrusions that allow for a twitching-like motility. Both forms of movement are linked to virulence, pili have also been linked to DNA uptake by bacteria used to incorporate and share DNA in the environment, which allows for sharing of adaptive and pathogenic features.

Another feature of gram-negative bacteria is a variety of secretion systems, which allow bacteria to secrete effector proteins, including toxins, proteases, and other useful enzymes into their environment. The type II secretion (T2SS) is a simple secretion system which secretes enzymes and proteins into the environment. The T2SS is made up of three parts, two translocons (TAT and SEC) in the inner membrane and one exportation pore (XCP) spanning all three bacterial cell membranes. The TAT and SEC translocons transport folded and unfolded proteins respectively into the periplasm. Once in the periplasm all proteins that are unfolded are folded ant then secreted by the XCP transmembrane pore outside the bacteria. (Figure 1.4 A)
The type III secretion system is one of seven known secretion systems employed by bacteria to secrete functional proteins outside the bacterial cell walls. It consists of an export apparatus, a basal body, a needle-like apparatus, and a translocon. The export apparatus consists of six structural proteins and four chaperones that help to package and transmit the necessary proteins through the needle. PscD makes up the basal section of the export apparatus, providing transport through the inner membrane; PscC spans the outer membrane. Removal of either of these export apparatus proteins prevents the needle from forming and thus precludes secretion of the T3SS effectors. The entire needle and the translocon (made up of two proteins, PopB and PopD) are formed within the bacteria and transported through the basal body and later the needle to construct the T3SS. The needle-like apparatus extends from the bacterial membrane into the host cell membrane, through which several effector proteins are secreted. The effector proteins in *Pseudomonas* are ExoS, ExoT, ExoU, and ExoY. Effector proteins ExoS and ExoT have a GAP domains and an ADP-ribosylating enzyme (Frank 1997, Frithz-Lindsten, Du et al. 1997) Exoenzyme U is an acute cytotoxic factor (also called PepA) (Finck-Barbancon, Goranson et al. 1997, Hauser, Kang et al. 1998), and ExoY is an adenylate cyclase. Each of these effector proteins eventually leads to cell death in mammalian cells. ExoS plays a role in modulating bacterial phagocytosis by phagocytes and in invasion into non phagocytic cells, and it induces apoptosis of epithelial cells, fibroblasts, and lymphocytes (Fleiszig, Wiener-Kronish et al. 1997, Frithz-Lindsten, Du et al. 1997). ExoS is also involved in intracellular survival within mammalian cells (Finlay and Cossart 1997). ExoU mediates rapid lysis (cytotoxicity) of a variety of mammalian cell types in vitro, including macrophages, epithelial cells, and fibroblasts (Fleiszig, Wiener-Kronish et al. 1997, Yahr, Mende-Mueller et al. 1997, Coburn and Frank 1999). (Figure 1.4 B)

Figure 1.4: The Type II and III secretions systems of *Pseudomonas*

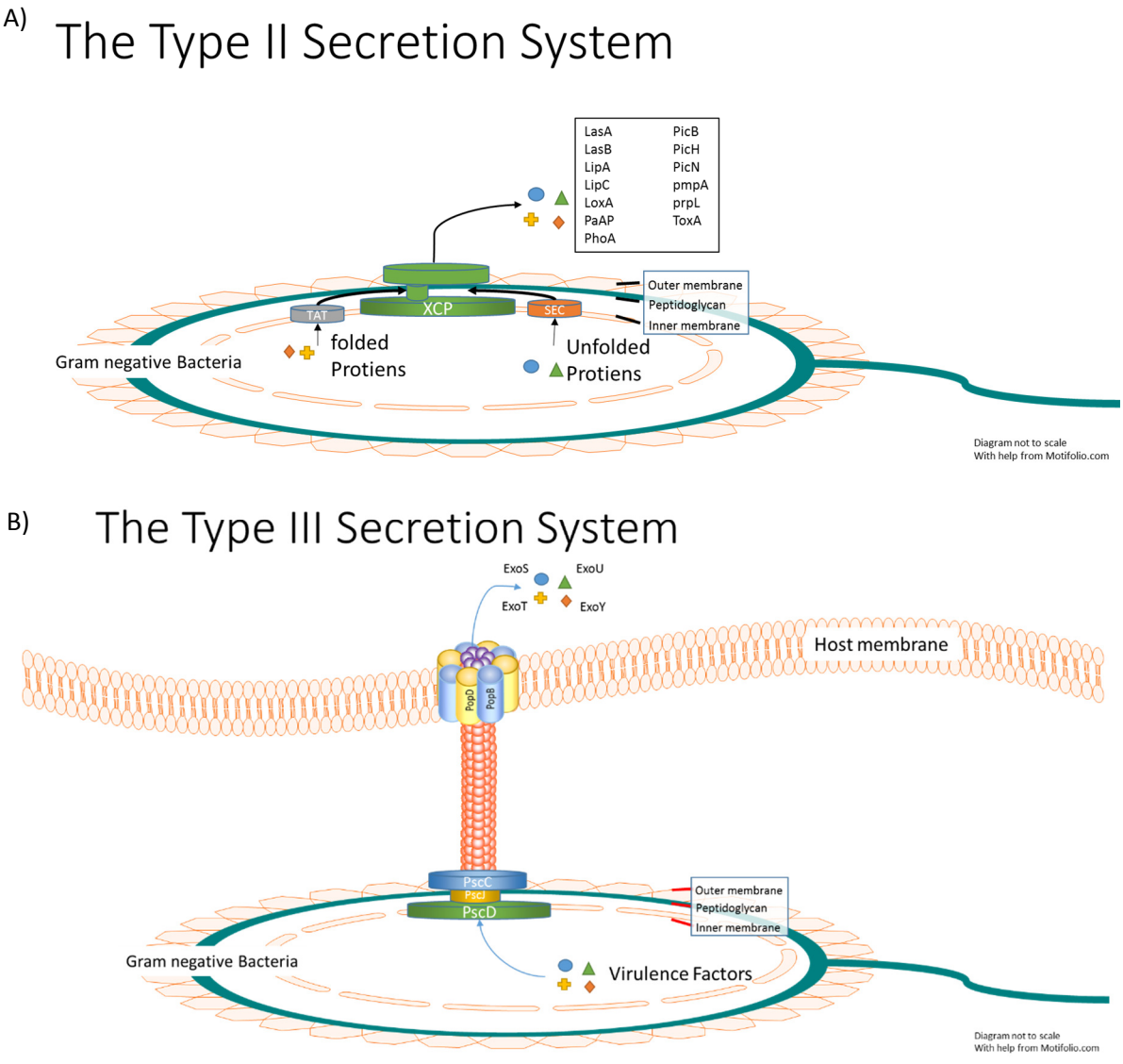

Gram-negative bacteria are often opportunistic pathogens, in that they do not normally cause disease unless assisted by some sort of Immunodeficiency of their host or other special circumstances. Contact lens wear is one such special condition in which *P. aeruginosa* causes infections.

Ocular Surface Microbiome

The questions of what components are in the eye and how they affect health are not new. We have long known that bacteria can be found in the eye (Ramachandran, Sharma et al. 1995) and that they can cause eye disease (Stapleton, Willcox et al. 1997, Willcox, Power et al. 1997). These bacteria have been always highly associated with disease, especially CL-related complications. Techniques for culturing these bacteria are a routine part of clinical practice, so it

is no surprise that the explosion in microbiome research has encompassed eye research. However, for many years discovering no bacteria in an ocular culture was considered the norm (McNatt, Allen et al. 1978, Jackson, Eykyn et al. 2003, Lab 2015). This would seem to indicate that presence of bacteria in the eye would be an abnormal or at least a transient event. New techniques that can discover non-culturable bacteria via 16s ribosomal DNA are at the forefront of microbiome analysis (Schabereiter-Gurtner, Maca et al. 2001, Muthappan, Lee et al. 2011). Application to the eye has been suggested (Willcox 2013), but with the caution that additional studies including longitudinal research are needed to establish the validity and impact of current findings.

The reason for caution about cutting-edge microbiome analysis is that DNA evidence is not by itself proof of the presence of living microbes. Indeed, DNA has a half-life of approximately 521 years (Which would average 1.5 million years of integrity) at least within geographically conserved fossils (Allentoft, Collins et al. 2012). However, progress in microbiome research has been substantial, and some studies that have unearthed varying numbers of hits in these screens (Aoki, Fukuda et al. 2013, Dong, Yang et al. 2013, Moreno, Moreno et al. 2014, Zegans and Van Gelder 2014, Zhou, Holland et al. 2014). Even popular scientific periodicals like *The Scientist* (Shaikh-Lesko 2014) have published articles on the subject of the ocular microbiome. Professor Suzanne Fleiszig of the University of California at Berkeley offered this advice when interviewed on the ocular microbiome: "The history of the microbiome field is that the methods were originally developed by environmental microbiologists looking for microbes that do not grow in the lab where conditions are generally optimized for clinical samples. So they found a plethora of previously unrecognized microbes in hot springs, high salt, extreme temperatures etc. and this completely redefined our understanding of the world around us. The problem is that people then started using them on clinical samples without considering the limitations of the methods" (OVS 2014).

Biome representational in silico karyotyping (BRISK) has become the norm for microbiome analysis. This is a general technique for analyzing all DNA present in a sample. It uses the Type IIB DNA restriction enzyme to create a defined representation of 27-mer DNA in a sample. Then parallel sequencing is utilized to construct high-resolution karyotypes and achieve identification of multiple species within the sample. This technique is very sensitive as it uses PCR to amplify the DNA present in the sample, thus allowing for analysis of even trace evidence of bacteria. To identify individual species of bacteria, it uses 16s ribosomal DNA, which is one of the most conserved DNA sequences in all species because it encodes the machinery for translating DNA and RNA into proteins. Because this is such a critical process for every living thing, alterations are slow to occur and can thus be used to fingerprint species. However, this DNA is ubiquitous, as every cell needs a large number of ribosomes to translate DNA and RNA constantly. This fact, combined with the extremely long half-life of DNA, means that it may remain around for a long time after the organism has perished. Dead microbes or free DNA may be detected by BRISK or other microbiome analyses as readily as live microbes in stable populations.

Despite the drawbacks of this technique in a clinical setting, it has led to many discoveries related to microbiomes all over the body. In particular, BRISK analysis has been instrumental in understanding the gut microbiome, which has a significant, systemic effect on the immune system as well as on metabolism. Several paradigms have been established as to how this

microbiome survives within a human host. The first thing to consider is compartmentalization. In the gut, bacteria are isolated to certain regions of the gut lumen and there is a defined barrier between the gut mucosa and the bacterial microbiome (Vaishnava, Yamamoto et al. 2011). That zone is 50µm and is sustained by both the gut surface and the bacteria that live above it. If we were to consider the ocular surface to be equal to the most understood microbiome, then we would expect similar conditions. However, the ocular surface has only 10-14ul of tear film on the surface (Creech, Do et al. 1998). When the eye is closed, this distance is halved as there are surfaces on either side of the tear film, and in addition the tear film is compressed further. If this were the only consideration then there would be only 10% to 15% of the space needed for this clear zone in the eye. This alone could make it difficult for a microbiome to coexist, but other factors are also involved. The tear fluid is both highly antimicrobial and bacterial static, containing several components that protect against microbes including lactoferrin, KDAMPs and immunoglobulins (McClellan, Whitney et al. 1973, Broekhuyse 1974, Holly 1980, Tam, Mun et al. 2012). The epithelial surface is also capable of repulsing and destroying foreign invaders. The surface itself has a glycocalyx, which makes it difficult for bacteria and other microbes to bind to the surface (Gipson, Yankauckas et al. 1992). Several defensive compounds are secreted by the epithelium and conjunctiva, including mucins and defensins (McNamara, Van et al. 1999, Gipson 2004).

When we consider the adaptability of the bacteria causing these eye diseases along with the many side effects of CL use, it seems obvious that risks will be associated with wearing CLs. The only way to prevent these risks is to further understand the initial events that bacteria utilize to gain access to the corneal epithelium and penetrate that barrier. Models of susceptibility are needed because of the eye's innate ability to resist infection. These models each tell us much about both the eye's defenses on which it relies to keep out microbes and the arsenal that the bacteria exploit to bypass them. The present dissertation focuses on the bacterial factors needed in these models to successfully breach the initial barriers to infection. Investigation of these factors leads to a question of the relevance of ocular microbiome publications from other researchers. Knowing the natural homeostasis of the ocular surface, which includes if microbial flora are present, will help us to better understand eye disease.

Chapter 2:

Methodology

Chapter 2: Methodology

Bacteria. Several strains of the *P. aeruginosa* strain were used, as detailed in tables I, III, and IV. PAO1 is an invasive strain that encodes three known type three secreted effectors, ExoS, ExoT, and ExoY, and is capable of traversing murine corneal epithelia in vivo and ex vivo (Alarcon, Tam et al. 2011, Tam, LeDue et al. 2011) and human corneal epithelia in vitro (Augustin, Heimer et al. 2011). Two sets of PAO1 bacteria were used for the protease experiments, which lacked LasA, LasB or AprA proteases. LasB was rescued on the double mutant of LasA and LasB with the pCOM plasmid, whereas on the other set of PAO1 with the LasB mutant, LasB was rescued with [pKSM3 or pLAFR2] (Brint and Ohman 1995, Hobden 2002). PAK, another strain used in this study, is an invasive strain that encodes the ExoS effector. The last strain used in this study, PA14, is a cytotoxic strain that encodes ExoU instead of ExoS. Mutations in ExoU, ExoT, ExoY, and PscD were used in the PA14 strain of bacteria. (Vance, Rietsch et al. 2005). For imaging, all bacteria and mutants were complemented (by electroporation) with plasmid pSMC2 encoding green fluorescent protein (GFP)(Bloemberg, O'Toole et al. 1997), and thus were grown on trypticase soy agar (TSA) supplemented with 300 µg/ml of carbenicillin overnight (~18 h) at 37° C. For use in experiments, bacteria were resuspended in serum-free tissue culture medium (DMEM, Gibco) without antibiotics to a concentration of approximately 10^11cfu/mL, confirmed by viable count. Plasmid-complemented strains grow equally well in vitro.

Ex-vivo murine models of *P. aeruginosa* epithelial traversal. All procedures were performed in accordance with the ARVO Statement for the Use of Animals in Ophthalmic and Vision Research, and they were approved by the Animal Care and Use Committee of the University of California, Berkeley. Wild type (WT) C57BL/6 mice (6 to 8 weeks old) or *myd88* (-/-) gene knockout mice of the same strain and age were used for all experiments. After sacrifice, the eyes were enucleated and rinsed three times with PBS and then placed in a 96-well tissue culture plate (Corning). Eyes were incubated at 37° C (5 % CO_2) or for microscopy in a chamber slide with a water jacketed heater set to 37° C. For each model described below, each experimental group contained 4 to 8 eyes and experiments were conducted on at least two separate days.
In model 1 (tissue paper blotting/EGTA), eyes of WT mice were blotted with a Kimwipe™ (Kimtech) before incubation in EGTA (100 mM in PBS) for 1 h at 37° C (Figure 2.1). Eyes were then rinsed three more times in PBS and transferred to bacterial suspension and incubated for 3 or 6 h. After bacterial exposure, eyes were rinsed with PBS to remove non-adherent bacteria, affixed to a glass coverslip with cornea facing up, and submerged in Hams F12 (Lonza) for imaging. Alternatively, eyes were preserved in 1% PFA (paraformaldehyde) and 1.25% GA (gluteraldehyde) overnight. The preserved eyes were then rehydrated in PBS with 0.3% Triton X-100 overnight to ensure that the tissue resumed its regular shape. No physiological differences were observed with tissue treated in either way.

Figure 2.1: Ex-Vivo experimental model used to study initial events of eye infections

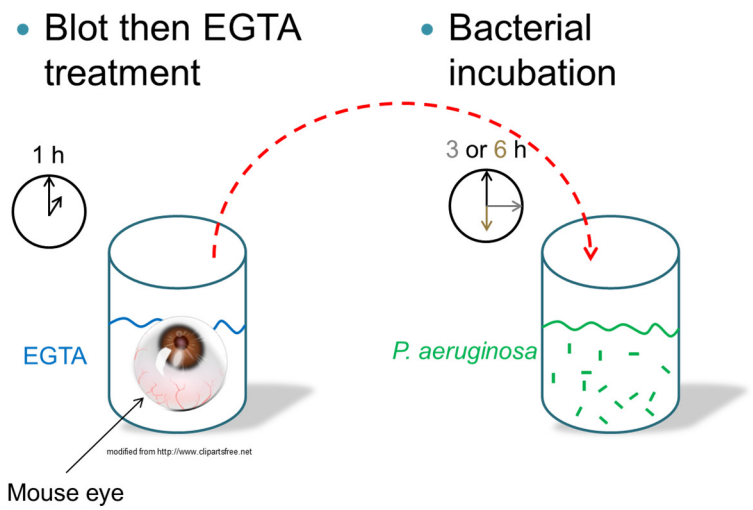

In model 2, eyes from C57BL/6 *myd88* (-/-) mice were used. These mice were kindly provided by Dr. Greg Barton (University of California, Berkeley) and bred in our facilities. Their eyes were neither blotted nor EGTA treated, and after three rinses with PBS they were placed in bacterial suspension for 6 h. After bacterial exposure, eyes were rinsed with PBS to remove non-adherent bacteria, affixed to a glass coverslip with cornea facing up, and submerged in Hams F12 (Lonza) for imaging.

In-vivo murine models of *P. aeruginosa* epithelial traversal and eye disease. In-vivo experiments were conducted in to accordance with the ARVO (Association for Research in Vision and Ophthalmology) Statement for the Use of Animals in Ophthalmic and Vision Research, and they were approved by the Animal Care and Use Committee of the University of California, Berkeley. C57BL/6 mice (6 to 8 weeks old) mice were used for all experiments. Mice were anesthetized with Ketamine (50mg/kg) Meditomadine (0.75mg/kg). 5µl of 10^11 CFU/mL of bacteria in DMEM (Dulbecco's minimum Eagle's media) media were used to inoculate one eye. The fellow eye was inoculated with 5µL of DMEM media to serve as a control. The mice were kept asleep for 4 hours before a counter agent, atipamezole (3.75 mg/kg) was injected to wake up the mice. They were either sacrificed immediately and the eyes were imaged live in a 2-photon Zeiss Meta 510, or the mice were held for 48h for observation of disease progression.
Mice observed for disease progression had pictures of their eyes taken with an Olympus stereo microscope.
In-vivo contact lens experiments were performed under the same protocol, but instead of 5µL of bacterial inoculum a contact lens was placed in the eye for 4h which had a biofilm of PA14 WT or PA14 –*exoU*. The biofilms were grown on the contact lens for one week either directly from the blister pack or previously soaked in PBS (overnight). Bacteria were grown in DMEM which was changed every other day to ensure healthy bacterial growth. Biofilm lenses were homogenized and bacteria were counted at 10^6 CFU/mL for each experiment.

Imaging of murine eyes by confocal and 2-photon microscopy. The imaging methodology

used was described previously (Tam, LeDue et al. 2011). Briefly, eyes were imaged using a Zeiss LSM 510 NLO META Axioplan confocal and 2-photon microscope equipped with Spectra-Physics MaiTai HP DeepSee for 2-photon imaging (700-1020 nm), and 458 nm, 488 nm, 514 nm, 543 nm, and 633 nm laser lines (Molecular Imaging Center, UC Berkeley). Achroplan 20x/0.5 W WD = 1.9 mm dipping objective and Achroplan IR 40x/0.80 W WD = 3.6mm dipping objective were used. A 720 nm laser was used to visualize auto-fluorescence of NADPH inside live cells. Corneal cells were also imaged without chemical fixing and labeling by using a 633 nm laser to obtain reflection of all cells (live or dead). For each eye, optical slices were taken at 0.5 μm intervals from the apical surface of the corneal epithelial cells (if present) through the entire thickness of the epithelium and into the anterior stroma (to ~ 50 μm depth). Reconstruction of 3D and transverse images for each sample was done using imaging software described previously (Tam, LeDue et al. 2011).
Confocal imaging was performed with an Olympus FV1000 confocal microscope. A 488nm laser was used for GFP imaging of bacteria, and a 635 nm laser was used to obtain reflection in the same method that was used for 2-photon imaging. The 488 nm laser was also used for auto-fluorescence of flavins to identify epithelial tissue (488/540 Excitation/Emission). Flavin auto-fluorescence was used instead of NADPH used in the 2-photon imaging because of the limitation that a confocal microscope cannot auto-fluoresce NADPH.

Measurement of corneal epithelial thickness and bacterial traversal. Corneal thickness was measured using the Zeiss LSM imaging software. Reflectance and auto-fluorescence confocal overlaid images were divided into a 3 x 3 grid, and the thickness of the epithelium was measured using measurement tools provided within the software package. At least 9 measurements were averaged across 4 to 8 corneas per test group, and means and standard deviations were calculated. Bacterial traversal was measured as described previously (Tam, LeDue et al. 2011). In some instances, lack of epithelial uniformity necessitated an alternate method for measuring epithelial thickness and bacterial traversal. Briefly, 3D models of epithelial surfaces and bacteria were generated using IMARIS (Bitplane, South Windsor, CT), and distances between the epithelial surfaces and bacteria were computed using a distance transformation via a Matlab (Mathworks Torrance, CA) plug-in within IMARIS. Distances to both the apical epithelial surface and bacteria were measured from the basal lamina to compute epithelial thickness and bacterial traversal respectively.

Alternative method for determining epithelial thickness and traversal distance. Distance

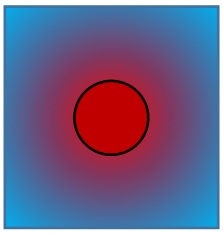

transformation was the key to solving this problem. A distance transformation takes an image and rates each pixel's minimum distance to an object. The figure to the left visualizes the distance from a point outside the circle to the edge of the circle (drawn in black). Points closer to the circle are more red, and points farther from the circle are more blue. By using the mask of the cells as the surface to create a distance transformation (e.g. the epithelium's surface becomes our circle), we can identify the distance from the bacteria to the surfaces of the epithelium (by asking what color zone the bacteria show up in). When this is done in 3D, we need to generate two surfaces: the apical surface of the epithelium and the basal lamina of the epithelium. A distance transformation is computed for each surface, allowing us to identify both bacterial distance from the surface and from the basal lamina of the

epithelium. In addition, we can identify the thickness of the epithelium by looking at the distance transformations along either surface.

However, the epithelial surface is not perfectly smooth, especially once the bacteria have damaged it while burrowing through it. This leads to an inaccuracy if we measure traversal solely from either the apical or basal surface. The figure 2.4 illuminates some of these issues. If we measure from the apical surface only, we will note that bacterium c is outside the epithelium, but will believe that the traversal by bacteria a and b are equal. If we measure from the basal surface, we would think that bacteria a and d have the same amount of traversal, and we would also mistakenly assume that b and c are equal. Not until we take measurements from both surfaces can we accurately assess how much traversal has occurred. We express this in terms of percentage of traversal:

Figure 2.2: Traversal Distance

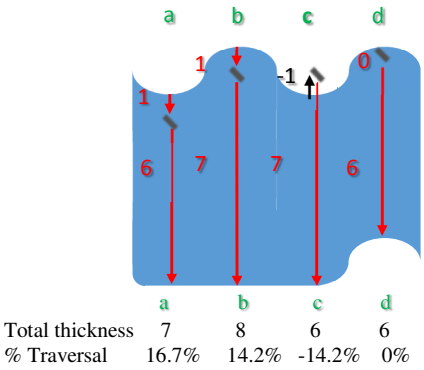

$$\% \, Traversal = \frac{distance \, from \, apical \, surface}{distance \, from \, apical \, surface + distance \, from \, basal \, lamina} \times 100$$

Figure 2.3 Epithelial Thickness measurments

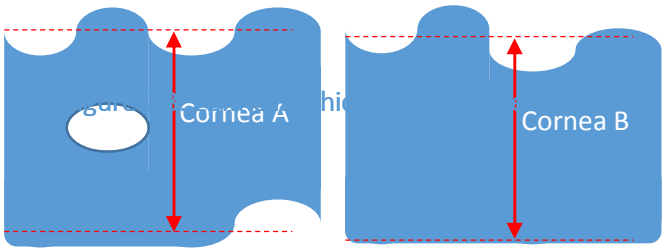

Lastly, we report two characteristics of the epithelium to identify corneal health: average thickness and volume. Average thickness must be combined with volume to accurately convey the status of the epithelium, because holes opened up in the epithelium are not adequately described if we take only thickness into account, and the volume of epithelium alone does not tell us whether the epithelium is uniform or has thick areas of epithelium followed by thin areas.

Cornea	A	B
Mean Thickness Standard Deviation	6.75 µm ± 0.95	6.75 µm ± 0.50
Area	45µm^2	50µm^2

When analyzing data from several images, one must keep in mind what one is looking for. Figure 2.6 shows two different methods for computing the number of bacteria found at each distance from the basal lamina. When the percentage of bacteria at each layer is calculated, the

median of each distance is clearly shown. However, when the number of bacteria per image is used instead, this reveals a discrepancy in the total number of bacteria recovered by each knockout-inoculated eye. Depending on the aim of the study, different presentations would be more appropriate in different situations.

Figure 2.4: Examples of absolute vs. percentage quantification

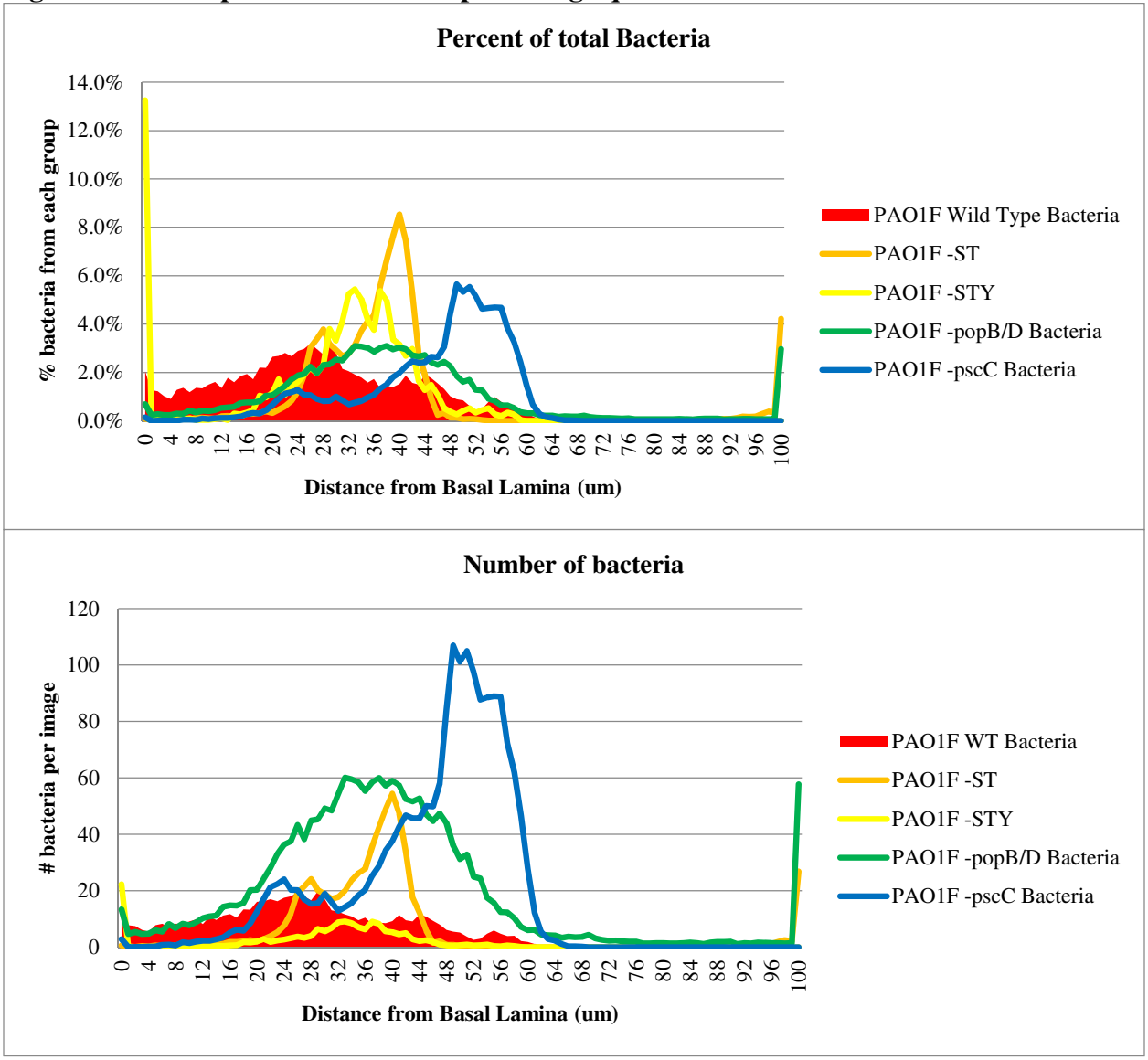

One of the methods used to quantify corneal epithelial health is to construct a plot of the epithelial characteristics on the X- and Y-axes. Volume data for each epithelium were plotted on the Y-axis while the minimum object-oriented bounding box was used for the X-axis. Object-oriented bounding box is a technique in which a box is drawn around an object so that it completely encases the object regardless of its orientation (Figure 2.5). Then the smallest length of that box is used to determine the maximum corneal thickness (Bounding Box OO length A). When it is compared to the volume of the epithelium, several characteristics can be identified. If the epithelium is within normal thickness range (40-50µm), then the volume can be assumed to be approximately 1.6k-2.0k mm^3:

V = 35 (+/-10) um * 212um * 212um.
The curvature of the epithelium must be taken into effect, so a maximum thickness (object-oriented bounding box minimum) of 40-60µm is assumed. A linear association with volume and thickness is assumed, so when volume increases without a commensurate change in thickness, edema is predicted.

Figure 2.5: Bounding Box

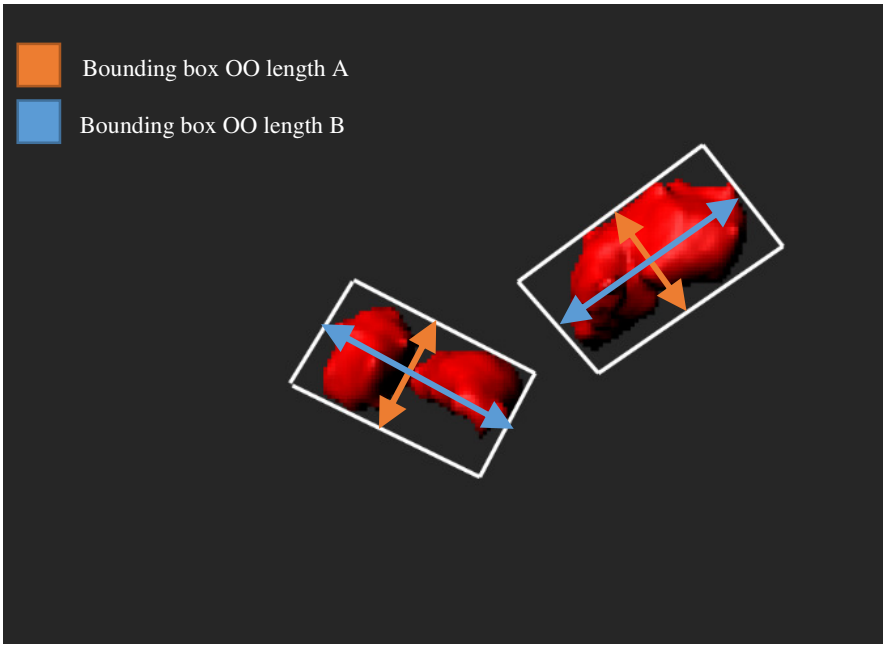

Figure 2.6 Examples of epithelial health characteristics

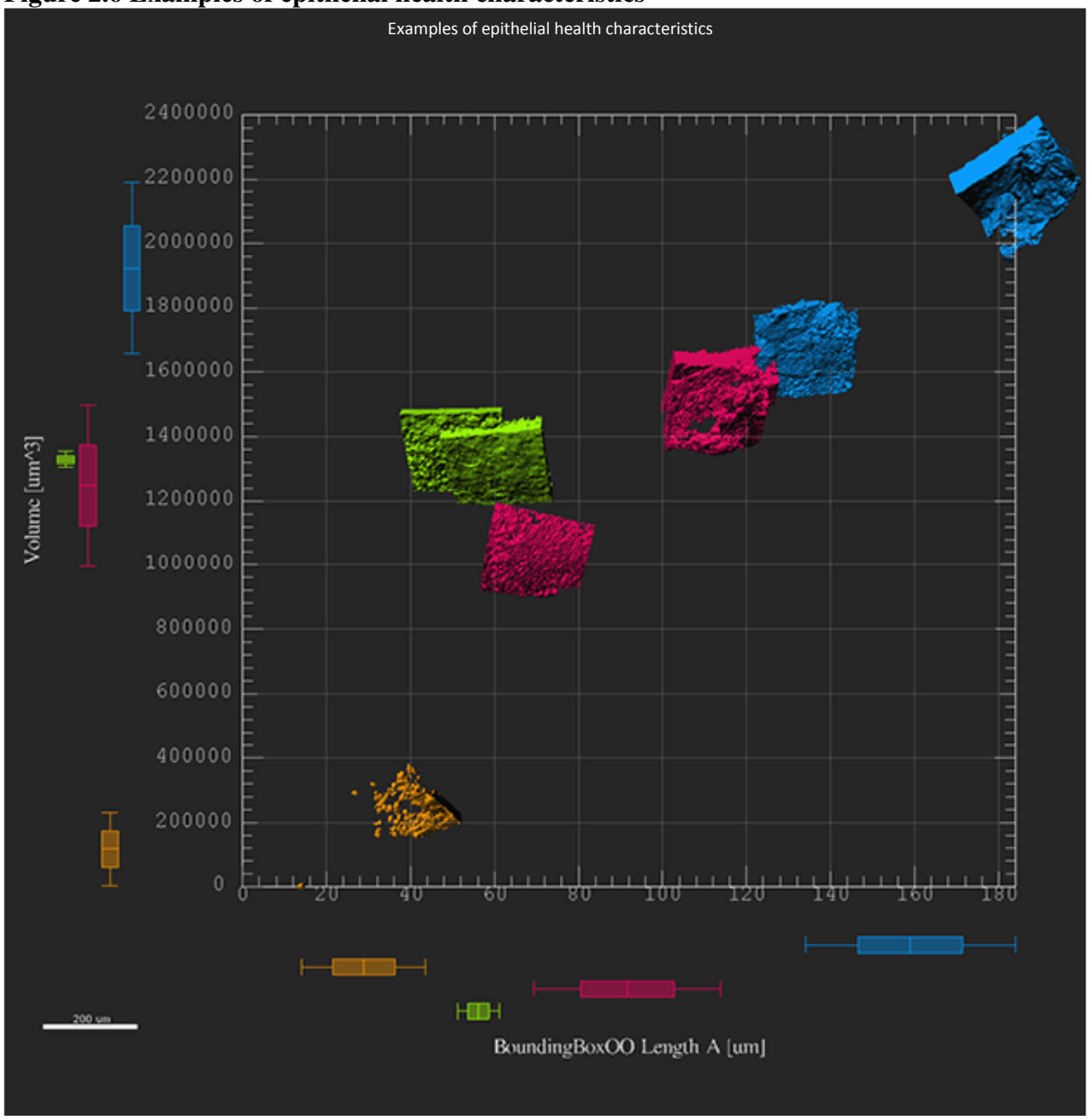

If thickness increases without an increase in volume, then the epithelium must be peeling away from the surface, thus giving the impression of a thicker epithelium. If there is a reduction in volume but not in thickness, then holes must be present in the epithelium, whereas if thickness appears to increase while volume decreases, then the epithelium has fragmented and the remaining pieces are floating away. Lastly, if a decrease in epithelial thickness is accompanied by decreases in volume then there is an absence of epithelium. Four examples are shown in figure 2.6; Absent or degraded epithelium is shown in orange, green epithelium is taken from healthy eyes, red epithelium shows minor peeling and holes, and blue epithelium shows extensive peeling. The differences in epithelium samples containing multiple characteristics are more difficult to quantify. For example, the red samples all have holes, but one image has only a

hole while the other has a hole and is also peeling. Also, epithelium that has thinned due to exfoliation and peeled is impossible to differentiate, using this method, from floating epithelium of the same thickness.

For this reason, fragment analysis is performed to determine if the epithelium is intact or has been broken into multiple fragments. This is done by first generating the epithelial surface in 3D with Imaris. Then the number of surfaces per image is counted, and the average and standard deviation are computed to determine the degree of fragmentation in the epithelium after treatment.

Accurate thickness of epithelium was measured by drawing 3D surfaces at apical and basal planes of the epithelium and then taking their mean distance. This was done by first generating a distance transformation, with Imaris's Matlab plug-in, from the epithelial surface and then using that information to generate two surfaces on the apical and basal surfaces of the epithelium. Next, statistics are generated by creating a channel in Imaris with a distance transformation for both apical and basal surfaces. Imaris computes the mean, median, and standard deviation automatically for these distance transformations to each surface.

All three of these metrics are used to determine the epithelial health after each treatment. One metric used alone often misses important information. For simplicity, the last two metrics, fragment and thickness analysis, usually suffice; however, should extensive holes or peeling appear in the samples, only the first method shows the differences between treatment groups.

Real-time PCR (RT-PCR). To determine *exsA* gene expression in vitro, bacteria were grown under T3SS-inducing conditions, i.e., tryptic soy broth (TSB) containing glycerol (1 % v/v), monosodium glutamate (50 mM), EGTA (5 mM), and $MgCl_2$ (50 mM) (Yahr, Mende-Mueller et al. 1997) at 37^{o} C to exponential growth phase, and harvested by centrifugation (~11,000 x g, 10 min). Non-T3SS-inducing conditions (TSB alone) were used for controls. RNA was isolated from bacteria using TRIzol (Life Technologies, Grand Island, NY). A DNase I kit (Fermentas) was used to eliminate contaminating DNA, and cDNA was made for RT-PCR using an Ambion® MessageAmp™ II-Bacteria kit (Life Technologies). RT-PCR was performed on an Applied Biosystems Step One Plus (Life Technologies). Primers were designed using Applied Biosystems Primer Express Software and verified by a BLAST search. Gene sequences were obtained from the *Pseudomonas* genome database (www.pseudomonas.com). RT-PCR primers were as follows: 16S ribosomal RNA for PAO1 [Fwd. GGCGCTAATACCGCATACGT, Rev. TGATAGCGTGAGGTCCGAAGA], exsA [Fwd. CATGGAGGCGGGCTTTT, Rev. CGAAACGGCGGCGATAG]. Primers were synthesized by IDT (Coralville, IA).

SDS-PAGE and Western immunoblot. Bacteria were grown under T3SS-inducing and non-inducing conditions and centrifuged as described in RT-PCR methodology, and culture supernatant was collected to determine the expression of the T3SS effector protein ExoS. Protein concentration of the supernatant was determined using a DC protein assay kit (BioRad, Hercules, CA) with a bovine serum albumin standard. Equal amounts of protein were resolved by SDS-PAGE (15% Ready Gels Tris-HCl, BioRad). Western immunoblot was used to detect ExoS by transferring proteins to nitrocellulose membranes, blocking overnight with a buffer of skim milk (5% w/v) in TBS-Tween 20 (0.05% v/v), and exposure to rabbit anti-ExoS antibody (New England Peptide, Gardner, MA) overnight, diluted in blocking buffer (1:1000). Bound antibody

was detected by chemiluminescence using a horseradish peroxidase–conjugated goat anti-rabbit secondary antibody (BioRad) diluted in blocking buffer (1:1000).

FDA-approved staining of bacteria for clinical diagnosis. FDA-approved dyes Fluorescein, lissamine green, and rose bengal were incubated with bacteria to determine if clinically approved dyes could be used to identify the live microbes on the corneal surface. Fluorescein (AKORN) strips were diluted in 1 mL of PBS and incubated with bacteria for 5 min, 15 min, and 30 min at 37^{o} C. The bacteria were then plated on a coverslip and imaged on an Olympus FV1000 confocal microscope system to determine the percentage of bacteria that fluoresced (488 nm excitation, 500 nm emission). Rose bengal (Sigma Aldritch) was used at the same dose as that used for clinical staining (0.1%). Bacteria were incubated for 5 min, 15 min, and 30 min at 37^{o} C. Lastly, lissamine green (Sigma Aldritch) [1% v/v] was applied to bacteria for 30 min at 37^{o} C. Bacteria were imaged on an Olympus Widefield phase contrast microscope.

Murine model of corneal and conjunctival clearance. C57 b/6 background mice were inoculated in one eye in accordance with ARVO guidelines for the ethical treatment of animals. Five microliters of 10^9 CFU/mL of bacteria (either *P. aeruginosa* or *S. aureus*) were inoculated into one eye, and DMEM was placed in the fellow eye as a control. For corneal wash, 20µL of PBS was applied to the corneal surface and removed by capillary tube to prevent the PBS from touching the mouse's eyelids. Mice were anesthetized with Ketamine Meditomidine cocktail (as described in in-vivo experiments above). After 1 h, they were given a counteragent Atipimazole (as described in in-vivo experiments above). Time points of 1 h, 6 h, 14 h, and 24 h were used to determine the course of bacterial clearance in both models. At 24 h, the mice were euthanized and the cornea were ground using Polytron pt 1200e (kinematica) tissue homogenizer. For conjunctival clearance, one mouse was used for each time point. Conjunctival samples were extracted from the mice after the lethal dose of anesthesia was administered, followed by cervical dislocation. Conjunctival samples were homogenized and then plated on TSA agar (Tryptic soy agar) for colony counts.

Plasmid construction for bacterial knockouts. Bacteria knockouts were generated via the same method that Arne Reitsch used in (Rietsch, Wolfgang et al. 2004) (Figure 2.9). A suicide vector excised *exoS* or *exoT* by replacing the gene with a blank cassette. PAO1 and E. coli (SM10 + plasmid) were streaked out on LB (Luteinizing Broth) agar plates overnight for single colonies. The bacteria were then conjugated for 1 h at 37^{o} C before being transferred to a LB gent/irgasan selective plate overnight (gentamycin 30ug/mL, irgasan 5ug/mL). The bacteria were transferred to a LB plate with no salt for 2-3 h and then placed on an LB 5% Sucrose plate (to kick out the plasmid) and incubated overnight. Colonies were selected and cross-checked for gentamycin sensitivity by plating on LB and LB gent/irgasan plates. The suicide vector ensured that only double crossovers were viable and no antibiotic resistance was conferred. A second cross-check was performed after every screen to ensure that antibiotic sensitivity was returned. The results were tested via colony PCR to ensure that the gene was knocked out.

Figure 2.7: pEX18GW exoS plasmid map

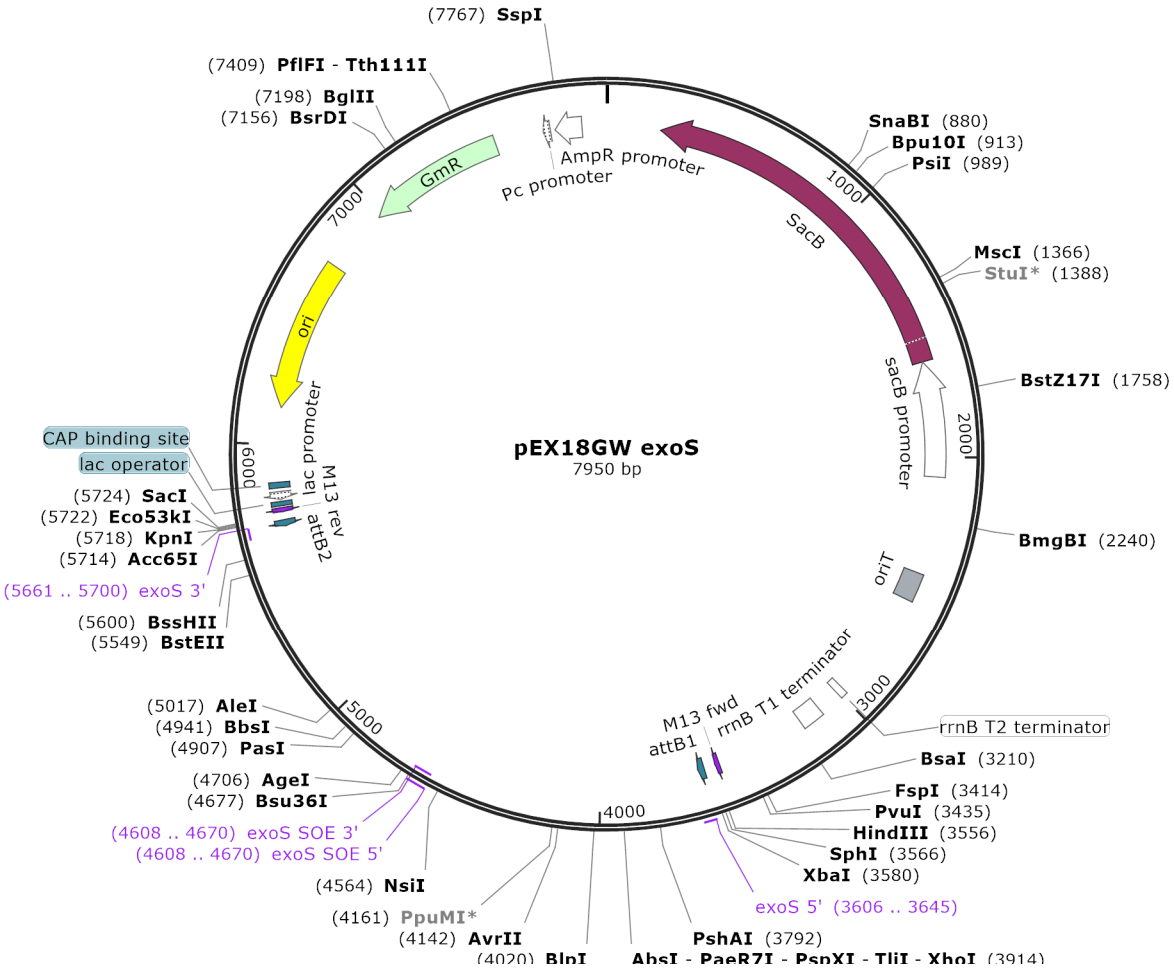

Statistics. Data were expressed as the mean ± standard deviation (SD) for each sample group. Statistical significance among three or more groups was determined using ANOVA with Tukey multiple comparisons post-hoc analysis. Unpaired Student's *t*-Test was used for two group comparisons of normally distributed data. *P* values of < 0.05 were considered significant.

Chapter 3:

The Role of the T3SS in Corneal Traversal and Epithelial Barrier Disruption in Both Cytotoxic and Invasive Strains

Chapter 3: The Role of the T3SS in Corneal Traversal and Epithelial Barrier Disruption in Both Cytotoxic and Invasive Strains

Introduction

The first line of defense for any infection is the epithelium and the barriers that this tissue can form. For a microbial infection to occur, invading bacteria must first get to and then breach the epithelial barrier. In the case of the cornea of the eye, this barrier is unique in that it is "immune-privileged". This status means that, under normal conditions, the cornea of the eye does not elicit an inflammatory response, because any inflammatory response in the cornea could compromise vision. Despite this, the cornea is remarkably free from disease, even though it is constantly bombarded with foreign particles that can carry a plethora of microbes. To better understand the pathogenesis of bacterial infections a closer look is needed at both unique innate barrier functions and the methods by which bacteria bypass them.

The immune-privileged status of the cornea makes it ideal for investigation of innate immune responses and their circumvention. No other area of the eye is both so accessible and under so much onslaught of foreign microbes. In this instance, the eye is the window into the innate immune system.

The number-one cause of corneal microbial keratitis (MK) is the bacterium *Pseudomonas aeruginosa.* This bacterium has been linked to MK both in contact lens–related eye disease and also without contact lenses. The type III secretion system has been linked to the virulence of *Pseudomonas* (Collazo and Galan 1996, Hauser, Fleiszig et al. 1998, Hirano, Charkowski et al. 1999, Sawa, Yahr et al. 1999, Abe and Nagano 2000), especially in cases of MK. The components of the T3SS target various processes that enable bacteria to be more successful pathogens. ExoS, for instance, has been linked to intracellular survival, whereas ExoU has been shown to be cytotoxic. In-vitro studies have shown that the T3SS is needed for traversal of epithelium grown on a transwell (Ramirez, Fleiszig et al. 2012). However, this has only recently been studied within the eye in an initial infection model (Sullivan, Tam et al. 2015) The evidence shows that the T3SS is involved as long as the secretion system is turned on to a sufficient degree, but the study did not identify which effector is involved.

Results

Invasive Strain Traversal

Two different strains of *Pseudomonas* were used to investigate the effects of the T3SS on corneal epithelial barrier disruption as well as bacterial traversal of the corneal epithelium. The first strain of *Pseudomonas*, PAO1\ is an invasive strain that encodes the T3SS effectors ExoS, T, and Y. The strain came from two different labs. The first lab strain, labeled PAO1 DF was seen in previous studies to be exceptionally virulent and destructive to the corneal tissue. I knocked out *exoS* and *T* using a suicide vector, pEX18GW (Rietsch, Wolfgang et al. 2004). The second PAO1 (PAO1F) came with an extensive number of knockouts of the type III secretion system components. These knockouts were made using the same method that I used to construct ExoS and ExoT knockouts of strain PAO1 DF. Although PAO1F did not have the same virulence or extensive traversal characteristics as PAO1 DF, it was still able to traverse the corneal epithelium and cause disruption of the corneal epithelial barrier (data not shown). Previous studies have shown differences between bacteria from the same strain but different labs

(Klockgether 2010). All strains are identified by source and are partnered with a congenic wild type for comparison. Table 1 lists the strain and the sources of their knockouts.

Table I Invasive Strains used

Bacterial Designation	**Type III Effectors Produced**	**T3SS Secretion**	**Reference**
PAO1 DF WT	STY	High	Frank et al. (1994)
PAO1 DF ExsA::Ω	None	None	Frank et al. (1994)
PAO1 DF -*exoS*.	TY	High	This paper
PAO1 DF -*exoT*	SY	High	This paper
PAO1 DF -*exoS* & -*exoT*	Y	High	This paper
PAO1F WT	STY	N/D	Vance (2005)
PAO1F -exoS & -exoT	Y	N/D	Vance (2005)
PAO1F -*exoS*, -*exoT*, & -*exoY*	None	None	Vance (2005)
PAO1 -*pscC*	STY	None	Vance (2005)

After generating the knockouts of -*exoS* and -*exoT* I confirmed that the parent strain PAO1 DF was still potent enough to traverse the corneal epithelium and its -*exsA* knockout remained unable to traverse the epithelium or cause epithelial disruption.

Figure 3.1 PAO1 (invasive) Traverses in a T3SS dependent Manner

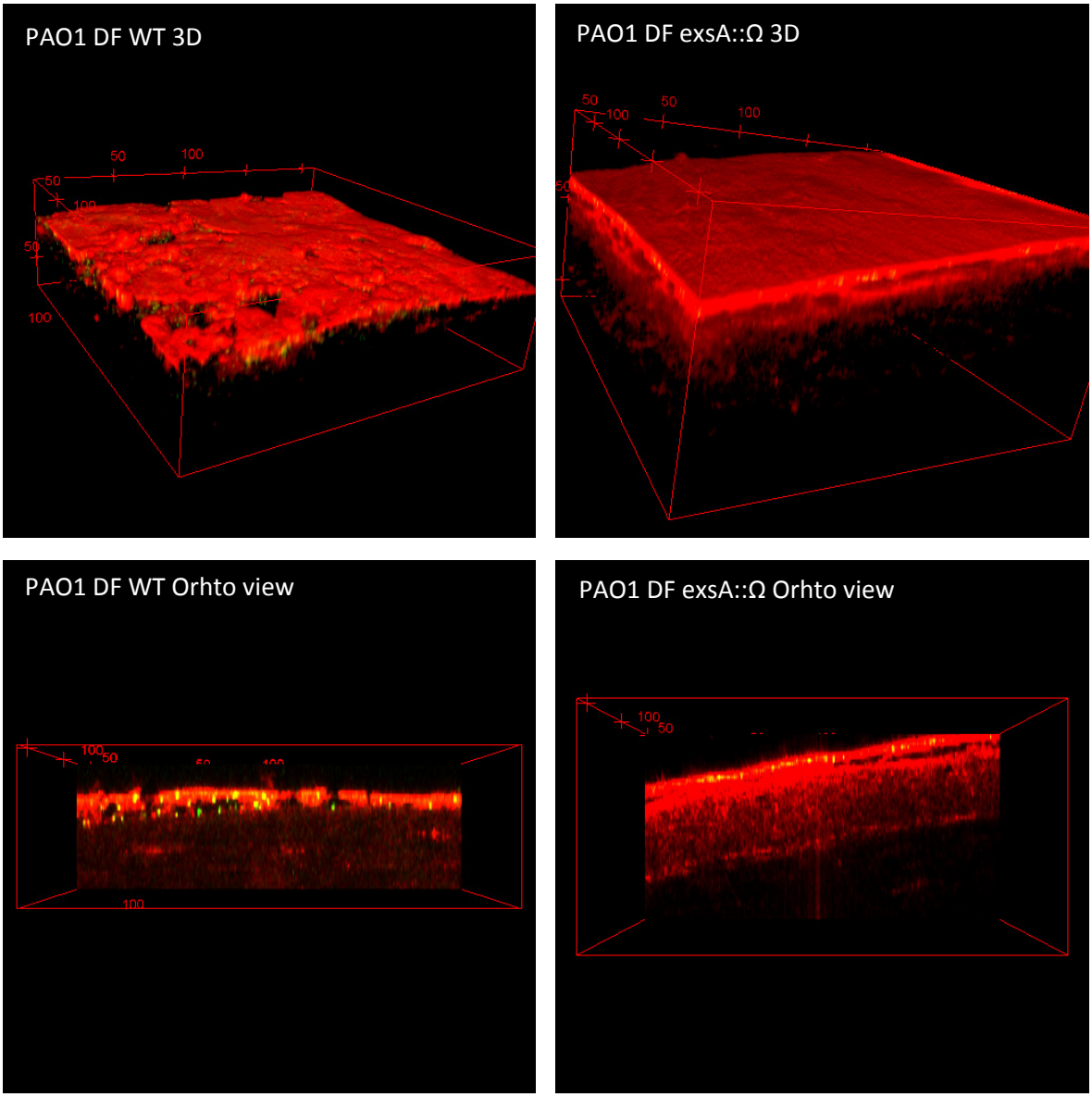

Previous findings show that when the master regulator for the T3SS (ExsA) is knocked out, the ability of bacteria to disrupt and traverse the corneal epithelial barrier is halted (Sullivan et al. 2015). Shown are representative confocal images of PAO1 Wild Type (WT) and the PAO1*exsA::*Ω lacking the T3SS. These are the parent strain used to make the *exoS* and *exoT*, KOs. Images here confirm that the parent strains retained their phenotype from previous findings.

Both the single knockout of *exoS* and double knockout of both *exoS* and *exoT* were able to cause epithelial disruption and traverse the corneal epithelium after 6 hours ex vivo. The tissue disruption was less severe in the T3SS effector knockout bacteria infections, but the barrier was breached. No statistical difference was observed between WT and effector knockout bacteria in terms of traversal depth. Epithelial thickness, however, was disrupted and had a higher variability as well as a larger number of fragments in WT compared to the ExsA control ($p<0.05$), which was whole and had no obvious holes. On average, -exoS had one epithelial fragment per image, which was lower than the -*exoS,T*, but the difference did not appear significant. Epithelial thickness tended to be thinner in the -exoS inoculated corneas as well.

There were an increased number of bacteria associated with the 70%-80% traversal depth with the ExoS, but ANOVA analysis of showed no significant difference between WT, -exoS and -exoS,T mutants. There was a significant difference between ::ΩexsA-inoculated eyes and the eyes treated with either WT or -exoS, -exoS,T mutants (ANOVA $p < 0.05$, Tukey post-hoc analysis).

Figure 3.2 T3SS effectors ExoS and ExoT are not necessary for traversal

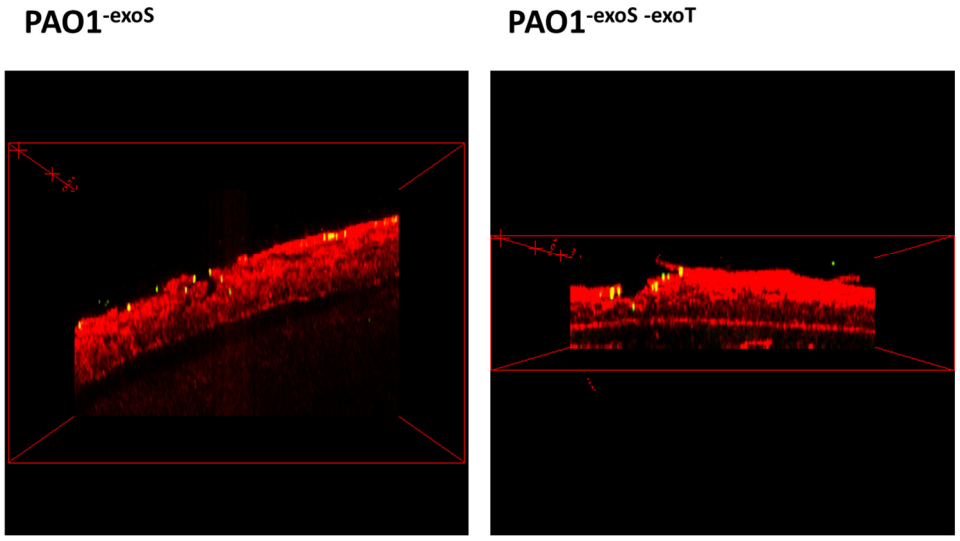

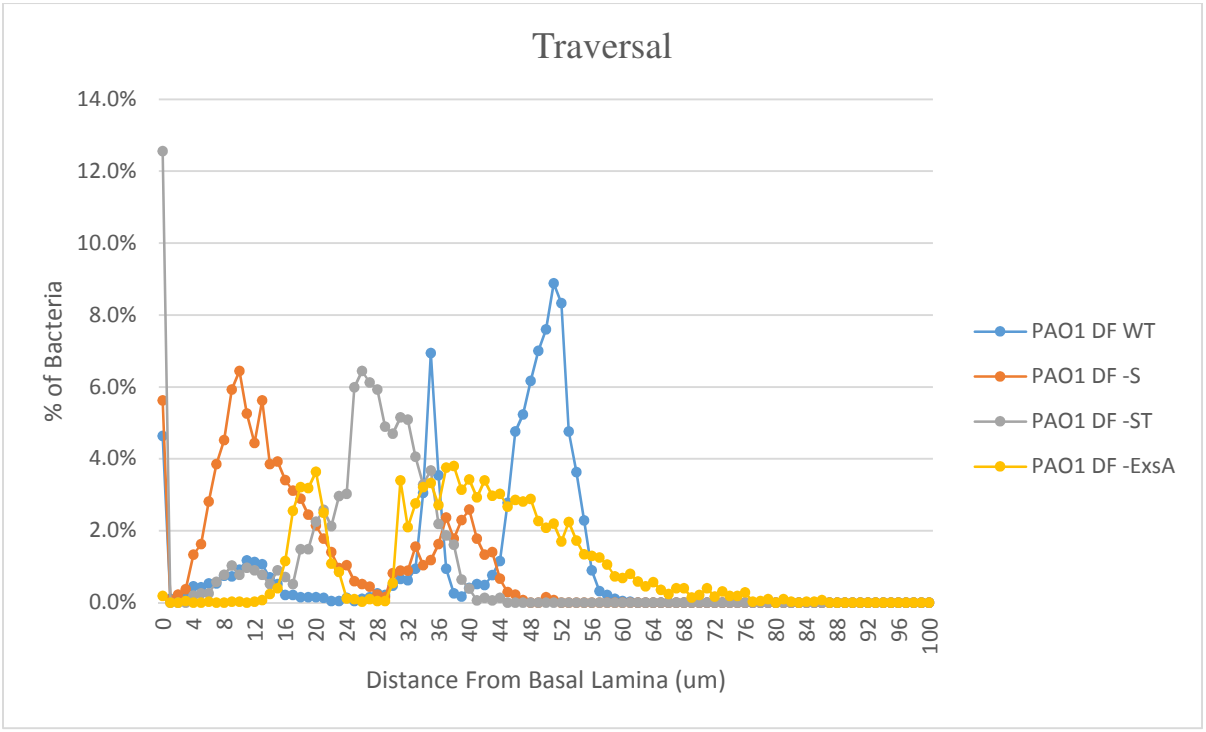

Figure 3.2 (continued).

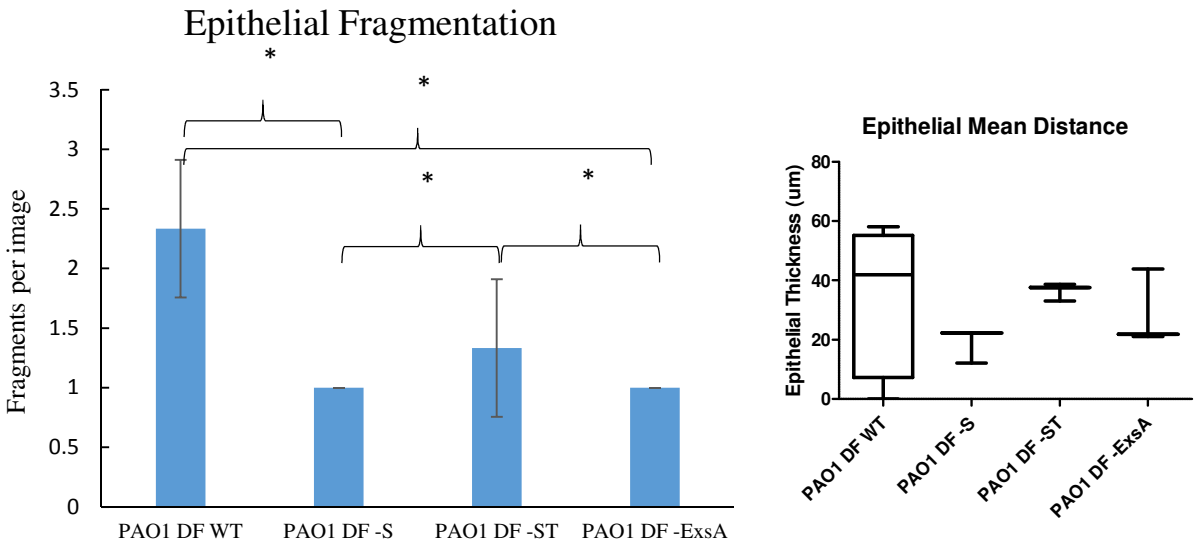

Knockouts of two T3SS effector proteins, ExoS and ExoT, do not halt the bacteria's ability to traverse the corneal epithelium. There is no statistical difference in traversal between the WT, -exoS. and -exoS-*exoT* mutants; however, there is a statistical difference between all three traversing bacteria and the *exsA* mutant. Interestingly, there seemed to be a large number of *–exoS* lacking bacteria at around 80% traversal. Epithelial thickness measurements show no difference, but the number of images captured with no epithelium was 50% with the WT and 0% with the ExsA MT. Both ExoS and -exoT showed some areas of no epithelium. The number of fragments found per image of epithelium differed between mutants. ExoS, T knockouts and WT both contained multiple fragments where ExoS-treated cornea along with ExsA-treated corneas only had a single fragment per image. (*p<0.05)

Table II Statistical analysis of PAO1 DF mutant traversal

Tukey's Multiple Comparison Test	Mean Diff.	q	Significant? P < 0.05?	Summary
PAO1 DF WT vs PAO1 DF -S	1.3	0.57	No	Ns
PAO1 DF WT vs PAO1 DF -ST	0.67	0.29	No	Ns
PAO1 DF WT vs PAO1 DF -ExsA	-15	6.5	Yes	***
PAO1 DF -S vs PAO1 DF -ST	-0.67	0.28	No	Ns
PAO1 DF -S vs PAO1 DF -ExsA	-17	7.0	Yes	***
PAO1 DF -ST vs PAO1 DF -ExsA	-16	6.7	Yes	***

Additional knockouts of the T3SS were then pursued using strain PAO1F, which had a more complete knockout library. Tests were run to confirm PAO1F's ability to traverse the corneal epithelium (data not shown), finding that it could satisfactorily could traverse the corneal epithelial barrier, although not as deeply or with as much tissue disruption as with strain PAO1 DF.

PAO1F included knockouts of all three secreted effectors (ExoS, ExoT, ExoY) as well as the translocons (PopB and PopD). Since a T3SS master regulator (ExsA) knockout was not available, I used a T3SS mutant (PscC), which disrupts the formation of the needle complex by eliminating the outer membrane pore that the needle complex needs in order to attach to the bacterial outer membrane (Figure 1.4 B). Further, PAO1F -*pscC* interrupts a positive feedback mechanism to maximally up regulate the T3SS (Yahr paper). As a result, the PscC MT was unable to traverse like the ExsA MT and was confirmed as a negative control in our assays. Knockouts of all three effector proteins as well as the translocon proteins had a minor effect on

epithelial disruption and bacterial traversal. Effector and translocon mutants were all able to reach the basal lamina as did the WT parent strain. However, the mean traversal distance was approximately 10 microns less than that for the WT bacteria. This seems to indicate that although they are not necessary or sufficient for traversal, they do have an impact on traversal.

Figure 3.3 Removal of any of the known secreted T3SS effectors, including the translocon, does not completely block traversal.

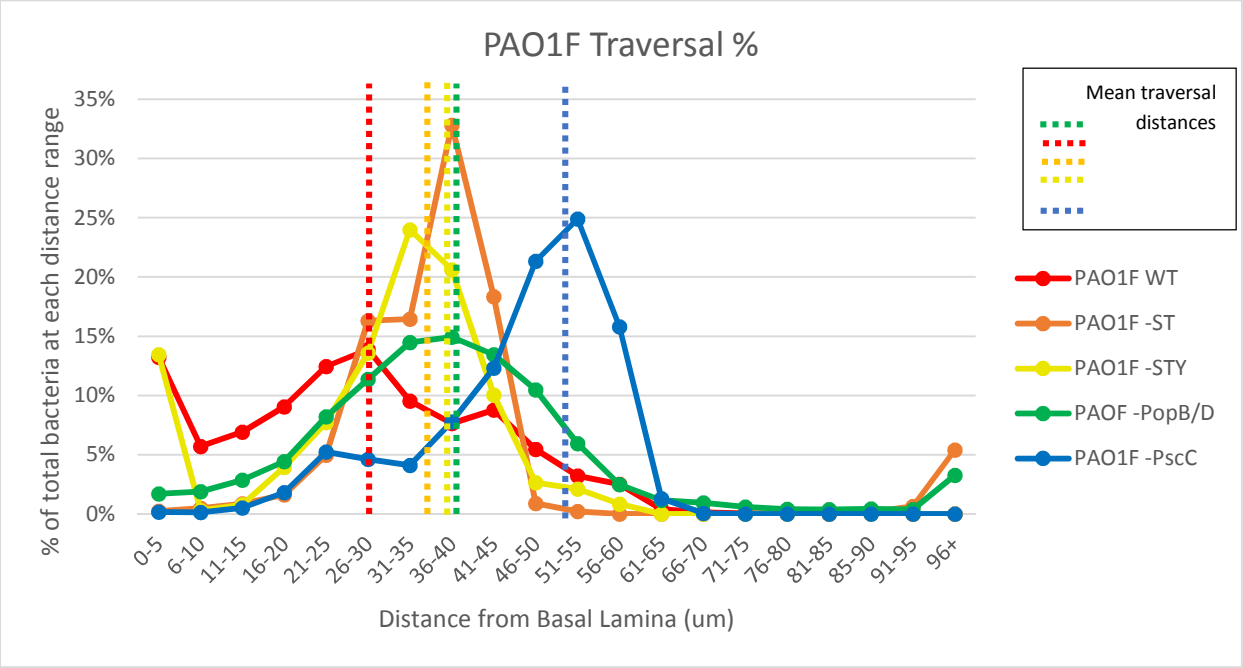

Using a similar strain of Pseudomonas, PAO1F, I observed that all three T3SS effectors and the translocons PopB and PopD are unnecessary for barrier disruption and traversal of the corneal epithelium. The percentage of bacteria per region shows the median traversal distance of ST, STY, and PopB/D mutants to be about 35-40 microns (10-15 microns further than the needle mutant PscC, used as a control). The Wild Type PAO1F traversed on average an additional 5-10 microns. When the data are evaluated in terms of the number of bacteria per image, the total number of WT and STY MT bacteria is found to be significantly lower than those of the other mutants.

Corneal epithelial health was measured in a variety of ways. By plotting the object-oriented bounding box shortest length (synonymous with epithelial thickness) and epithelial volume on an XY graph, we could determine if the epithelium was healthy, edematous, peeling, floating away from its main body, full of holes, or absent. PAO1F WT was found to cause epithelial absence or holes; some sections of the epithelium were also observed to be floating away from the corneal surface. PAO1 –ST had the majority of epithelium peeling with some sections of absent and floating epithelium. PAO1 –STY was characterized with mostly edematous epithelium, whereas translocon mutant PAO1 –PopB/D was evenly split between healthy, edematous, peeling, and absent epithelium. The needle knockout PAO1F –pscC had a few replicates that were edematous, but most samples of the epithelium tested were at a thickness consistent with health. The cutoff for each category was based on mean corneal thickness from untreated mice (data not shown).

Figure 3.4 Epithelial health is significantly impacted by traversing bacteria regardless of T3SS knockouts.

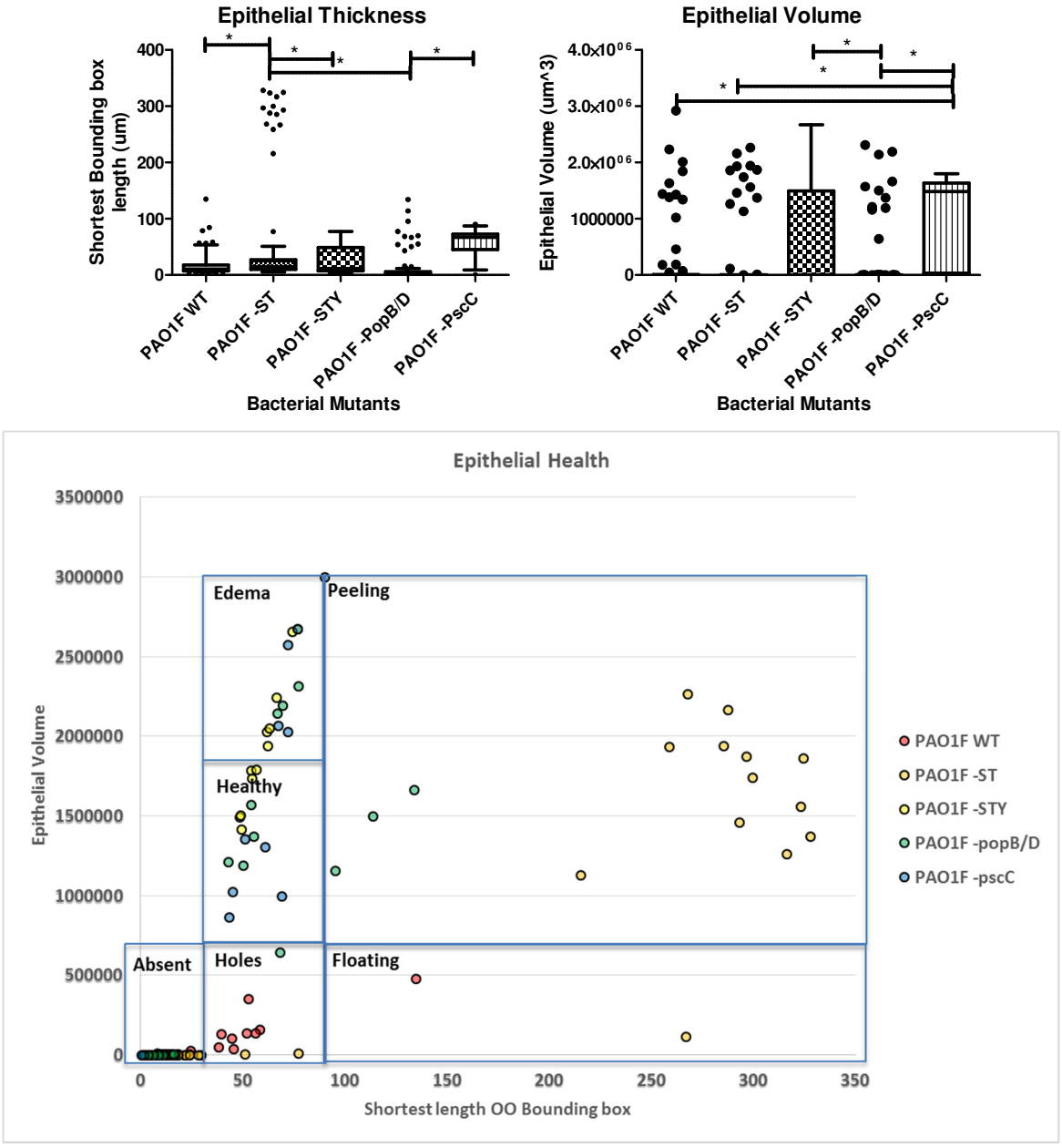

Figure 3.4 (continued)

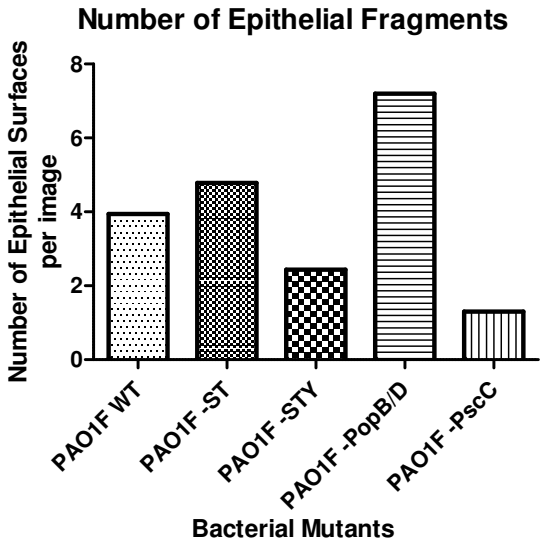

Three metrics were compared to identify corneal epithelial health. (The methodology is explained in chapter 2.) Maximum epithelial thickness, is plotted against epithelial volume is used to determine epithelial health. The number of epithelial surfaces found in each image are also reported here to indicate the extent of epithelial damage not covered by the other metrics. PAO1 *–exoS,T,Y* and -pscC negative control had surfaces showing no statistically significant differences between volume and maximum epithelial thickness. However, when plotted on an XY-coordinate system, the pattern of epithelial health can be delineated. Edematous cornea appear to be dominated by –STY inoculated cornea and healthy cornea by PAO1 -pscC, whereas PAO1 –exoS dominate the cornea that are peeling and WT-challenged cornea dominate the absent epithelium and cornea with significant holes. Translocon mutant PopB/D bacteria–challenged cornea appeared to be evenly distributed between edematous, healthy, and peeling cornea.

Cytotoxic Strain Traversal

Cytotoxic strains are associated with most cases of CL-related MK, and in-vitro data show that -exoU and to a lesser extent -exoT and -exoY contribute to corneal epithelial traversal. These strains have been shown to affect traversal in-vitro but were never tested in an ex-vivo eye study for traversal, which has a much more complex barrier. I used the same model of initial infection (ex-vivo null infection model) as with the invasive strain to determine if there were any differences in ex-vivo traversal, since there were differences in human subjects being susceptible to disease. Table III outlines the bacteria used in this study and their characteristics.

Table III Cytotoxic Strains Used

Bacterial designation	Type III Effectors	T3SS Secretion	Reference
PA14 WT	UTY	High	Myata et al. 2003
PA14 -*exoU*	TY	High	Myata et al. 2003
PA14 -*exoU*,-*exoT*,-*exoY*	None	None	Myata et al. 2003
PA14 -*pscD*	UTY	None	Myata et al. 2003

Initial results looking at traversal 3 h after inoculation showed that the T3SS, in particular PA14 -*exoU*, was needed for traversal of the corneal epithelium. PA14 -*exoU* and the needle knockout

(*-pscD*) were both equally unable to traverse. Traversal distances were equal to average epithelial thickness, showing that the bacteria remained on the surface.

Figure 3.5 3h Inoculation ex-vivo shows T33SS dependent traversal

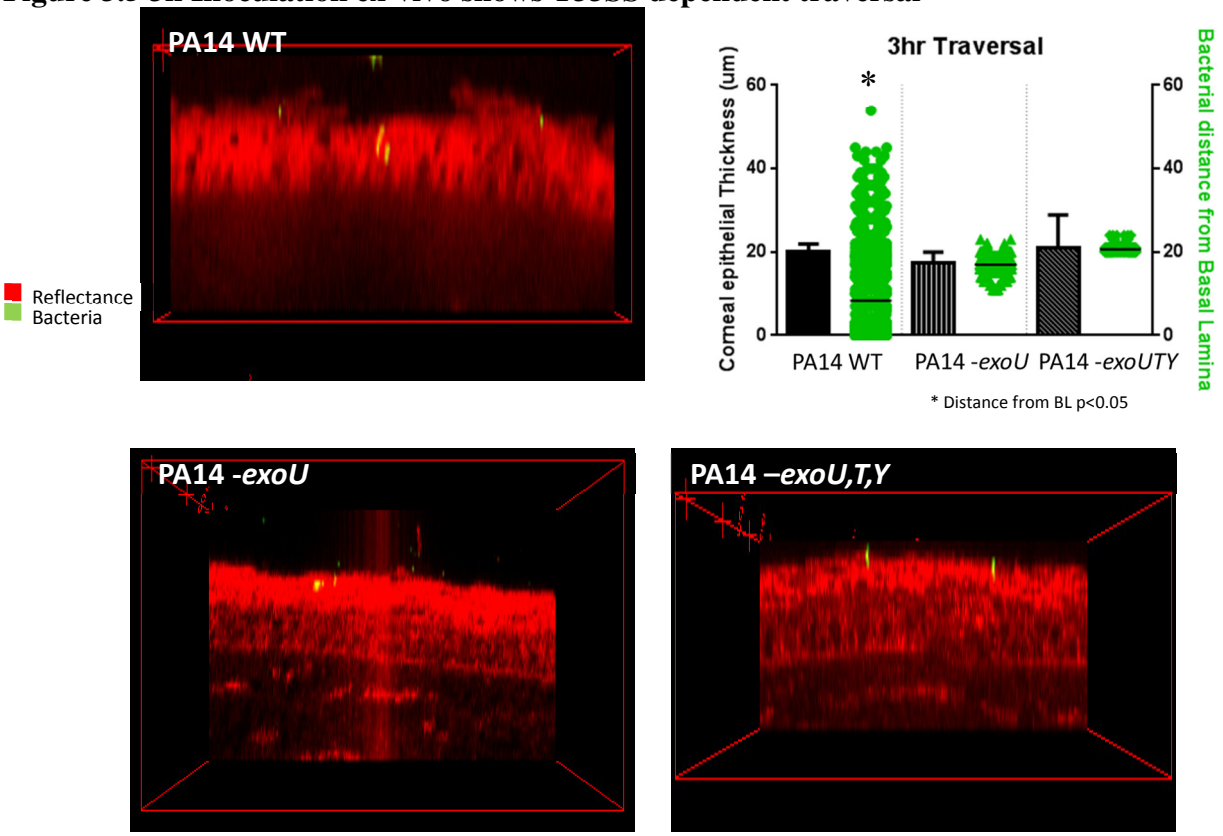

After a 3h exposure to the eye, only Wild Type PA14 bacteria were able to traverse the corneal epithelium. Epithelial thickness measurements showed no differences in thickness among the corneas treated with any of the bacteria. $*p < 0.05$.

When the inoculation was extended to 6h, all bacteria regardless of T3SS expression were able to disrupt as well as traverse the corneal epithelium. WT bacteria and those lacking ExoU did not totally eliminate the epithelium, whereas triple knockout (*-exoU, -exoT, -exoY*) and needle knockout (*-pscD*) [*-pscC* data not shown] bacteria eliminated all epithelium by 6h. These data show a difference in barrier disruption and traversal inversely proportional to the number of T3SS effectors produced. These data differ significantly from previous findings in vitro.

Figure 3.6: 6h inoculation ex-vivo allows for T3SS independent traversal of the cornea

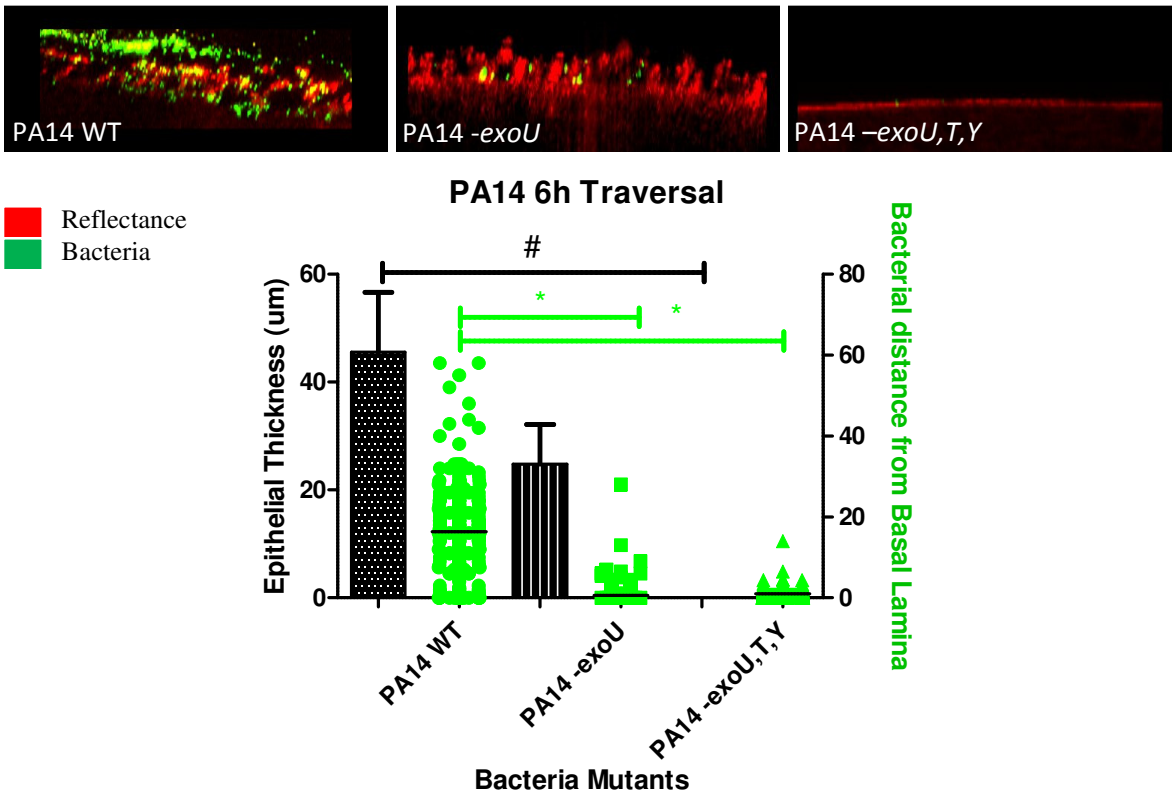

When the cytotoxic bacteria PA14 were exposed to the eye for 6h, all mutants were able to traverse and disrupt the corneal epithelium. Epithelial thickness was significantly greater in WT treated eyes than PA14 *–exoU,T,Y* treated eyes # $p<0.05$. Traversal of WT treated eyes was also significantly different from both *exoU* MT bacteria and PA14 *–exoU,T,Y* treated eyes * $p<0.05$. The epithelium was completely absent in the triple mutant (ExoU, ExoT, ExoY) and needle mutant (PscC) cases. (PA14 *–pscC* data not shown)

To ensure that the differences were not due to the pretreatment of the corneal epithelium, the ex-vivo model was tested without EGTA treatment and blotting. Unlike PAO1 (invasive strain), PA14 was able to traverse the corneal epithelium without EGTA treatment and blotting. These data point to significant differences in cytotoxic strain PA14's ability to achieve barrier disruption and traversal of the corneal epithelium when compared to invasive strain PAO1. In chapter 6 we discuss the differences between PA14 3h and 6h traversal further.

Figure 3.7 Ex vivo w/o EGTA still shows 6h T3SS-independent traversal

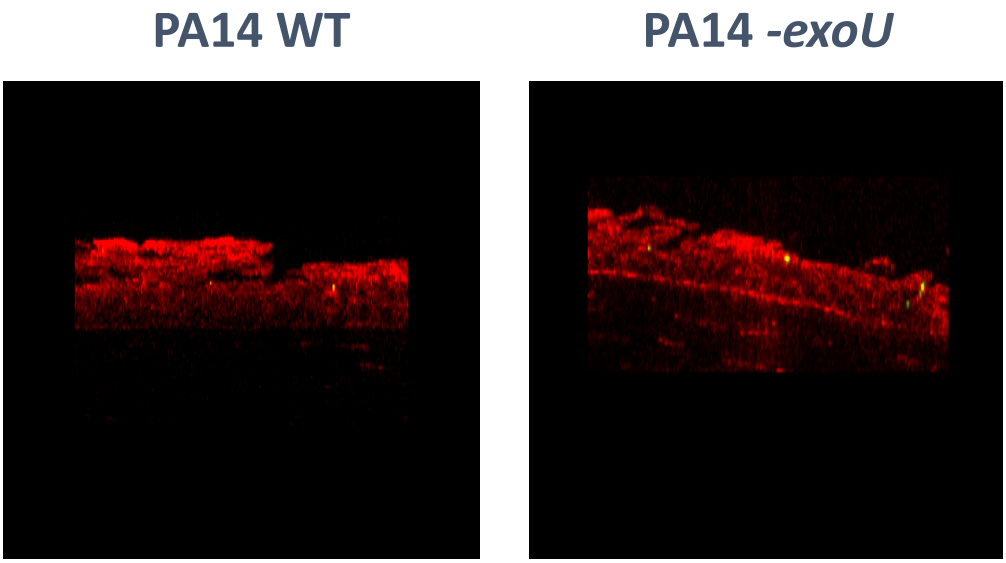

In order to determine whether traversal was due to blotting or EGTA treatment, eyes were inoculated without blotting or EGTA treatment first. In both cases, cytotoxic bacteria PA14 were able to traverse the eye and cause epithelial disruption.

Because the cytotoxic bacteria were able to cause barrier disruption and traversal without the need for EGTA or blotting, I tested the bacteria in an in-vivo model which used neither blotting nor EGTA treatment. Bacteria were optimized for inoculation time as well as inoculation amount (see Appendix). A dose of 5uL of inoculum was placed on the anesthetized mouse for 4h before the animal was awakened with a counteragent and observed for 48h.

Taking the ex-vivo model into a living system showed similar results as far as tissue dissruption at early time points was concerned. In the living system, we were also able to correlate disease progression to bacterial knockouts. The inoculum in the eye shows that after 24h, only ExoU containing PA14 were able to cause disease. However, after 48h an opacity appeared to be forming in even the eyes inoculated with PA14 -*exoU*. These findings showed a delay of approximately 24h in the onset of disease. Only 50% of the eyes treated in this manner had this disease outcome, but this outcome was present without EGTA and blotting treatment. EGTA-treated and blotted eyes were also examined but showed no difference in infection rate when compared to non-pretreated eyes (data not shown).

Figure 3.8 In-vivo disease requires ExoU

Bacterial inoculum covers the entire eye during infection

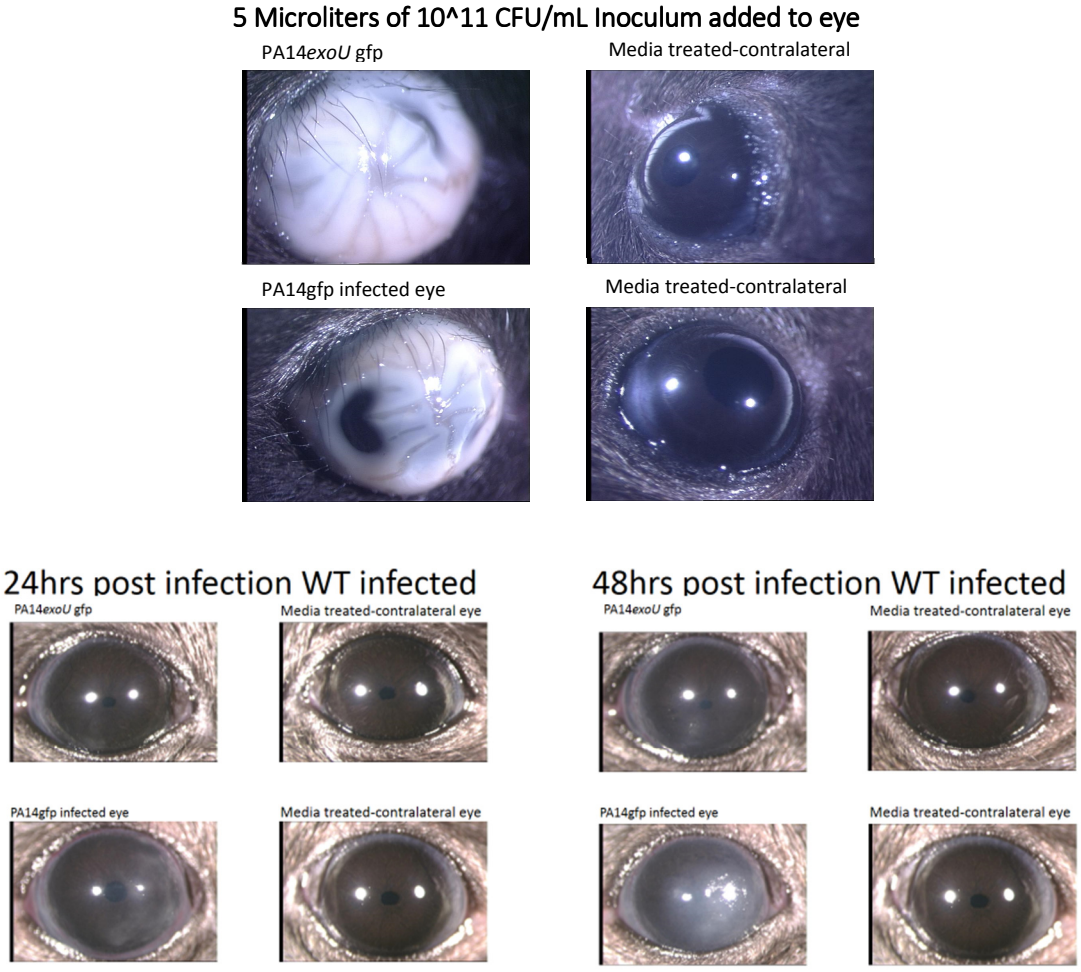

10^11 CFU/mL of bacteria were added to the surface of the eye. Representative images show that 5 microliters of this concentration covered the eye completely. After 4h of inoculation, disease began to occur 24h later in PA14 WT treated eyes but not ExoU MT treated eyes. After 48h, the differences in disease are clearly much more prominent in PA14 WT eyes, although a slight opacity occurred in PA14 ExoU MT treated eyes. (Images collected in collaboration with Julio Ramirez.)

Traversal of the ExoU MT appears to be halted after 4h of inoculation. However, the eyes still were able to show some disease after 48h, though not at 24h. These data suggest that progression through the epithelium for mutants lacking components of the T3SS, especially ExoU in the case of PA14, have a much more retarded rate of epithelial barrier disruption and traversal to the basal lamina.

Figure 3.9 In-vivo traversal requires ExoU after 4h inoculation

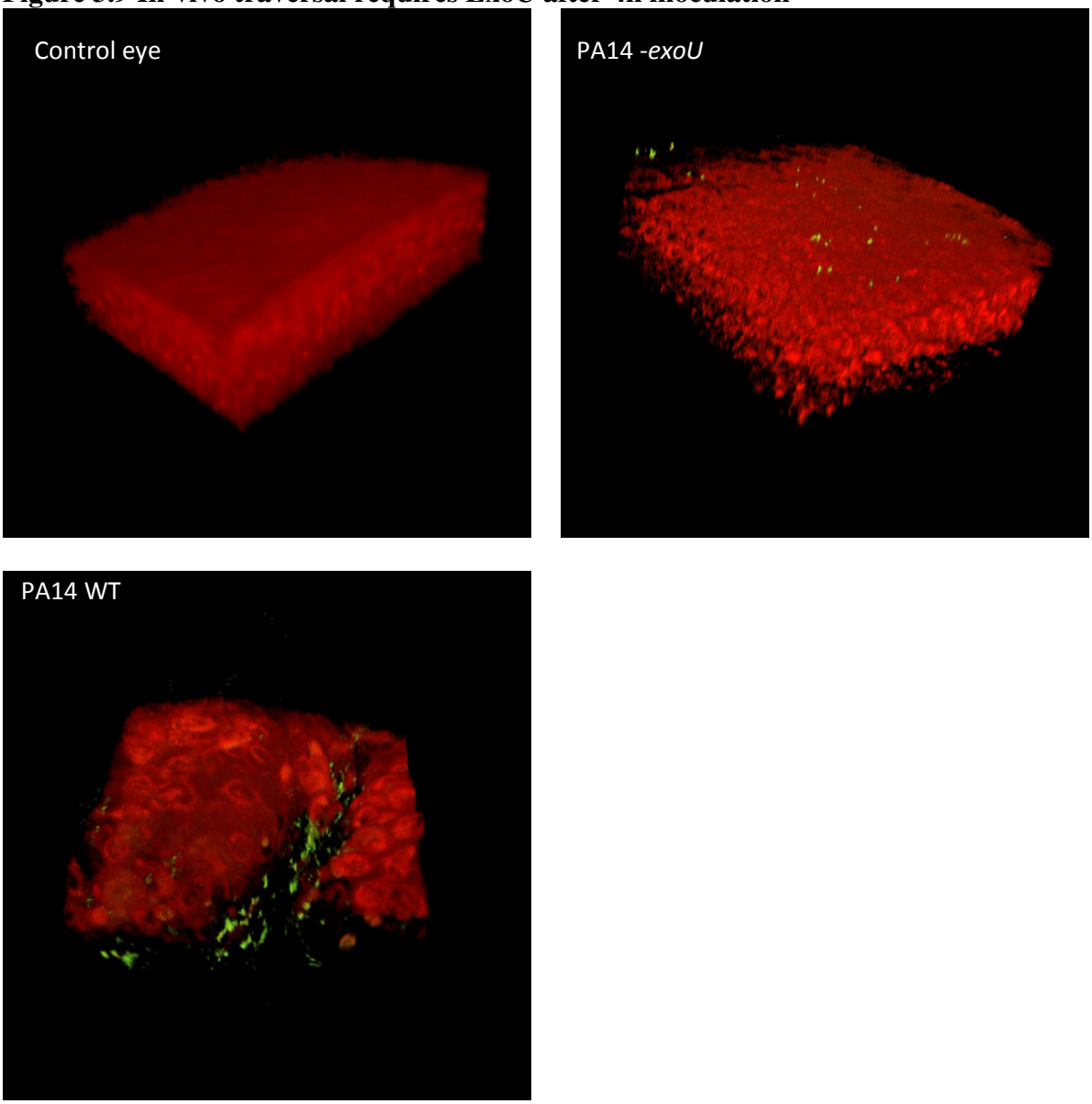

Traversal pictures of the in-vivo eyes treated with PA14 and PA14 ExoU MT show traversal only in WT treated eyes. These data agree with the ex-vivo data for 3h of inoculation, showing that traversal does not occur in a time span under 3 to 4h. (Images collected in collaboration with Julio Ramirez.)

Ex-vivo and in-vivo models of traversal and disease showed similar results. Unfortunately, due to health concerns regarding the mice, we were unable to extend inoculation to further time points. Chapter 5 outlines some further attempts that we pursued in the attempt to look at extended inoculation times.

Discussion

When I first started exploring the involvement of the T3SS in corneal barrier disruption and bacterial traversal of the corneal epithelium, the answers appeared to be straightforward. The level of T3SS expression correlated directly with the amount of corneal epithelial disruption and

traversal of the bacteria (Sullivan, Tam et al. 2015). However, this new evidence brings several factors into play that make the picture much more complex. First, all three of the secreted factors ExoS, ExoT, and ExoY appear to have minimal effect on traversal. Even the absence of the translocon (PopB/D Knockout) did not significantly affect the bacterial traversal and epithelial disruption. However, elimination of the needle through PscC knockouts or the master regulator of the T3SS (ExsA) halted traversal in invasive strain PAO1. These data seem to suggest one of two possibilities: either there may be an unknown effector that is secreted through the needle and does not require translocation for traversal in PAO1, or the T3SS influences regulation of either some additional bacterial virulence system. Considering that, given enough time, the cytotoxic strain PA14 was able to disrupt barrier function and traverse the corneal epithelium, the second option is most likely. This is, of course, unless these strains are utilizing separate methods of traversal.

Another possibility is that there is an unknown effector in PAO1 or an effector-less means of traversal. Identification of the unknown effector is currently ongoing, but there is evidence of a T3SS-independent cytotoxicity that kills cells after approximately 24h (Wu and Jin 2005).

One system shown to be linked with the T3SS is the Type 2 secretion system (T2SS), a simple secretion system to export bacterial proteins into extracellular spaces, which unlike the T3SS contains no needle or translocon. This is an extracellular system secreting several effectors, including several proteases, lipases, phospholipases, and Exotoxin A (Sandkvist 2001). The T3SS has been shown to have regulatory effects on the T2SS proteases (Cowell, Twining et al. 2003) as well as the ability to degrade ExoS. Also, in endothelial traversal the protease LasA from the T2SS has been shown to degrade VE cadherin, allowing *Pseudomonas* to gain access to the basal surface of the endothelium where the T3SS injects its effectors (Golovkine, Faudry et al. 2014).

This evidence showing traversal without T3SS effectors differs from our in-vitro studies done in 2012, but those studies were done with the cytotoxic bacteria PA14. With PA14, the T3SS seems to be involved in traversal only in initial events. It appears that despite the lack of T3SS involvement epithelial barrier disruption at later time points, the T3SS effectors are needed to cause disease later in the eye when exposure is limited to 4h or less. This raises a major concern regarding users of extended-wear contact lenses, as cytotoxic strains are the predominant bacteria found in cases of MK. During pilot experiments, I found that 1h of inoculation of PA14 was enough to cause cloudiness in the eyes of mice (see Appendix). This fact alone underscores the risk of wearing a contaminated contact lens for any length of time.

Contact lens wear is associated with an increase in fluorescein staining, which indicates an ocular surface with minor defects such as those that an object rubbing on the ocular surface or dry eye would cause. In addition, EDTA is a calcium chelator (less specific than EGTA, used in our studies) present in many contact lens solutions. This makes the blotting/EGTA treatment appear more favorable for creating conditions similar to CL-related eye disease. However, PA14, our representative for cytotoxic strains of *Pseudomonas aeruginosa,* showed no difference in either barrier disruption or disease due to blotting/EGTA treatment. PAO1, an invasive strain, has been previously shown to require both EGTA and blotting to allow for traversal (Tam, LeDue et al. 2011). Although these treatments are clearly important in indicating which barriers need to be broken down to allow for disease, they do not seem to be directly related to contact lens wear conditions.

The need for pretreatment does show that additional barriers need to be disrupted to enable invasive strains to cause eye disease. It is possible that correlations between contact lens care solutions with and without a calcium chelator have not been factored into this equation, but it is clear that all the cytotoxic strains need is to be brought into close proximity to allow both barrier disruption and disease. Professor David Evans Touro University, California postulated in his review of CL-related MK (Evans and Fleiszig 2013) that the key relevant features of CL wear are that they allow bacteria both close proximity to the corneal surface and freedom from being washed away by the tear film and blinking. Our in-vivo model provides both these conditions, as the mice under anesthesia do not blink and the bacteria remain on the ocular surface for up to 4h before the mouse is awakened.

The exact contributions of each T3SS effector to traversal remains unclear, but there is evidence of its importance. In invasive strain PAO1 it was correlated with better ability to disrupt and traverse the corneal epithelium, and in cytotoxic PA14 it was negatively correlated with disruption and traversal. Either way, it does play a role in initial stages of infection, but differences in strategies from one strain to another alter what is needed. This could be one reason why the exact nature of the T3SS's involvement is so difficult to discern. Depending on the strain used, not only will there be variations in T3SS production and thus in effectiveness, but also the T3SS may be used in a different manner.

Chapter 4:

Proteases and Their Relationship to Type 3 Secretion System–Mediated Traversal

Chapter 4: Proteases and Their Relationship to Type 3 Secretion System–Mediated Traversal

Introduction

Proteases are well known for their part in bacterial virulence, but their role in initial stages of infection is not well understood. Elastase A, Elastase B, and Protease IV are all part of the type II secretion system (T2SS). They are responsible for a number of virulence effects including enhancing host shedding, destruction of elastin, collagen and complement, and inhibition of immune cell function. Below is a list of the various effects associated with these proteases.(Figure 4.1) Alkaline protease has similar effects on virulence and disruption of the immune system but is secreted by the Type I secretion system (T1SS). (Sandkvist 2001, Hobden 2002, Marquart, Caballero et al. 2005, Leduc, Beaufort et al. 2007, Hoge, Pelzer et al. 2010, Kuang, Hao et al. 2011)

Figure 4.1: Known protease activities

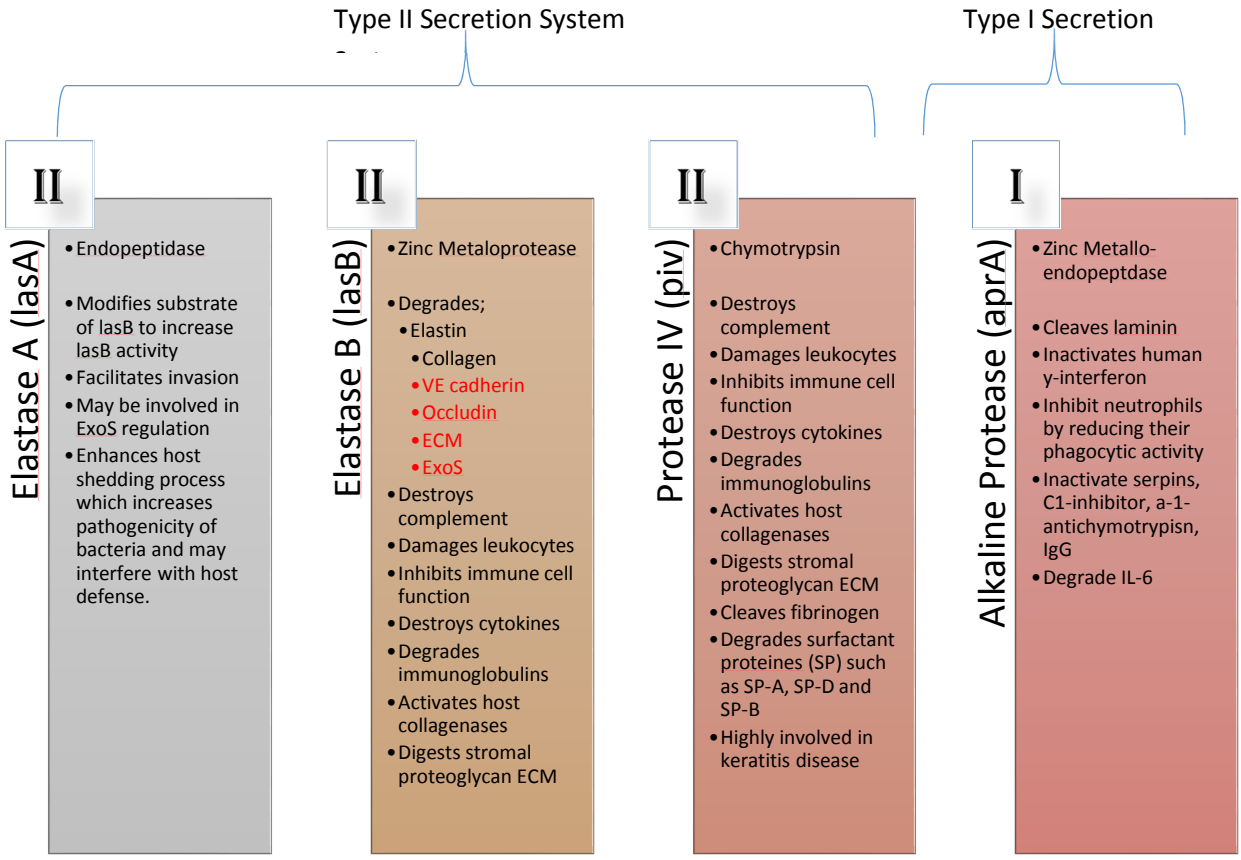

Type II secretion proteases are secreted in a two-step process (Figure 4.2). In brief, the genes are translated within the cytoplasm (CP) and transferred across the inner membrane (IM) through the Sec translocon. In the periplasm (PP), the proteins are folded along with their prepeptides for export across the outer membrane (OM). They are shuttled across the OM via the Xcp transmembrane pore to the extracellular space (EC), where a final cleavage step activates the proteases. In the case of elastase A, this step requires both activated elastase B and protease IV.

Alkaline protease has a similar mechanism through the Type I secretion system. It is important that the proteases are activated only once outside the bacteria. They would cause significant damage to the bacteria if they were activated prematurely.

Figure 4.2 Type II Secretion System

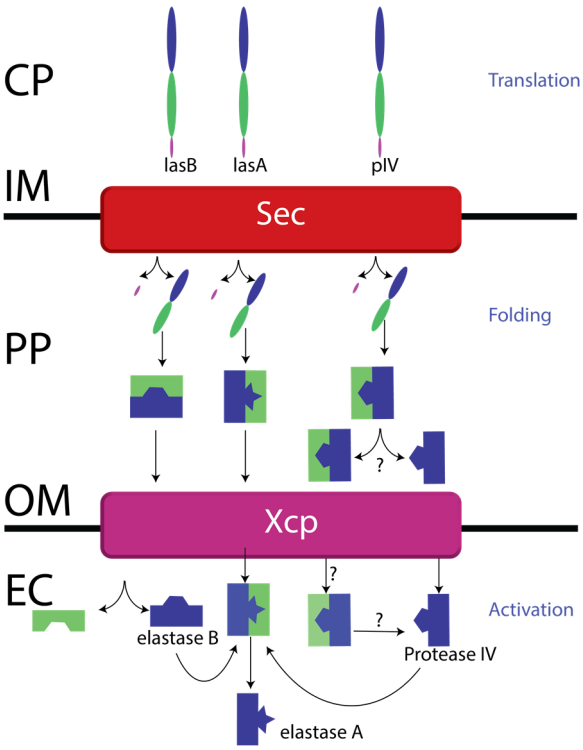

Outside the bacteria, these proteases cause a variety of effects that promote disease, as listed in the above Figure 4.1. In vascular endothelial tissues, LasB has been shown to degrade VE cadherin. This allows bacteria to traverse the endothelium and gives them access to the basal surface of cells for T3SS injection (Golovkine, Faudry et al. 2014). Even though VE cadherin is absent from the cornea, I believe that proteases are still relevant due to the presence of several other cadherins in the cornea. However, LasB has not been shown to be important in the virulence of *Pseudomonas* in the cornea (Hobden 2002).

One of the main reasons for this apparent lack of LasB activity in corneal disease virulence could be the models used. Corneal scratch and interstromal injection are the two most common methods of studying eye disease, because without access to the corneal stroma the bacteria do not cause disease. However, not all diseases start with an injury like the scratch and injection methods model, especially diseases like microbial keratitis. By bypassing the initial stages of infection, studies of disease models can miss vital processes that a pathogen could be using to cause disease. For this reason, our lab has developed several models that we use to study barriers to infection, called null infection models. We believe that using our null infection models will enable us to determine the first stages of diseases that do not require an initial injury or immunodeficiency.

Results

Experiments: To investigate the role of proteases in T3SS-independent traversal.

Several strains of *Pseudomonas* were used in this study. PAO1 is an invasive lab strain of *Pseudomonas aeruginosa* that our lab obtained from three different labs. Each lab provided a matching congenic wild type and several knockouts. The strains are designated PAO1 DF, PAO1 JH, and PAO1 DO. In addition, the invasive strain PAK was used in this study. Table IV indicates the characteristics of each strain type and mutant.

Table IV Bacteria Used for Protease Secretion–Mediated Traversal

Strain Name	Type III Effectors	Proteases	Reference
PAO1 DF WT	STY	LasA, LasB, AprA, pIV	Frank et al. (1994)
PAO1 exsA::Ω	None	LasA, LasB, AprA, pIV	Frank et al. (1994)
PAK	STY (Hyper expressed)	LasA, LasB, AprA, pIV (under expressed)	Frank et al. (1994)
PAO1 JH WT	STY	LasA, LasB, AprA, pIV	Hobden (2002)
PAO1 JH -LasA -	STY	LasB, AprA, pIV	Hobden (2002)
PAO1 JH -LasA,- LasB -	STY	AprA, pIV	Hobden (2002)
PAO1 JH -LasA, -LasB KO +pCOM LasB	STY	LasB, AprA, pIV	Hobden (2002)
PAO1 JH -AprA	STY	LasA, LasB, pIV	Hobden (2002)
PAO1 JH TPM (-LasA, -LasB, -AprA)	STY	pIV	Hobden (2002)
PAO1 DO WT	STY	LasA, LasB, AprA, pIV	Ohman (1995)
PAO1 DO –LasB	STY	LasA, AprA, pIV	Ohman (1995)
PAO1 DO –LasB +LasB	STY	LasA, LasB, AprA, pIV	Ohman (1995)

During our investigation to discover the effects of the T3SS and levels of expression on corneal epithelium traversal, I discovered a unique finding when I applied PAK (a known hyper secretor of the T3SS) to eyes under the EGTA/blotting conditions ex vivo. Despite the fact that these bacteria have a significantly higher level secretion of T3SS effectors when compared to other strains like PAO1, (Colmer and Hamood 2001) the bacteria were unable to traverse the corneal epithelium. This result was unexpected, given that previous studies (Sullivan, Tam et al. 2015) showed that levels of T3SS directly correlated with traversal ability. PAK bacteria when inoculated in the ex-vivo model showed neither epithelial barrier disruption nor traversal through the epithelium, unlike PAO1 WT. PAK's traversal looked identical to that of PAO1*exsA::*Ω.

Figure 4.3: Protease mutants of PAO1 and PAK are unable to traverse the corneal epithelium despite being normal T3SS expression.

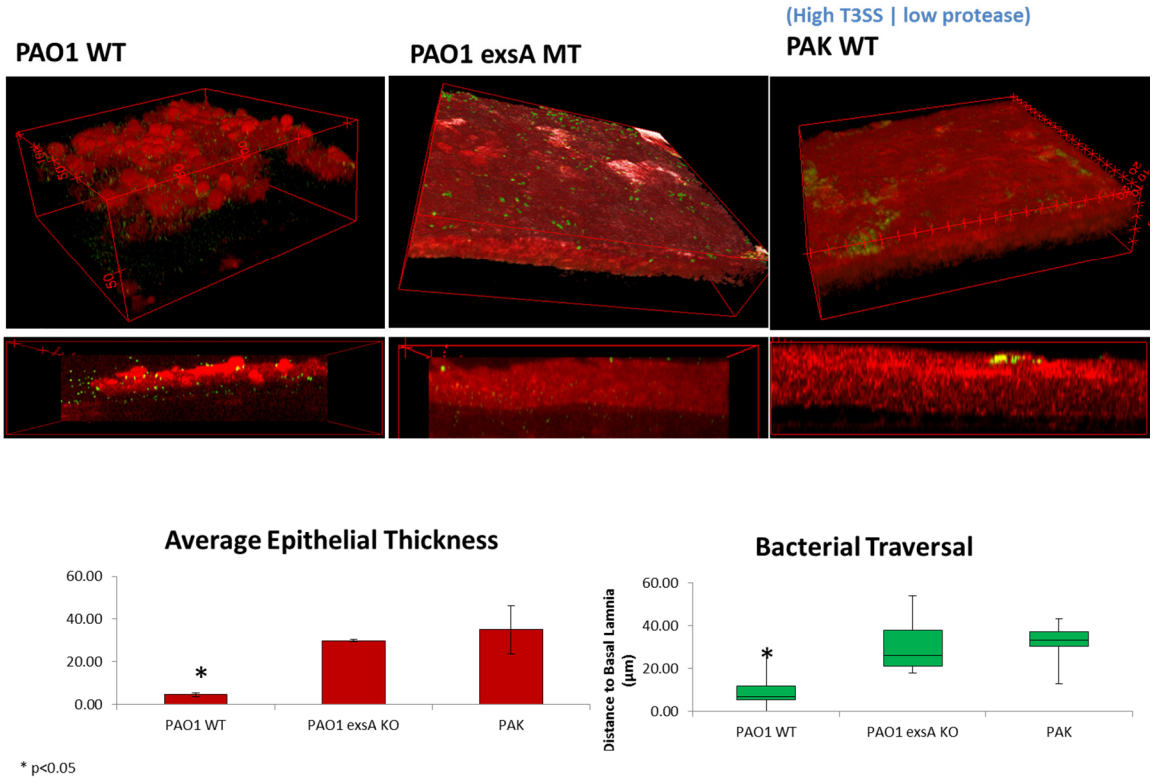

PAK, a hyper secretor of the T3SS effectors, was unable to traverse the corneal epithelium. Corneal epithelial thickness and distance traversed were at the same level as with the T3SS knockout. PAO1 wild type had a statistically significant reduction in corneal epithelium thickness and distance to basal lamina when compared to both PAO1 ExsA mutant and PAK (ANOVA $p < 0.05$).

One of the other hallmark features of PAK bacteria, in addition to their hyper secretion of the T3SS, is their significantly low levels of protease secretion (Soscia, Hachani et al. 2007). Therefore, I decided to investigate the role of proteases on bacterial traversal of the corneal epithelium.

Triple protease knockouts (lacking LasA, LasB, and AprA) were similarly unable to traverse. These triple mutant bacteria had the same lack of traversal characteristics than did PAO1 DF - exsA bacteria. I then proceeded to look at individual knockouts of the proteases. Bacteria lacking LasA had nearly identical statistics to the WT PAO1 JH. However when both LasA and LasB were knocked out, the PAO1 was unable to traverse. A rescue experiment with LasB added back on a pCOM plasmid into the bacteria lacking both LasA and LasB proteases found that these bacteria were not only able to traverse the corneal epithelium, but were so destructive as to obliterate the entire epithelium from the surface of the eye. These results showed that LasB could cause corneal destruction and traversal.

Figure 4.4: Bacteria lacking protease LasA traverse significantly better than do WT or triple protease mutants

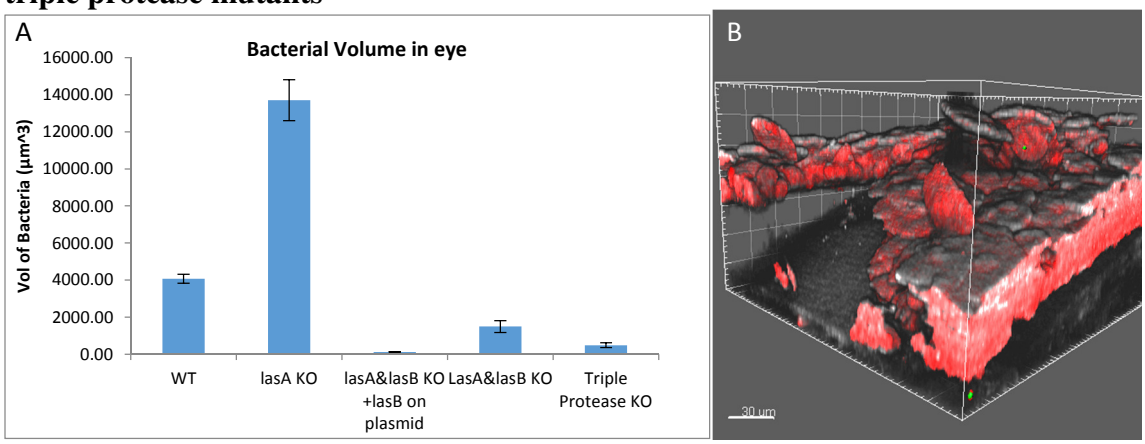

A significantly greater volume of bacteria was found in LasA KO bacteria–treated eyes compared to wild type and all other knockouts. In addition, one can see the peeling epithelium of LasA KO–treated eyes. These peeling sections contain a great many bacteria and could be responsible for the lack of bacteria found in the rescue bacteria (LasA & LasB KO + LasB on plasmid) There is a notable reduction in bacteria in both LasA & LasB KO and triple protease knockouts when compared to wild type.

Previous research shows that there may be a coregulatory effect with the protease knockouts that is related to T3SS expression (Cowell, Twining et al. 2003). Real-time PCR under inducing conditions shows no significant difference between the protease knockouts and their matched congenic controls. Although there appears to be a trend in expression differences between two different PAO1 sources (PAO1 JH and PAO1 DF), the difference was not significant (ANOVA $p > 0.05$). Relative expression is compared to non-induced PAO1 JH wild type.

Figure 4.5: LasB required for traversal

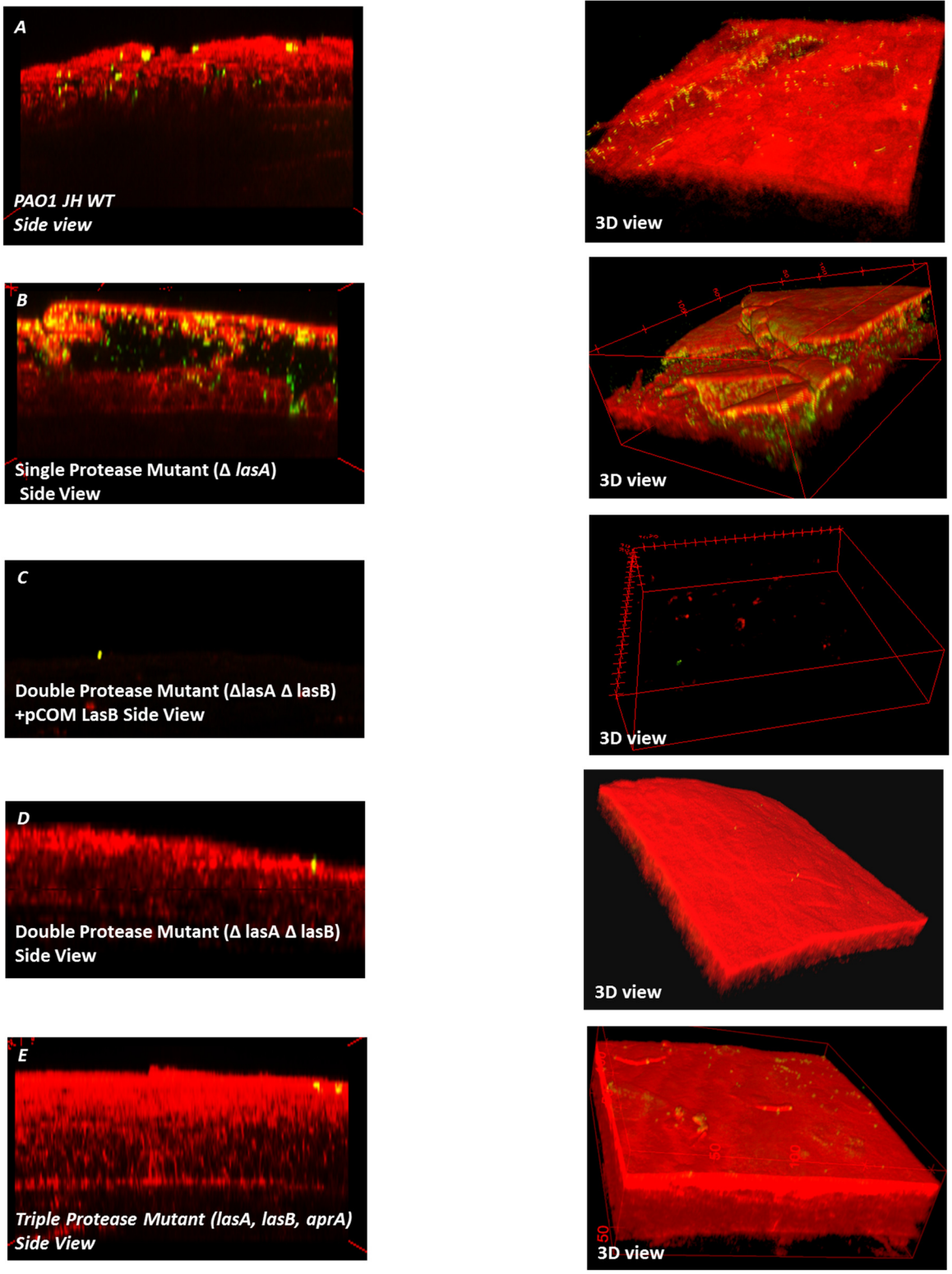

Figure 4.5 (continued)

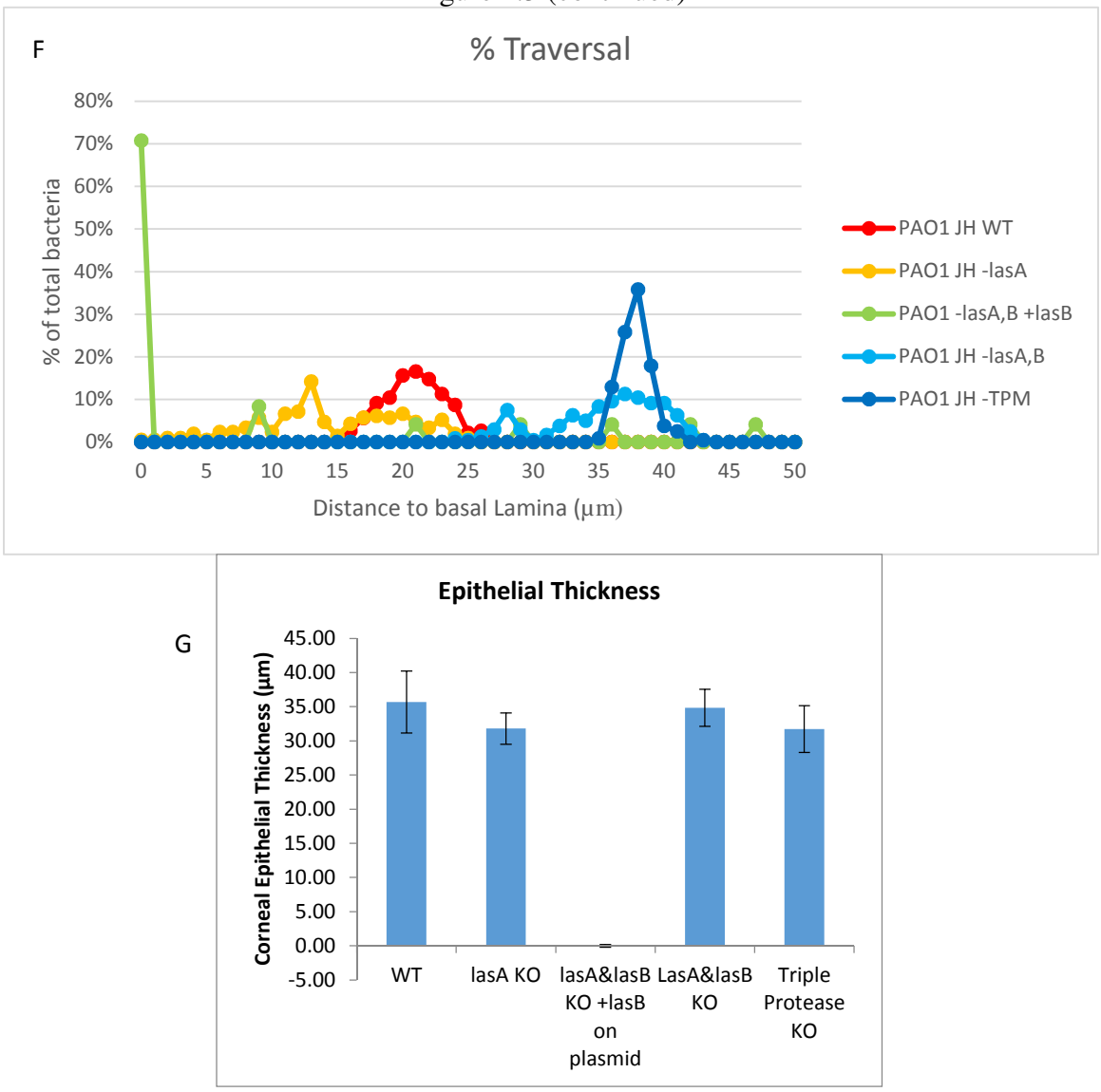

Traversal is reduced when LasB is knocked out of bacteria, as a rescue experiment with LasB on a plasmid confirms. A-E are representative images of bacterial traversal in protease mutants. F shows traversal depths of the protease MTs and their WT parent. Epithelial thicknesses (G) remained the same in all but the samples with LasB added back on a plasmid (ANOVA $p < 0.05$).

The PAO1 single protease mutant (LasA) caused significantly more epithelial damage than its isogenic wild type, although they traversed in similar patterns and had similar epithelial thicknesses. This was due to a peeling of the corneal epithelium caused by LasA KO bacteria. Figure 4.5 shows the peeling effect seen in LasA KO bacteria treated eyes; note the separation between layers of epithelial cells (B). In addition, the number of bacteria increased significantly when compared to WT (A). The epithelium was absent in the LasA & LasB KO, with the rescue plasmid containing LasB (C). Both the double and triple protease mutants (D, E) showed no epithelium loss, and the bacteria appeared to be on the surface. Measurements of the percentage of traversal [Distance from apical surface/(distance to apical surface + distance to basal surface)] showed that most of the bacteria remained within the upper 5% of the epithelium in both the LasA & LasB and triple protease knockouts. The WT, LasA KO, and LasA & LasB KO + LasB

all have significant numbers of bacteria at least 50% through the epithelium. These data suggest that LasB is needed for traversal. Epithelial thickness was reduced in the LasA & LasB KO + LasB on plasmid-inoculated eyes only (ANOVA $p < 0.05$).

Volumetric data (Figure 4.5 A) of bacteria in each of the mutants show that LasA KOs were found in the greatest quantity where LasA & LasB KO + LasB on a plasmid had the least number of bacteria. I believe that the reduction in bacteria seen in the LasA & LasB KO + LasB is due to the tissue destruction caused by these bacteria. When the epithelium is seen lifting off the surface of the cornea, bacteria are carried away with the removed epithelium. As shown in the LasA KO image, most of the bacteria are contained within epithelial layers and significant amounts are removed while the epithelium exfoliates.

Figure 4.6 T3SS regulation remains unchanged in protease knockouts.

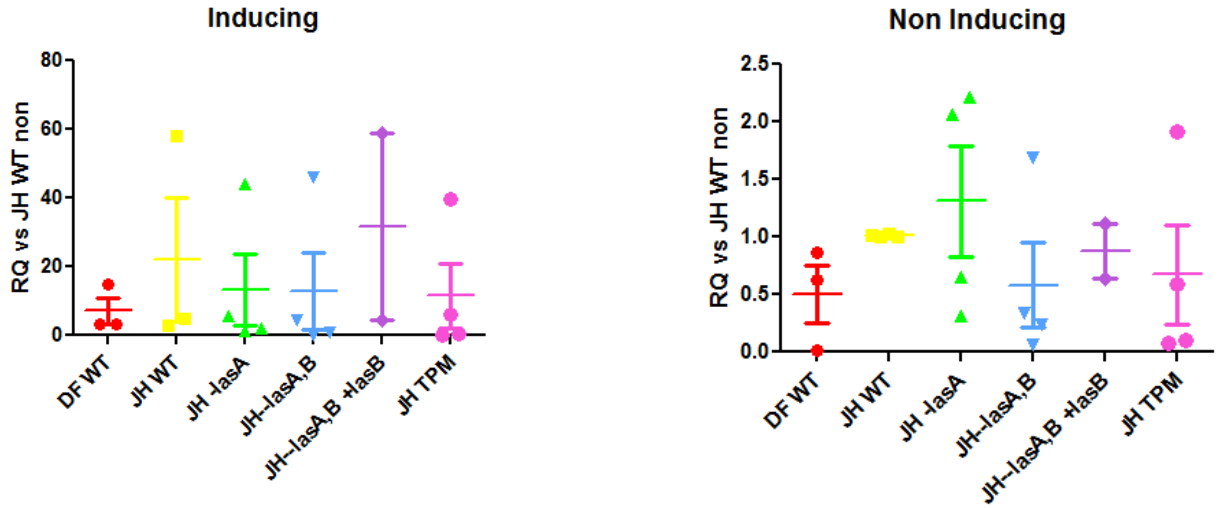

Bacteria were cultured overnight and then 100 µL was inoculated into 10mL of TSB media. The TSB media either contained calcium chelators and other agents known to induce the T3SS (Victoria's paper), or was non-inducing (TSB only). After 3h bacteria were spun at 8000g for 5 min to settle bacteria and collect bacteria for PCR. Real-time PCR showed no change in T3SS expression. The expression had a trend of being slightly lower than that of the WT PAO1, but the differences were not statistically significant (Mann-Whitney).

Discussion

One of the most challenging aspects of categorizing the activity of proteases like elastase is that they are nonspecific enzymes. They have multiple targets, so it is difficult to identify, in a particular situation, their effect on a disease process. Las B's photolytic activity works by hydrolyzing internal peptide bonds of proteins and peptides on the amino side of hydrophobic residue, with phenylalanine as the preferred residue in position P1′ (Maeda and Morihara 1995, Kessler, Safrin et al. 1998). The sequence specificity shows that the substrate carbobenzoxy-Gly-X-NH2 is most susceptible to digestion when X is an aromatic or bulky amino acid residue such as Phe, Leu or Tyr (Galloway 1991). *Pseudomonas* LasB shows less specificity than pancreatic elastase but a more complete breakdown of elastin (Saulnier, Curtil et al. 1989). I believe that this factor, along with the limitations in standard models of infection, explains why their role is so poorly understood. Their role in the initiation of disease, however, is beginning to

become clearer as better models are being developed. VE cadherin degradation by LasB has been shown to precede T3SS injection to the basal surface of the vascular endothelium (Golovkine, Faudry et al. 2014). Similarly, I found that, like the T3SS in corneal epithelial barrier disruption and traversal, LasB is a key component in bacterial success. Quite possibly a similar relationship exists in the cornea to this synergistic relationship in endothelial tissue.

Because the removal of either LasB or the T3SS halts corneal barrier disruption and traversal in invasive strains of *Pseudomonas*, it is most likely that both processes must occur together to breach this barrier to infection. The exact nature of their relationship is still not well understood, but several possibilities exist. The most obvious one is that bypassing the corneal epithelial barrier is a multistage process. LasB has already been shown to disrupt connections between cells, and this would allow bacteria access to lower depths where the T3SS is more effective (Fleiszig, Evans et al. 1997, Bucior, Mostov et al. 2010). Another possibility is the existence of a co-regulatory element between the T3SS and LasB of the T2SS. There is already evidence of this, (Twining, Kirschner et al. 1993) but real-time PCR did not corroborate that LasB has an effect on the T3SS; however, regulation taking place in the opposite direction is still possible. Both systems are induced by the same quorum-sensing cascade (PQS), so the effect may be upstream of the production of proteases LasA and LasB. In any case, it is certain that barrier disruption and traversal involve multiple systems, some of which may be either redundant or complementary.

One curious observation in this study occurred when LasA was knocked out in our traversal model. The increased amount of tissue damage in the LasA KO is difficult to explain. LasA has been shown to enhance the activity of LasB (Cowell, Twining et al. 2003). When LasA is translated into Elastase A, the final step is a cleavage of the product exported by XCP across the outer membrane. Both Protease IV and Elastase B (the final product of LasB) work together to activate Elastase A (Hobden 2002). It is possible that because LasB isn't being occupied in cleaving LasA into its final product, it has greater enzymatic activity, thus allowing the LasA mutant to be more virulent. Another possibility is that the organization of the corneal epithelium is layered and that each layer has a different organization of junctional proteins. At the apical surface, most of the junctions are tight junctions; in the middle there are few tight junctions and adherens junctions make up the majority of junctions seen between cells. At the basal layers, desmosomes are the predominant junction. It is possible that without LasA aiding LasB activity, the lower junctions are more difficult for LasB alone to degrade; thus more peeling is found and these pockets form where the bacteria are found.

Given that LasB appears to be such an important factor in initial stages of disease, and that LasB has already been shown to be an initiation step in effective delivery by the T3SS, this may be an even better target than the current attempts to generate anti T3SS vaccines (Coburn, Sekirov et al. 2007). By preventing bacteria presenting the T2SS and eliminating those that are secreting these proteases, we would be able to stop the barrier disruption needed to cause disease. Not only would this make T3SS-mediated disease difficult, but also, by protecting the barriers to infection, we would prevent the host from losing these barriers and becoming more susceptible to other infections.

Still, the connection between the T3SS and LasB is not well understood. It is important to determine whether these two systems are working together. Since knocking out either system halts this process, it is clear that both are needed in some fashion, but it is unclear whether that

connection is directly connection to each system's regulation. With the growing need for combatting antibiotic-resistant strains, targeting the machinery of infection is our best bet for preventing death and disease caused by these highly adaptive bacteria. By doing so, we will be able to create a future in which antibiotics—which are truly a limited approach, as they don't discriminate between beneficial and pathogenic bacteria—are used less often in favor of a more precise and directed approach to preventing bacteria pathogenicity.

Chapter 5:

Corneal epithelial traversal models

Quantification Method Development for position of bacteria within a degraded epithelial tissue

Null Infection Models

The Ocular Microbiome

Chapter 5: Corneal epithelial traversal models

Quantitation method development for position of bacteria within a degraded epithelial tissue.

Figure 5.1: PSF

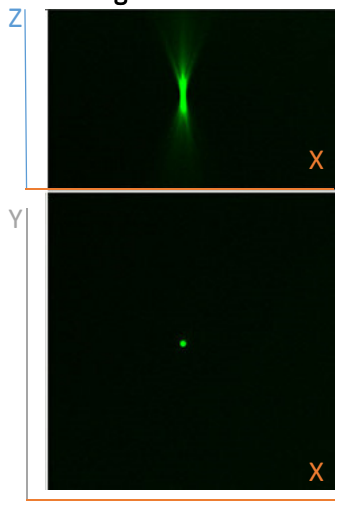

In this chapter, I will discuss the difficulties involved in quantification of 3D microscope images of bacteria traversing a degraded epithelial surface and the challenges of accurately quantifying the location and number of bacteria. I will discuss how image defects affect 3D reconstruction to define the borders of the epithelium, how to use machine learning accurately to count irregularly shaped bacteria, how to measure distances from an irregular surface to a bacterium, and how to quantify traversal between two irregular surfaces.

Microscope imaging technology has advanced rapidly in the past years. One of the difficulties entailed in these advances is how to use the imaging data quantitatively. The field, which lends itself beautifully to qualitative images, has such a dynamic environment that turning these images into data that can be assessed statistically is very difficult. The fault lies partially in how the images are overloaded with information, including position, color (from fluorophore[1]), luminance, and orientation, all of which can vary significantly from image to image if not properly controlled.

For my project, a series of images at different elevation was taken through the cornea to enable 3D reconstruction of the eye. These images will be used for analysis of bacterial penetration and traversal of the corneal epithelium, and to look at corneal epithelium health during such an event. These image sets are termed Z-stacks, with Z representing the depth direction on an XYZ-coordinate system. The first decision and potential area for difficulty is setting the Z height for each image. The further apart the images are, the faster the images can be taken, but the greater the lack of data between images is. A big lack of data leads to a blur in the Z direction of every image. However, if Z-stacks are taken too close together, time exposure to laser light used to excite fluorophore will cause photo bleaching and the image will no longer be visible. The ideal step size for maximum resolution of an image is equal to half the maximum resolution in the Z direction of a microscope. Anything above or below this amount will not improve image quality and may degrade it. However, maximum Z resolution isn't always the goal when speed is of greater need. In these cases, a step size at least equal to maximum Z resolution is recommended. This should double acquisition speed while still keeping resolution within an acceptable range. Further step size increases can be utilized if further speed increases cannot be accomplished in any other way. Our maximum Z resolution is 1.8 microns therefore, one micron Z direction step size were used for imaging mouse corneas.

The second difficulty is light scattering. Fluorophores are used to visualize certain structures and bacteria in fluorescence microscopy. However, the fluorescently tagged objects are in a complex environment, which can scatter emitted light as the light from the fluorophore crosses the various

[1] A fluorophore is a fluorescent molecule that can absorb light at a lower wavelength and then glows with a color at a higher wavelength than what was absorbed. Fluorophores are used as markers that bind to a particular type of tissue or protein of interest. Green fluorescent protein (GFP) is a common fluorophore that excites (absorbs) 488nm (blue) light and then emits (glows) at 510nm (green) light.

layers of the cornea before being detected by the imaging system. This scattering is called a point spread function (a mathematical *function* that expresses how a *point* of light is *spread* out when it passes through various surfaces). This will make the light from the fluorophore appear in planes beyond its physical location. This result is partially caused by the fact that excitation light is also scattered before reaching the fluorophore. The scattering means that the light is disrupted while it is traveling to the fluorophore from the microscope's lasers and then disrupted again when it is traveling back to the microscope camera or detector. This is best described when looking at a point spread function of refractive error of a point of light. Figure 5.1 shows an object located in the center (bottom), but the light emitted by a fluorescent bead fans out in an irregular pattern above and below the object's actual location (top). If there were no refractive errors, the light would appear as a point, but we see this pattern because the local environment of the object is not optically perfect. If we were to construct a 3D image from this picture, we would have a stretched object erroneously appearing larger in the Z direction that it truly is. This same sort of pattern is seen when we take a Z-stack down through the cornea.

Correcting for this problem is paramount to accurately addressing object location, but it has another important feature as well. The better the correction for the point spread of the object, the better resolution one can obtain. This will allow us to see bacteria that otherwise would overlap and be impossible to see. Shown to the left Figure 5.2 is a Line Spread Function (LSF), which is the same as a point spread function except that it is located in 2D space. The figure shows how blurring can make two objects appear as a single object. This potential problem can be corrected by a process known as deconvolution. There are two different approaches to deconvolution; the first involves measuring fluorescent beads in the imaging system used to calculate a psf, and the second entails estimating computational models of the refractive indexes of all the materials in the sample. Either of these methods allows the amount of blurring to be calculated for the image and then removed. This improves resolution of the image (especially along the Z-axis) and increases our accuracy in identifying small objects.

Figure 5.2: Line spread function

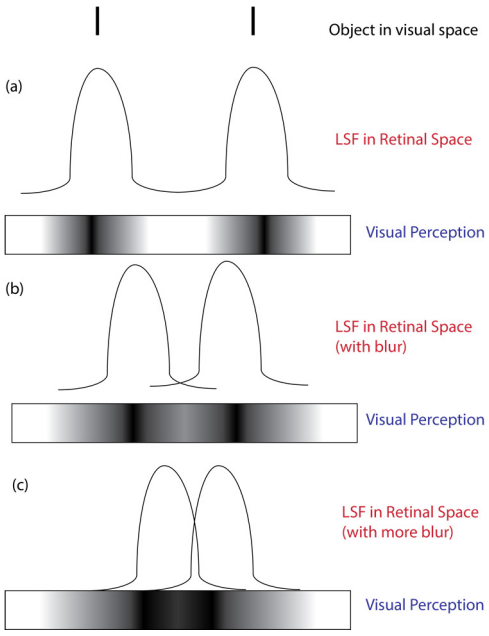

After we have cleaned up the image by applying deconvolution, the next step is to start separating the color channels of the image for quantification. In figure 5.3, MatLab code was applied to separate the red, green, and blue channels of an image of bacteria invading cells on a coverslip. In the image to the left, the green channel illuminated the bacteria, the blue auto-fluorescence of the epithelial cells. The red channel contained no data in this experiment. However, the color channels can vary depending on which fluorophore are used to tag different objects in an image. For my research, bacteria are almost always green.

Figure 5.3 Color separation for analysis.

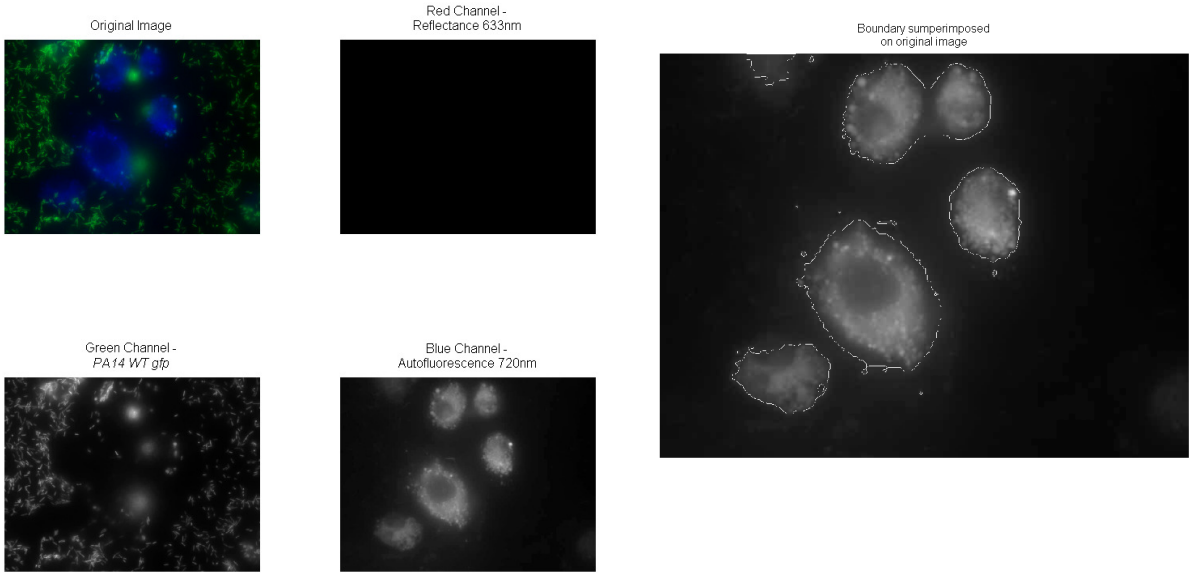

Sobel edge detection was used to compute cell borders from the blue channel data. Sobel edge detection is a mathematical model used to detect edges of objects in digital photographs. The Sobel operator is based on the following filters:

$$L_x = \begin{bmatrix} -1 & 0 & +1 \\ -2 & 0 & +2 \\ -1 & 0 & +1 \end{bmatrix} \times L \; and \; L_y = \begin{bmatrix} -1 & 0 & +1 \\ -2 & 0 & +2 \\ -1 & 0 & +1 \end{bmatrix} \times L$$

Given such estimates of first- order derivatives, the gradient magnitude is then computed as:

$$|\nabla L| = \sqrt{L_x^2 + L_y^2}$$

While the gradient orientation can be estimated as:

$$\theta = atan2(L_y, L_x)$$

(Wikipedia 2015)

Figure 5.4: 2D example of isolating bacteria inside tissue for identification.

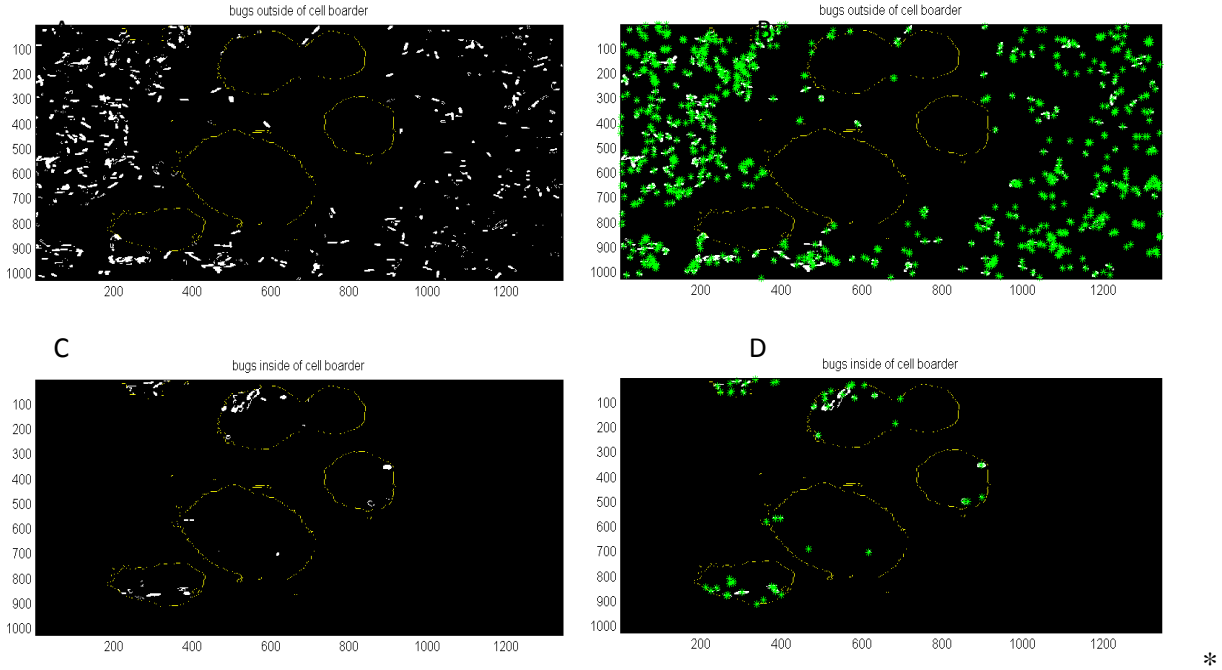

*

Indicates individual bacteria counted

This was used to create a mask that can be applied to the other channels to identify what bacteria from each channel are inside or outside the epithelial cells identified by the blue channel. This information was then used to create two new images from the overlay of this mask upon the green channel, as shown bottom panels of Figure 5.4 A and C.

With the identification of which bacteria were inside (Figure 5.4 D) and outside (Figure 5.4 B) the epithelium, we can now begin to analyze the quantity and location of the bacteria. When taken to three dimensions, this method can identify bacteria within tissue layers as opposed to those floating above the tissue. The green asterisk indicates the bacteria counted.

However, upon closer examination we can see that overlapping bacteria are counted as a single unit instead of as multiple bacteria. This problem has two causes. First, Sobel edge detection did not discern the shape of the object that it was counting. This worked well for cells, which did not touch, but for bacteria that are overlapping each other it is a rather large problem. Since I wished to count individual bacterium, this method would not work.

Figure 5.5: Cell profiler machine learning counting algorithm

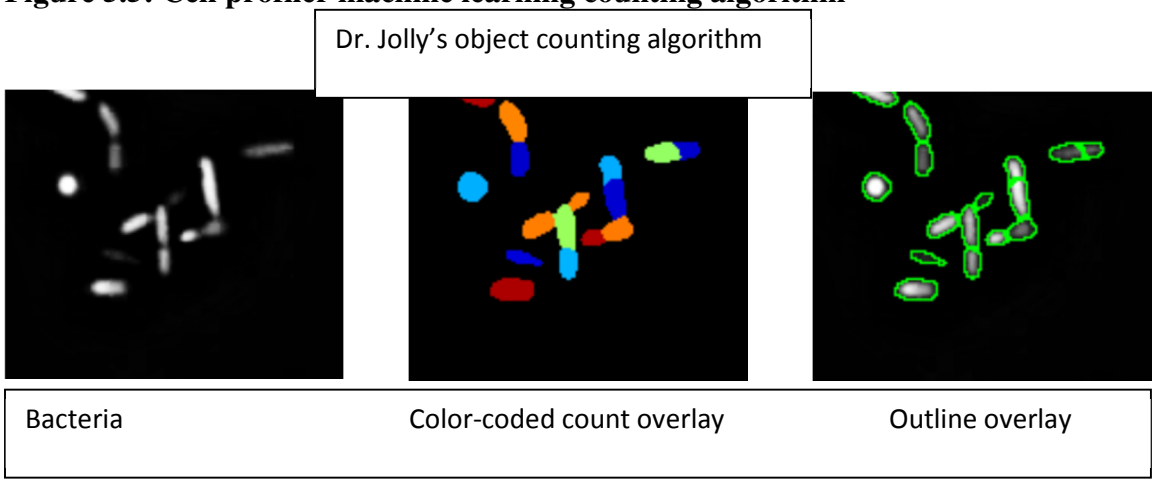

The solution to this problem came from Dr. Amber Jolly. She had been working on an algorithm in CellProfiler, a microscope imaging and quantification software. By using a self-learning algorithm, she was able to input multiple parameters for the code to identify vesicles within cells regardless of their ever-changing shape and luminance. As shown in Figure 5.5, the luminance of the bacteria has a large degree of variance, and Dr. Jolly's algorithm corrects for this beautifully.

Null infection models of eye disease

The eye is remarkable in its ability to resist infection. Most of what is known about eye infections has been learned through studies of eye disease using models that bypass the corneal epithelial barrier. Three main methods are employed for this purpose: corneal scratch, substromal injection, and chemical burn. Newer models have been developed to study initial stages of disease that do not allow bacteria direct access to the corneal stroma. The first is the scratch-and-heal model (Lee, Evans et al. 2003), which allows the corneal to heal for six hours after a substromal scratch the epithelium knits back in place. This leaves epithelium covering the entire cornea, but the junctions are not fully reformed and disease is possible. Another method established by this lab (The Fleiszig Lab) is the blotting/EGTA treatment method (Tam, LeDue et al. 2011). In this method, bacteria are able to adhere to the corneal surface and traverse. ZO-1 staining confirmed that junctions were weakened as their staining became less punctate in nature and more diffused. When tested with 1-micron beads, the barrier remained able to prevent their penetration through the layers of the cornea. However fluorescein staining revealed that small molecules were now able to penetrate the entire cornea past the epithelium and into the stroma. These models still require some junctional destabilization of the corneal epithelium with synthetic means, but currently they are the only models of interaction between an intact epithelium and bacteria during the initial stages of disease.

A new method of corneal susceptibility was discovered during an attempt to extend the length of time that ocular tissue would survive outside the host. DMEM +5% FBS has been shown to keep tissue cultures of the eye alive for an extended amount of time (Engelsberg and Ghosh 2011). In our ex-vivo model, we were able to keep the eye alive for at least 48h using this method. Propidium iodide staining confirmed that the amount of corneal epithelial cell death remained the same as when the eye was newly excised. Tissue culture media allows for longer survival of corneal epithelium, but also permits increased traversal.

Figure 5.6: PI staining with 24 and 48h

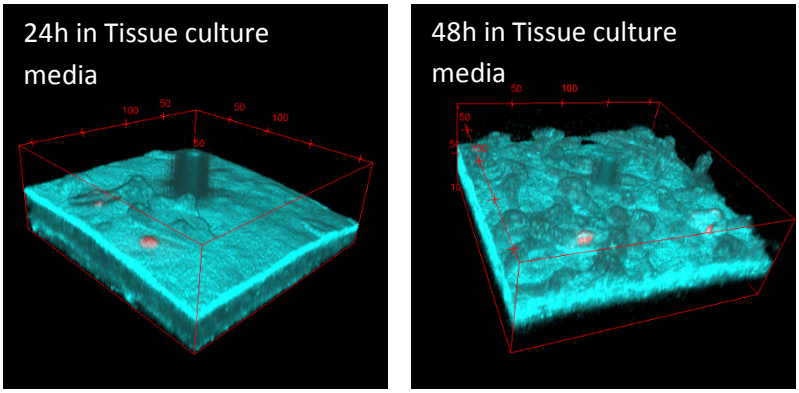

Propidium iodide staining shows minimal cell death in the corneal epithelium after 24 and 48h.

Figure 5.7: Bead experiments

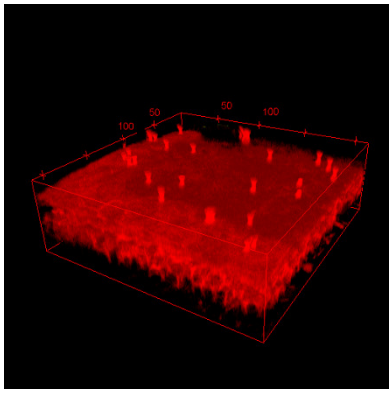

Fluorescently labeled beads were added to an ex-vivo eye to determine if passive processes could allow for traversal of the corneal epithelium. This was done to ensure if the corneal epithelial barrier remained intact for objects of the same size as bacteria. After 6h the beads were unable to traverse, showing that the barrier function remained intact for objects larger than one micron.

When we used this model to study T3SS-dependent traversal, we discovered that wild type bacteria previously unable to traverse (PAO1 AR), as well as T3SS KOs, were both able to traverse in a T3SS-independent manner (Figure 5.7). Time course studies showed a rapid effect allowing for traversal as early as 3h after inoculation. These data point to a disruption of the barrier function of the corneal epithelium, which differs from the blotting/EGTA method previously described because these eyes are susceptible to traversal in a T3SS-independent manner. The exact nature of their vulnerability is still unknown, but it is possible that since the epithelial surface is normally exposed to air or tears, exposure to factors in serum, a component seen only in tissue that has been vascularized, causes some signaling that yields a less effective barrier. Indeed, when in-vitro models are established, they must be "airlifted" or exposed to open air for a week before multilayers form. When this situation is considered in terms of the normal epithelial organization, it seems a likely cause. The epithelium junctional organization differs between the layers of the corneal epithelium; the top layers have extensive tight junctional complexes while the middle layers contain a greater number of adherens junctions and the basal layers contain mostly desmosomes and anchoring junctions.

Figure 5.8: Type III independent bacterial traversal

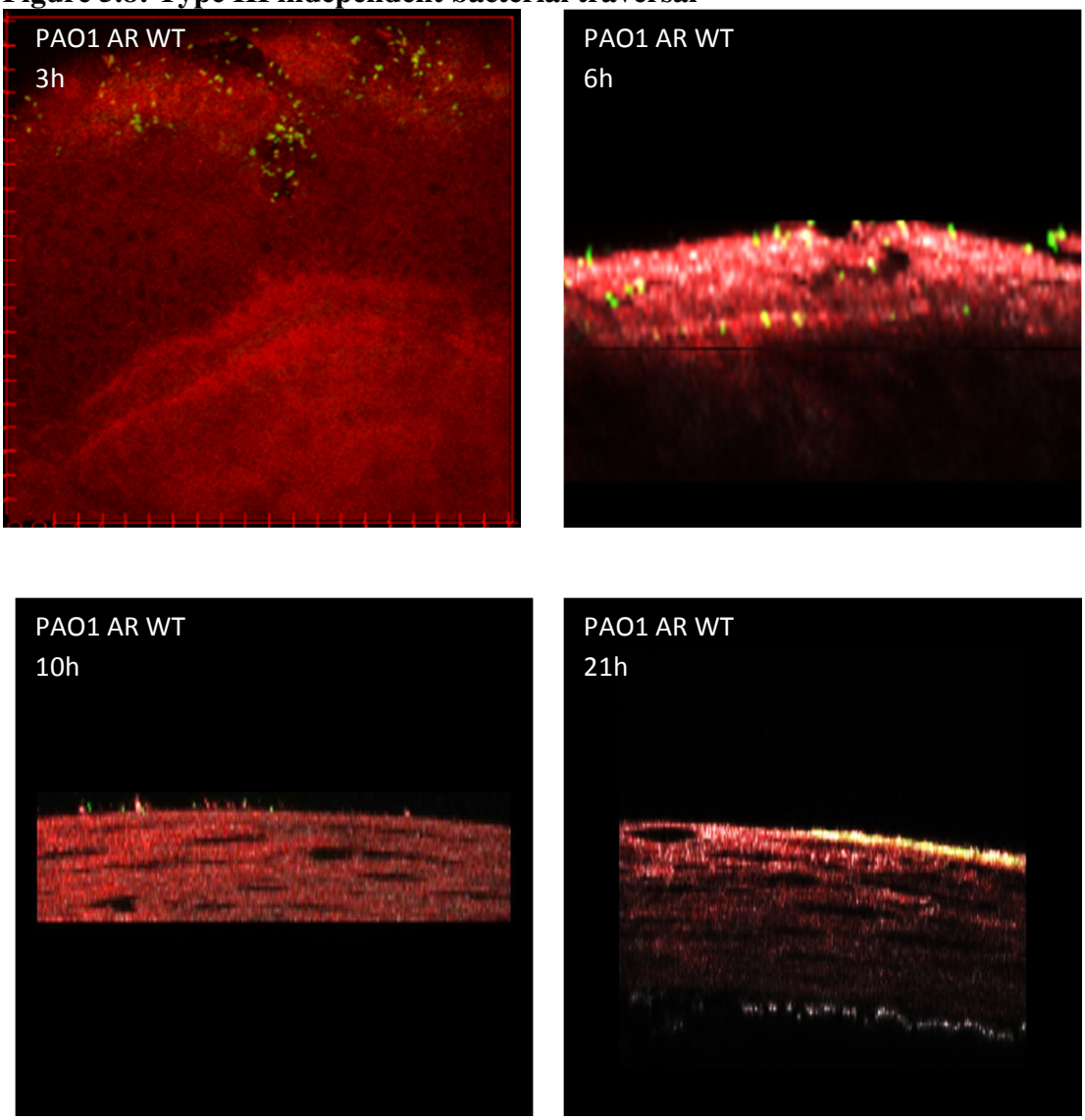

PAO1 AR was unable to traverse the corneal epithelium in the blotting/EGTA model, but when this bacteria was used in the tissue culture method we say traversal as early as 3h. Note that the 3h image is taken at a different angle than the rest of the images. An image taken at the same angle was not available for the 3h time point. Also in the 10h and 21h images the epithelium is completely absent. When the epithelium is absent the stroma is seen as very bright fibers in the red (reflectance) channel which is different than the cuboid epithelium visible on the surface when the epithelium is present. This issue can be corrected for by using auto-fluorescence to identify the epithelium instead of reflectance.

The other model used in for looking at initial stages of traversal is by the use of a MyD88 KO mouse. This mouse is susceptible to traversal without blotting and EGTA treating however bacteria are able to traverse in a T3SS independent manner.

Figure 5.9: MyD88 KO mice have T3SS independent epithelial barrier disruption

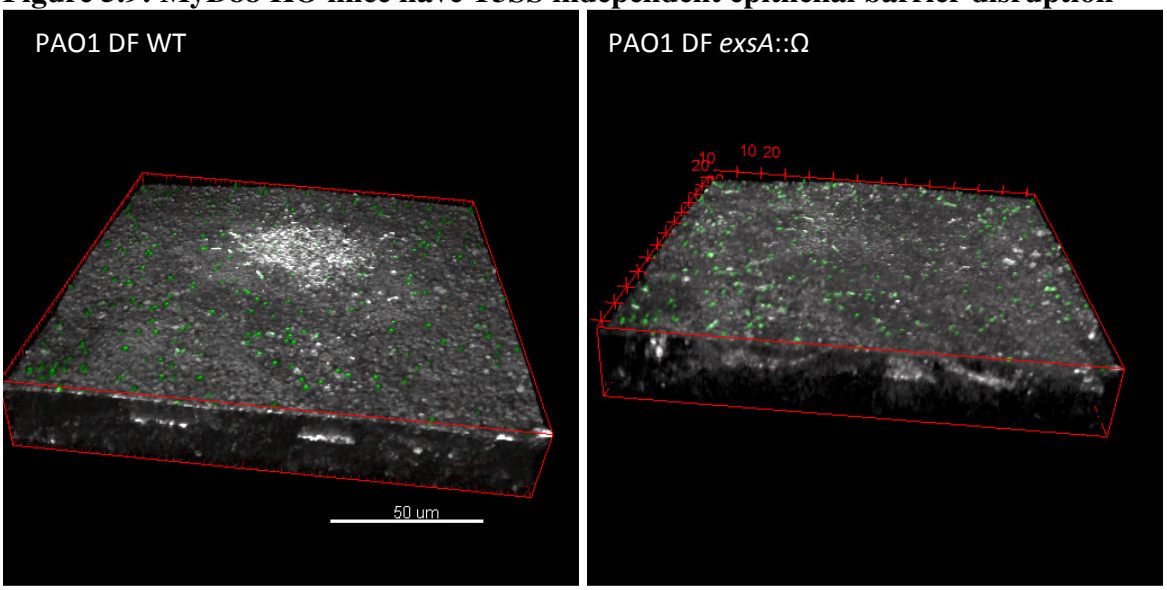

Ex-vivo inoculation of eyes with WT and bacteria lacking ExsA are both able to traverse and destroy the corneal epithelium when they are applied to the eye of a MyD88 KO mouse.

MyD88 KO traversal has led to several TLR as well as IL-1R KO mice being tested for their susceptibility to traversal. However this work is being done by another in the Fleiszig lab and won't be discussed here.

The last model is contact lens wear susceptibility to infection. In this study contact lenses specially fit for mice were incubated with bacteria to create a biofilm before they were applied to a sleeping mouse for 4h. The contact lens was removed prior to waking the mouse and the mouse eye was scored for disease 24h and 48h post infection (p.i.).

Figure 5.10: Contact lenses solution Control

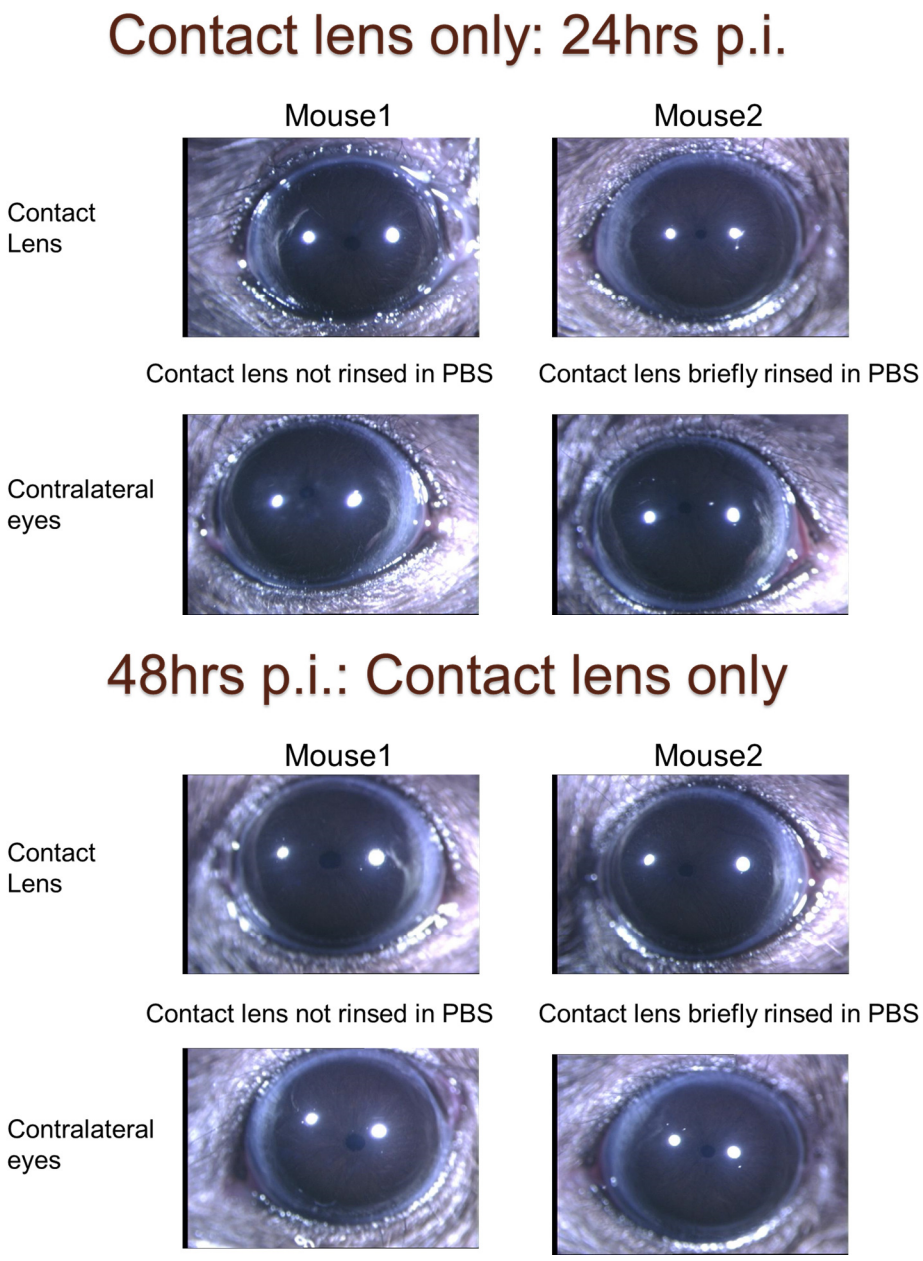

Contact lenses were fitted to mice eyes for 4h either being first pre-rinsed with sterile PBS or unrinsed from the storage solution provided by the contact lens manufacturer. All eyes showed no irregularities after being placed in the eyes of mice 24h and 48h later.

PA14 WT were allowed to create a biofilm over the course of a week before the contact lenses were put in the eye of C57 b/6 mice. For the safety of the mouse only one eye had a contact lens place within.

Figure 5.11. Contact lens solution effects virulence of bacterial biofilm**.**

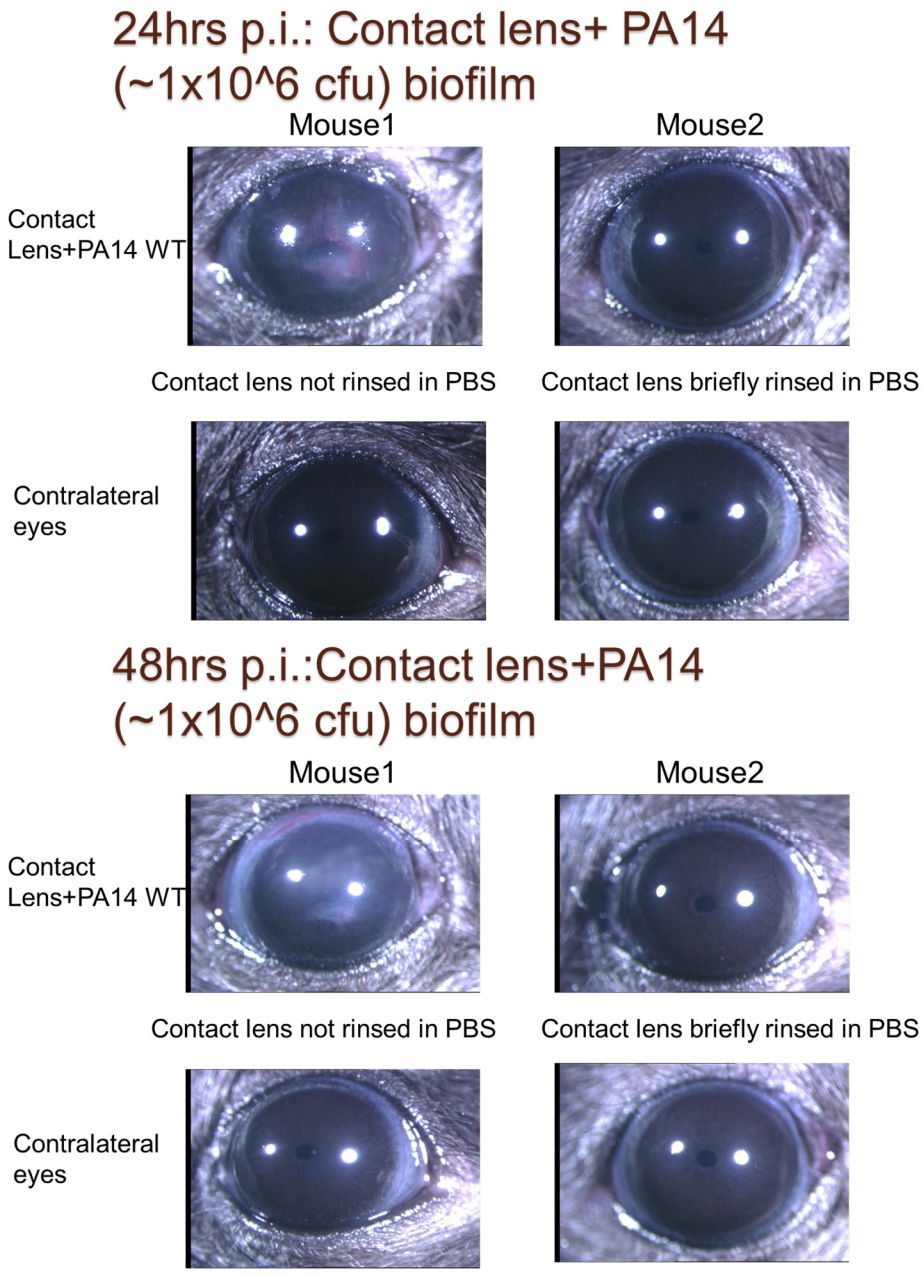

Biofilms of 10^6 cfu/mL were grown on the anterior surface of contact lenses either pre-rinsed in PBS or un-rinsed from the contact lens storage solution. The contact lenses which were un-rinsed showed microbial keratitis in the eyes with the biofilm. Lenses which were pre-rinsed in PBS showed no sign of disease.

When we observed the eyes 24h and 28h p.i. only the contact lenses which were not rinsed prior to biofilm formation caused eye disease. The PBS rinsed lenses were soaked in PBS overnight to ensure that all chemicals which are part of the storage solution have ample time to diffuse from the contact lens. It is unclear what part of the CL solution interacted with the bacteria to make a more virulent biofilm, but it was clear that the storage solution was responsible for a change in bacterial behavior.

The natural environment of the eye: Is there a microbiome on the ocular surface?
The ocular surface has long been believed to be a microbe-free site. This is because microbes are rarely found in the eye, and when they are discovered it is usually in connection with disease or contamination from the skin flora falling into the eye. However, prior research used standard culturing methods, which select for microbes that grow in normoxic (normal levels of oxygen) conditions and at 37°C (normal body temperature). These techniques do not account for what are referred to as "non-culturables," or bacteria that have more specialized requirements for growth and do not grow under normal oxygen and temperature conditions. A new technique has been established in recent years for finding microbiota within any growth condition utilizing DNA analysis. BRISK, or biome representational in silico karyotyping (Muthappan, Lee et al. 2011), was developed from metagenomic characterization methods to sample total genome samples from mixed populations and thereby identify individual microbes within microbiomes. Recent microbiome analysis of the ocular surface has provided evidence that there may indeed be a microbiome in the eye (Zhou, Holland et al. 2014). These studies focused on the conjunctiva but do show the distinct differences between the epithelial surface of the cornea and the mucosal tissue of the conjunctiva.

However, the flora discovered in these studies are similar to contamination that could come from the skin flora surrounding the eye. In addition, these DNA-based studies do not verify whether the microbes found are alive or dead. This is a crucial but difficult distinction that needs to be addressed. The current microbiome analysis method is so incredibly sensitive that free DNA contaminations could contribute to the discovery of organisms. In this study I use a combination of techniques to verify the presence of live bacteria within the ocular surface. In addition, I separate the ocular surface into two distinct zones, the conjunctiva and the corneal surfaces. These surfaces cover the entire ocular surface from the tips of the eyelids all the way across the cornea.

These two surfaces have distinct characteristics both physically and immunologically. The conjunctiva is a mucosal membrane spanning the area from the eyelid margin, looping around the orbital socket, and attaching to the limbal region of the sclera (the white part of the eye). It has normal immune function and secretes mucins, which are a major component of tears. The cornea is the transparent membrane across the front of the eye, covering the area from the limbal region of the sclera across the pupil. This site is a smooth epithelial surface able to withstand the tremendous shear stress of blinking and is phagocytic in nature, or able to consume and dispose of bacterial invaders (Niederkorn, Peeler et al. 1989, Cowell, Chen et al. 2000). It is unique in that it is one of three immune-privileged sites in the body and the only one exposed to the outside environment. Inflammation and immune responses are repressed in the cornea to prevent destabilization of the cornea, which would cause optical impurities and blindness.

Three experiments were devised to assist in the study of the microbiome of the eye: (1) the use of FDA-approved diagnostic dyes in the eye, to evaluate if they can be used to stain bacteria in a clinical setting; (2) bacterial clearance animal models, to establish whether bacteria can remain within the eye; and (3) impression cytology and ocular washes in human subjects, to determine whether any bacteria can be found alive within the ocular surface.

FDA-approved dye staining is to be used on bacteria alone and within the eyes of an animal model to assess the accuracy of using these approved dyes in a clinical setting to determine eye health and to confirm if commensal microbes are normally present. Some of these dyes

(fluorescein in particular) are already known to stain bacteria such as *P. aeruginosa* (Augustin, Heimer et al. 2011). In this study, I tested the ability of fluorescein as well as rose bengal and lissamine green to stain common gram-negative and gram-positive bacteria believed to be within the microbiome of the eye.

Bacterial clearance of gram-negative *P. aeruginosa* has already been established in the cornea (Mun, Tam et al. 2009), but gram-positive bacteria's clearance of the conjunctiva has not been tested. Using *S. aureus* as an example of gram-positive bacteria (and one that was identified in microbiome analysis) along with *P. aeruginosa*, I explored both corneal and conjunctival clearance.

In the third and last experiment, I took corneal eye washes from subjects and used multiple culture techniques to determine if any detectable microbes were living on the ocular surface. The techniques use agar plates of various composition as well as anaerobic and aerobic conditions to allow for culturing of and extended range of microbes beyond what standard lab practices can show. The reasoning behind this is that some of the bacteria found are listed as "nonculturable." But this statement means only that the standard methods don't yield microbial colonies. All bacteria by definition can be grown if one provides the correct conditions. I chose nutrients and environmental conditions that simulate the extremes within the eye to determine if any microbes could be cultured given the limitations of the eye environment. These conditions should be able to culture most of the microbes identified as part of the ocular microbiome, although they do not cover every possible condition.

Results

Table V: Bacterial staining with FDA-approved dyes

Bacteria	% Stained by Rose Bengal	% Stained by Fluorescein	% Stained by Lissamine Green	Gram + /Gram -
P. aeruginosa	58%	50%	0%	-
S. aureus	87%	0%	0%	+
S. epidermidis	81%	0%	0%	+
S. pyogenes	96%	0%	0%	+
S. marsescens	37%	0%	0%	-

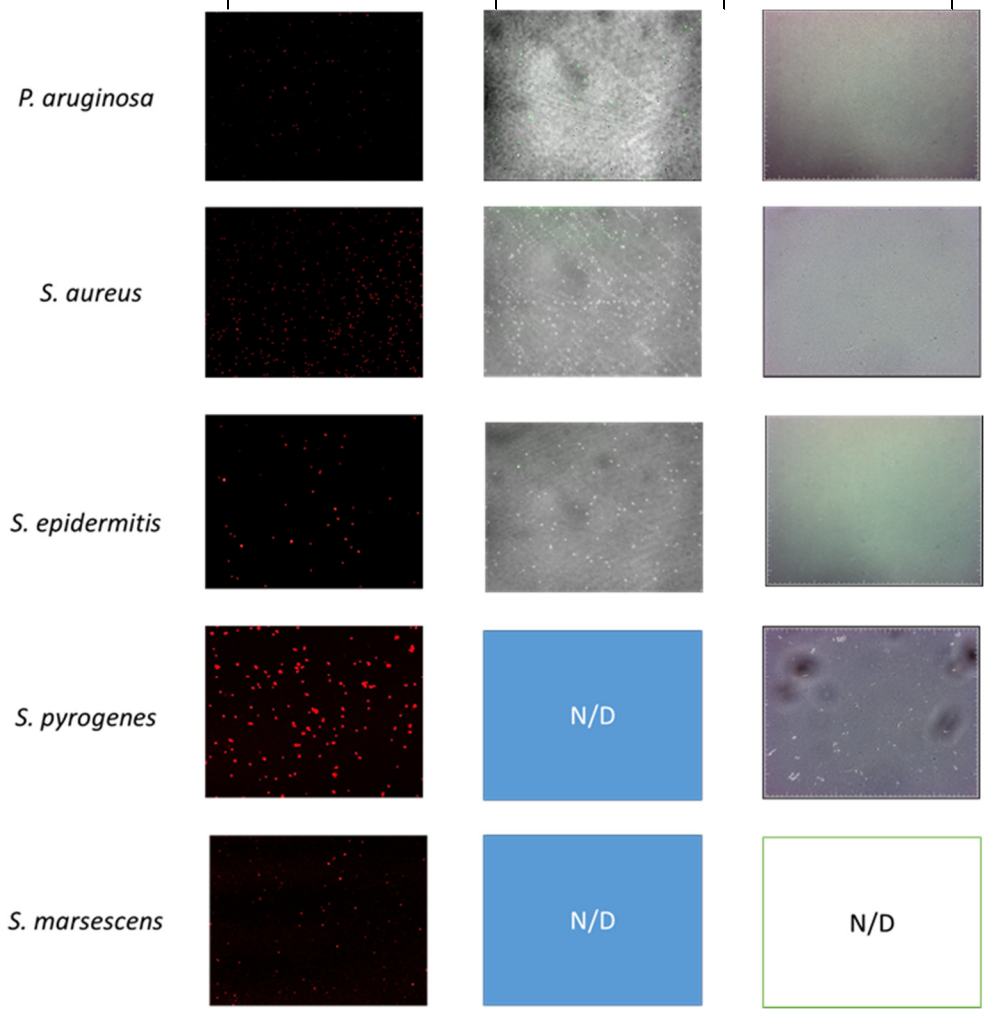

Figure 5.12 Rose Bengal staining in the eye

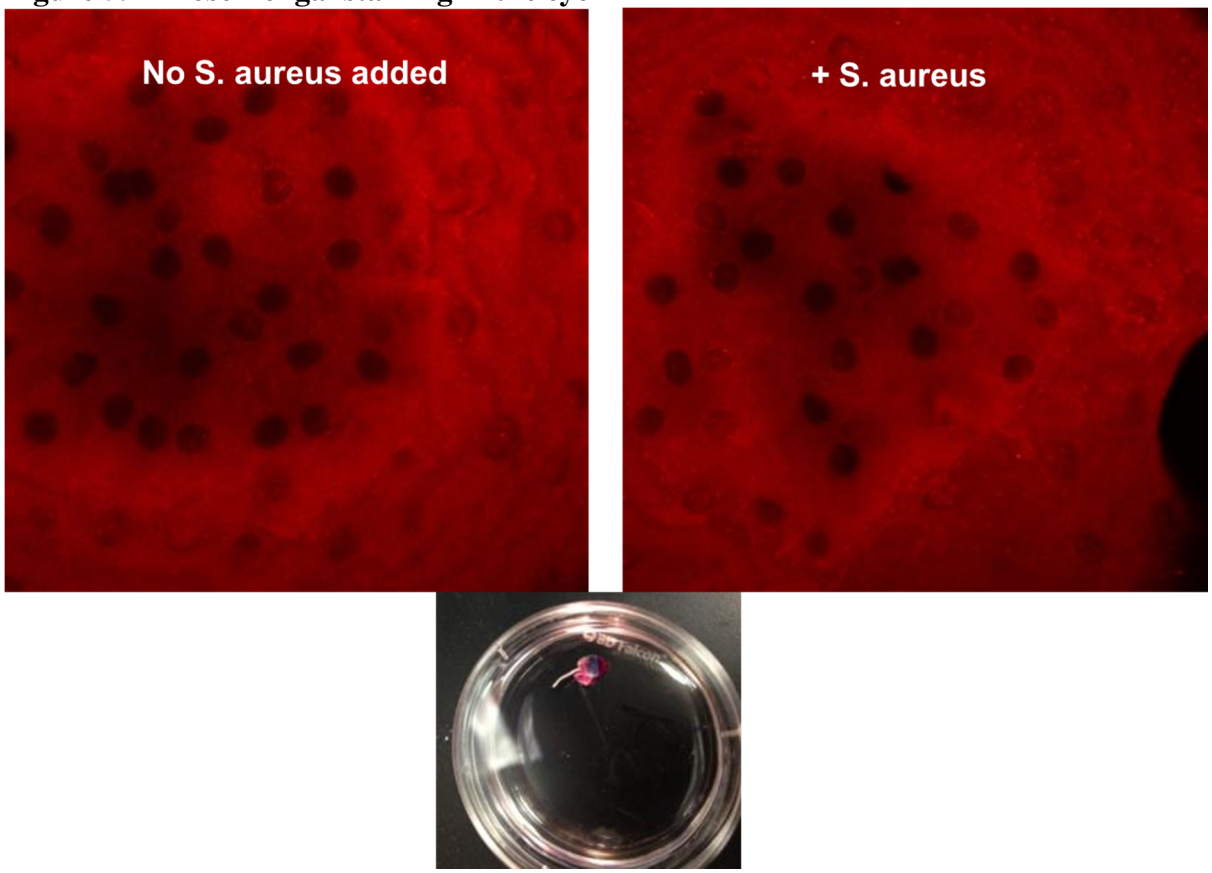

The eye of a mouse treated with 10^6 CFU/mL S. aureus were stained with Rose Bengal for 30 min ex vivo. The eyes were then imaged with an Olympus FV1000 confocal microscope. The staining of the ocular tissue prevented us from identifying bacteria also stained with Rose Bengal.

Three dyes that are FDA-approved for use in the eye were tested on several gram-negative and gram-positive bacteria believed to be part of the ocular surface microbiome. Lissamine green failed to stain any of the bacteria, whereas fluorescein was able to stain only *P. aeruginosa*. Differential interference contrast (DIC) illumination showed that only 50% of the bacteria were positively stained with fluorescein. Rose bengal was very efficient at staining gram-positive bacteria but less so with gram-negative bacteria.

Figure 5.13 Bacterial clearance of the ocular surface

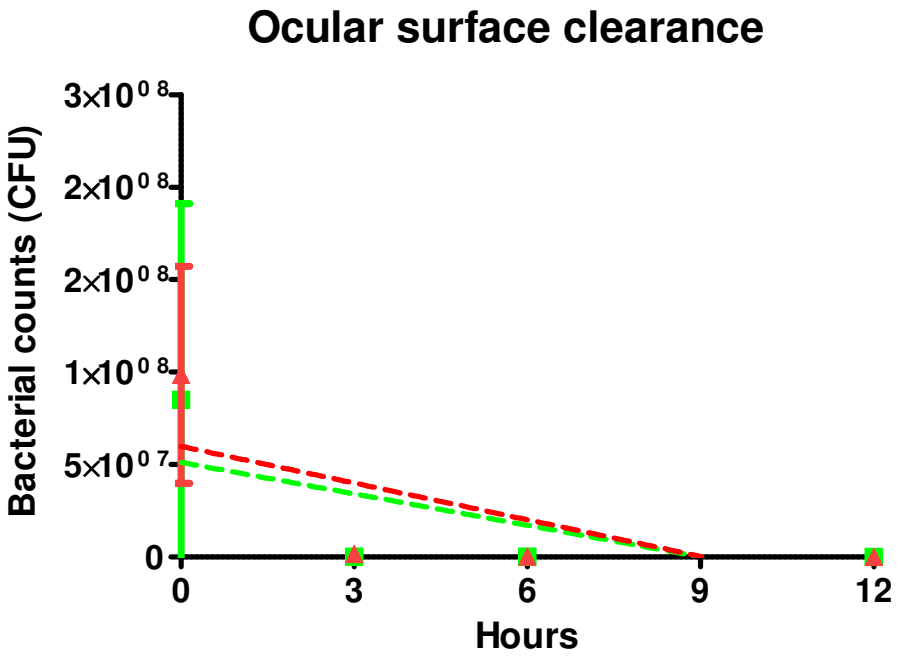

T	% PA remaining	% SA remaining
0		
3	15.75%	43.14%
6	2.13%	31.14%
12	0.0025%	0.0957%
12 (Homog)	0%	0.0229%

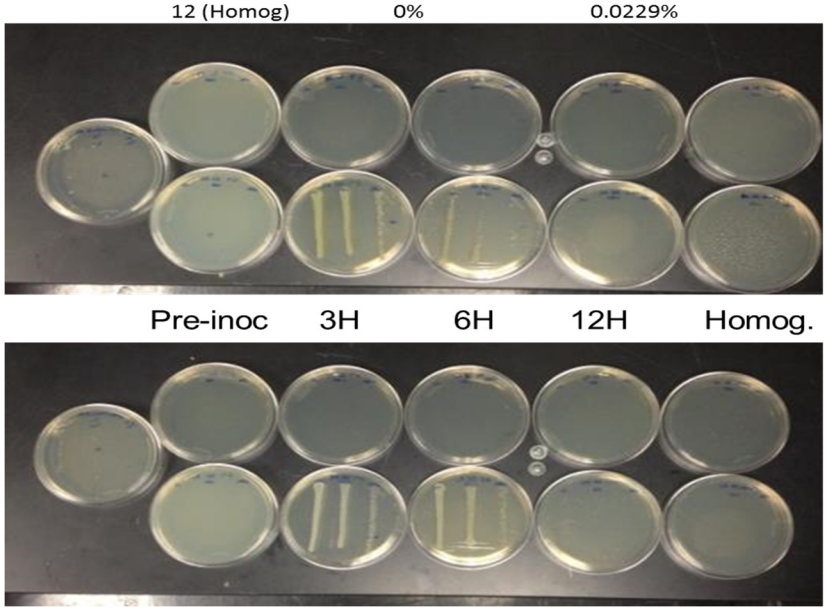

Corneal washes of 10µL were plated at 3h, 6h, and 12h after being given a 1h inoculation of 10^11 CFU/mL of bacteria. Linear regression analysis indicated that the rate of clearance between *S. aureus* and *P. aeruginosa* had both the same slope and Y-intercept.

Bacterial clearance from the ocular surface (cornea) was determined by ocular washing with 20ul of PBS. The bacteria were then serially diluted and platted on TSA agar for counting of colony forming units (CFUs). Both *S. aureus* and *P. aeruginosa* cleared from the eye rapidly. After 12

hours, 99.98% of the bacteria were cleared. *S. aureus* showed slightly more bacteria and a slower clearance, but the difference in clearance rates was not statistically significant ($p = 0.86$). When the corneas were ground after 12h, no bacteria were found within the cornea of animals treated with either *P. aeruginosa*, but some were found in the *S. aureus*-treated eyes.

Figure 5.14 Bacterial clearance of the conjunctiva of the eye

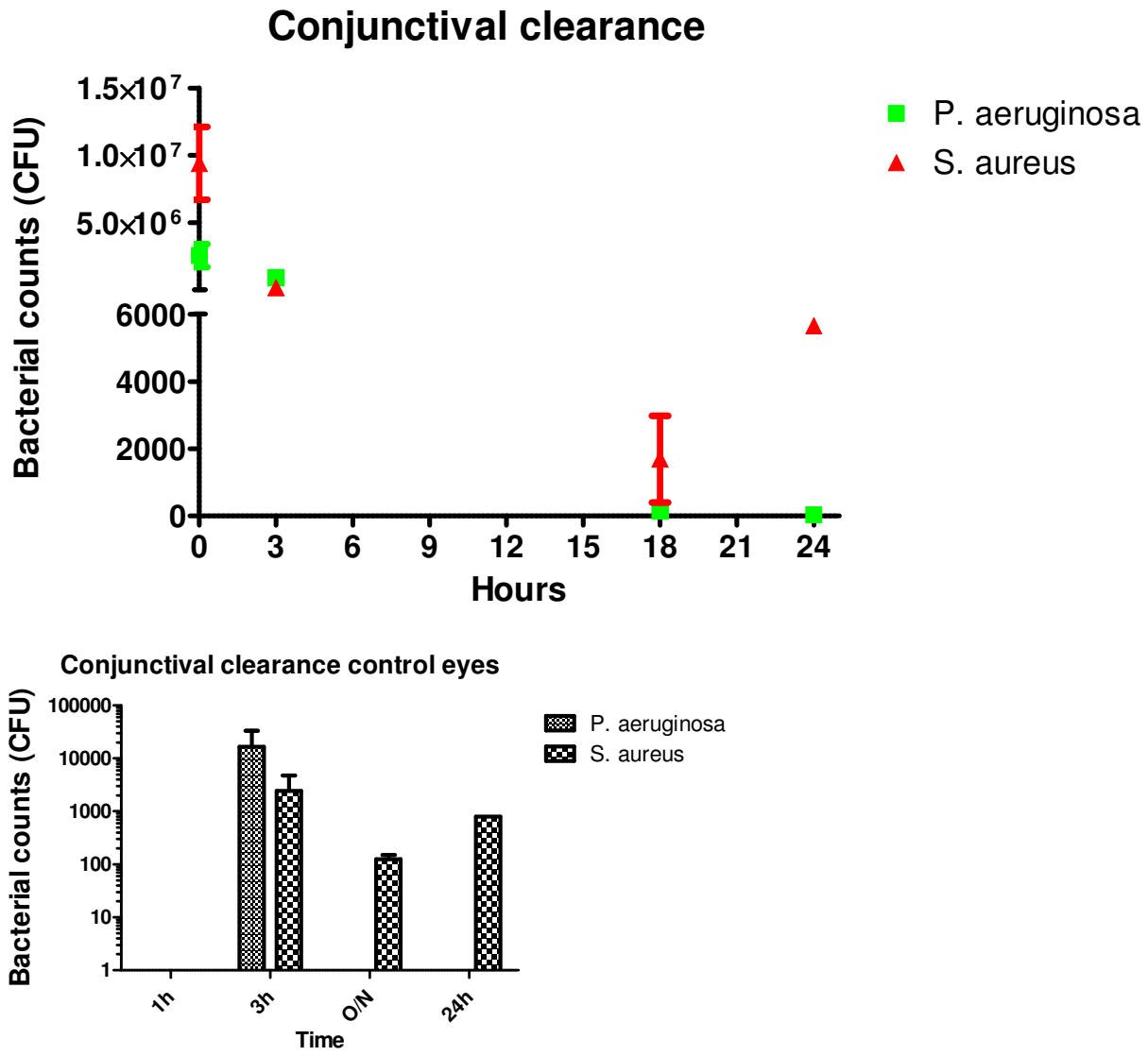

Clearance of the conjunctiva appears be the same rate as that of the cornea. The difference between conjunctival clearances had a trend towards slower *S. aureus* clearance, but it was not statistically significant ($p = 0.07$). ANOVA analysis showed that only the difference in 1h conjunctival clearance between PAO1 and *S. aureus* was statistically significant ($p < 0.01$). The 24h conjunctival clearance was unfortunately based on only a single sample, because the mouse for the experiment died before the study could be performed. All other conjunctival data represent at least two data points. Contamination of the control eye appeared to happen more often with S. aureus and occurred only once with *P. aeruginosa.*

Figure 5.15 Culture of eye wash from human subjects

Human subjects had their ocular surface washed using the apparatus depicted below. Sterile saline (1.5-2mL) were rinsed over the eye of the subject and collected in a sterile beaker. The sample was then placed on agar plates in various growth conditions to determine if there were any microbes on the ocular surface. Four subjects had their eyes washed and had their eyewash plated on two independent days. There was one unrepeated fungal growth in a single patient and a hypoxic bacterial growth on chocolate agar on a separate patient which also didn't repeat. Other than these two outliers there were no recovered microbes.

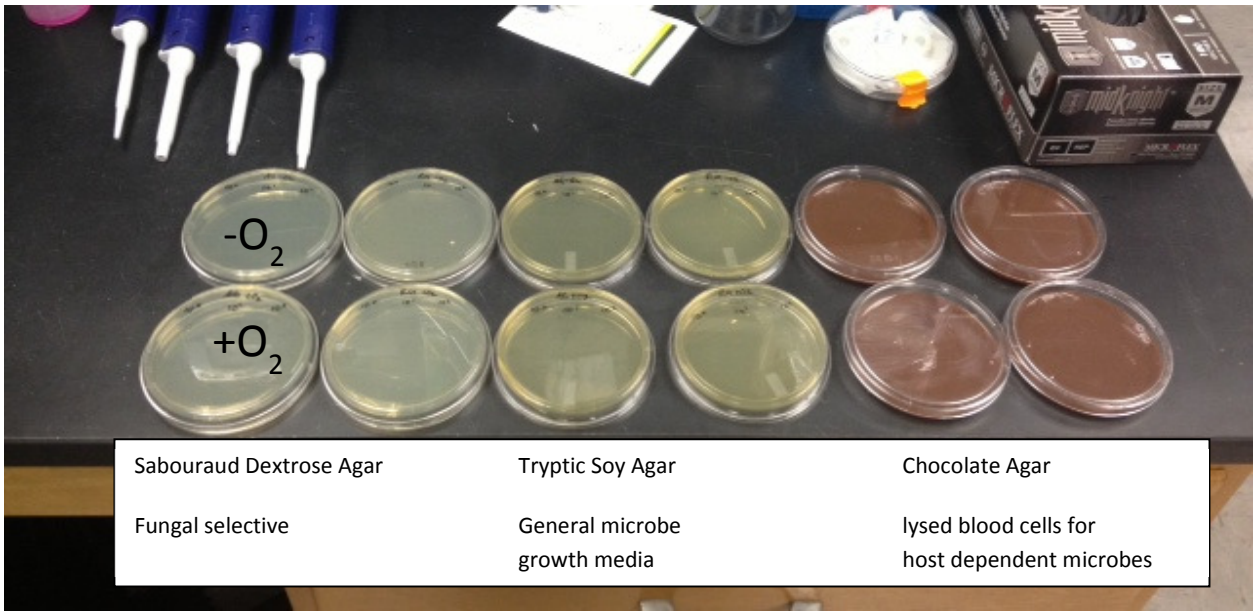

A corneal eyewash designed by Suzanne Fleiszig (Fleiszig and Efron 1992) was used to obtain ocular washes of subjects and to determine if any bacteria could be cultured under nonstandard growth conditions. Four subjects were tested; each subject was tested twice, at least one week apart. Contaminant fungal growth was seen in one subject but was not present in the next eye

wash; another had unknown bacteria growing on chocolate agar under anaerobic conditions in the first wash, but it did not appear after the second wash. With these two exceptions, no growth was detected.

Conclusions and future experiments planned

The first difficulty that I encountered is the most basic of problems: despite all the advances in microscopy and staining, it is still hard to see the bacteria in a human subject. This is in part because there exist few dyes that are safe for administration in the eye, but also because microorganisms have such varied structures that it is difficult to identify them. One of the dyes that worked best for identifying both gram-negative and gram-positive bacteria also stained the corneal tissue. Unfortunately, when this dye was placed in the eye of a mouse infected with bacteria, the staining of the corneal tissue was so great that it was impossible to identify the bacteria on the surface (Figure 5.10). However, I did not test this staining technique in the conjunctiva, from which the most reliable reports of a microbiome's presence have come, so it is possible that this technique could be used there. The stain took a full 30 min to become effective, but the rate at which that the stain fades has not been tested using either bacteria or the ocular tissue. There could be a difference in dye uptake in which even more sophisticated techniques such as Fluorescence Lifetime Imaging (FLIM) could assist us in the distinction of ocular from microbial cells. All these techniques combined with further advances in ophthalmic microscopy will eventually lead us to the point where we can actually see the microbes in the eye, even if they are transient and not in a commensal relationship. Once we can see the microbes, there will be no doubt as to their presence.

This brings us to the interesting conclusions about gram-positive versus gram-negative bacterial clearance from the ocular surfaces. Both bacteria were implicated as part of the ocular microbiome, so if the data can be believed, then we would expect their ability to remain in the eye to be similar. Ocular surface washes showed bacterial clearance of both *S. aureus* and *P. aeruginosa* at the same rate. However, the conjunctival clearance showed that only *S. aureus* leveled off in the number of bacteria cleared from 14h (overnight) to 24h. Further time points must be established to determine when, if ever, the bacteria are cleared from the conjunctiva. In the cornea and conjunctiva, although *Staphylococcus* was cleared at the same rate as *Pseudomonas,* there appeared to be a slightly larger amount left in the endpoint samples. The evidence that clearance appeared to halt in the conjunctiva is the strongest evidence to date that the existence of an ocular microbiome is possible, but further repeats need to be performed before these results can be tested for statistical significance. However, it is still a concern that these bacteria, which are easy to culture in standard lab settings, are not readily cultured from human subjects.

Indeed, when we attempted to culture the microbiome from several human subjects using both standard and nonstandard conditions, I were unable to obtain any reproducible data concerning regular colonies of the types of microbes found via the microbiome DNA analysis methods. Currently, the Fleiszig lab is pursuing conjunctival samples to determine if perhaps the two ocular surfaces, the conjunctiva and the cornea, have different characteristics with regard to living microbiota on their surfaces. But as our current data and the evidence of decades of failure to consistently culture multiple strains of microbes from eyes in a clinical setting indicate, the presence of microbes in the eye is still an elusive target.

Our next attempt to identify microbes within the eye will involve spiking bacteria into the ocular surface in several states: live, dead and purified bacterial DNA. By adding these samples, which have known marker plasmids, we can assess whether the DNA-based microbiome analysis can differentiate between these populations. If the dead and purified bacterial DNA are significantly degraded beyond the point of detection, then this will lend credence to the use of DNA as a tool for identifying living microbes within a microbiome. However, if the dead and DNA fragments are equally detected, then the data would indicate that this analysis is a model of encountered microbes rather than of the existence of a microbiome.

The existence of a microbiome on the ocular surface may help us to determine how this unique tissue maintains its immune-privileged state. However, the evidence that such a microbiome exists remains in dispute. The DNA evidence does show bacteria present, and the evidence both of universally found microorganisms and of changes in populations is useful whether or not it proves the presence of a living microbiome. The DNA evidence may point instead to the presence not of a microbiome, but of a necrobiome of encountered microbes that help to shape the eye's health. This necrobiome could serve in a similar way to the browser history of someone's computer, telling us the most recent events that have occurred and giving us an idea of which microbes the tissue has successfully survived. Functionally, the DNA may also be utilized by the corneal immune system to prevent further disease. The true nature of the microbiota within the eye is still poorly understood.

Chapter 6:

Concluding Remarks

Chapter 6: Concluding Remarks

Human beings are highly visual creatures. One needs only to consider our recreational activities to realize how many of them depend heavily on our vision. At least one million Americans a year are diagnosed with microbial keratitis, representing a significant number of individuals whose vision is at risk. Since any scars in the visual axis of vision cause impairment of vision, identifying initial stages of infection and the natural barriers that prevent disease is paramount to protecting eyesight. Understanding how pathogens can break down these barriers not only helps us to identify which barriers are most important but also gives us better targets for therapy and drug development to prevent disease. This is increasingly important as antibiotics are becoming less and less effective due to the growing antibiotic resistance of bacteria.

The eye is an ideal setting for observation. It presents circumstances where we can not only look at how pathogens cause eye disease but also observe the interaction of host and microbe to better understand all infections. *Pseudomonas* is an opportunistic pathogen that infects the eyes of contact lens wearers, the lungs of cystic fibrosis patients and those on ventilation, the skin of burn victims, and people who are recovering from surgery or are immune-compromised. It is an environmental bacterium, in that we encounter it in our daily environment, in the soil, and in our water. It is highly adaptable and often resistant to antibiotics, so better understanding is needed to combat *Pseudomonas* and other bacteria like it.

Recently, drugs targeting the T3SS have been devised to prevent these opportunistic pathogens from causing disease. However, the T3SS is an inducible system and is not always present. This is advantageous in that it does not encourage treatment-based selection; however, the T3SS isn't necessarily needed for all diseases caused by bacteria capable of creating a T3SS. In our own studies, we have found certain conditions (MyD88 KO, FBS exposure, cytotoxic strain PA14 infection) where the T3SS is not required for these bacteria to inflict tissue destruction and/or cause disease. This makes us reconsider the effectiveness of such treatments, especially considering that because *P. aeruginosa* is an opportunistic pathogen, these conditions mentioned above where the T3SS is not required are the ones most likely to need additional antibacterial treatments.

Our findings showing the importance of LasB in initial stages of infection in PAO1 give us another plausible target for protection against bacterial infection. By stopping the bacteria's access to the underside of a tissues surface epithelial layer, we can preserve barrier function and help to prevent infection. This effect would be similar to the theory behind how the scratch model works. If the scratch isn't deep enough to breach the stroma and is only through the epithelium, then the scratch model fails to yield infection when bacteria are applied (Preston, Fleiszig et al. 1995). Similarly, if LasB is unable to break down the barriers needed, we should be able to prevent bacteria from entering a space where they are most effective in causing disease.

The synergy between the T2SS-secreted proteases and the T3SS may lead us to a more ubiquitous solution to preventing bacterial pathogenicity. The results with PAK have shown us that the T3SS, even when hyper expressed, is not the only route to virulence. This discovery helped us identify that proteases like LasB are important in the initial stages of infection. Notably, studies have shown that not all *P. aeruginosa* strains produce LasB under inducing conditions (Twining 2003-2015). PA103, a cytotoxic strain like PA14, was shown in these

studies to produce a different protease under these conditions. These data point to a possible difference between cytotoxic and invasive strains other than production of ExoU versus ExoS. This alternate protease could explain the T3SS independence in cytotoxic strain PA14 and make it difficult to reliably target either T3SS or T2SS for therapeutic protection. The exact nature of the synergy of the T3SS and T2SS still needs further exploration, but it is clear that knocking only one of them out is not enough in all cases.

Some of the difficulty in modeling which system is needed to produce infection is related to the challenge of modeling the conditions in which the bacteria become successfully pathogenic. We have established several models in order to both test a variety of conditions and also to mimic certain situations that have proved to be risk factors in patients with MK. The blotting/EGTA model remains one of our best models, since it retains the best barrier function and can be performed outside the animal for up to 8h, giving us the opportunity to test a greater number of conditions without risking the animal's health or causing its discomfort. It is also advantageous when compared to cell culture techniques because the entire organ is evaluated intact. It does, however, have some limitations. It is isolated from the rest of the immune system, tears, and the mechanical protection of blinking. Also, the tissue begins to suffer morbidity after 8h, so longer studies are not possible. The use of tissue culture conditions dramatically increases the time during which the eye can be kept alive outside its host, but there is some alteration in the barrier function of the corneal surface that we do not yet completely understand. This vulnerability eliminates the need for the T3SS in PAO1 traversal. Understanding the changes in the barrier function, or the activity of *Pseudomonas* under these conditions, may shed some light on the nature of this relationship. However, the causal ingredient in FBS remains unknown.

Microscopy is advancing and allowing us to capture these events in detail in a way that we have never been able to accomplish. Along with the influx of 3D data comes the need for more sophisticated analysis of these images. I have outlined several methods that have been useful for turning that information into reliable, quantifiable data. However, the limitations of the image capturing techniques are still the deciding factor in what we can accomplish. Deconvolution and 3D surface generation are amazing technologies, but nothing can completely replace the need for accurate, clean images. So the first step in imaging is understanding the limitations of the microscope and understanding what questions one wishes to ask. The same is true for the process of quantification. For example, when one is imaging the corneal epithelium in a confocal microscope, the imaged section must include a distance above and below the region of interest equal to 50% of the maximum resolution of the microscope. This is to ensure that stray light can be properly deconvolved. It also allows us to ensure that the entire section of the epithelium is taken into account when making depth measurements. With the adequate resolution and field of view, we can reconstruct the events in 3D accurately and have the relevant amount of information to turn this picture into numbers for quantification. By processing data with high throughput and 3D distance modeling techniques, we can eliminate the ambiguity of disease scoring. This will hopefully yield more reproducible results and eliminate much of the error attributed to a highly labor-intensive process.

The ocular surface has been under close scrutiny for almost as long as we have had eyes. Evidence of microbes living in such a highly scrutinized part of our anatomy could shed much light on how that surface interacts with the environment and how it is protected from infection. However, the ocular surface lining needs to be broken down into regions due to differences in

anatomy between the cornea and the multiple regions of conjunctiva. Since the cornea is an immune-privileged site, and is also critical to vision, it is unclear why it would intentionally support a live microbiome. The antimicrobial activity of tears constantly washing over its surface, combined with the powerful brushing off of the surface by the eyelids that also ensures the tear fluid remains extremely thin, makes for the impression of a very tidy and orderly surface. Indeed, unlike the conjunctiva there is a lack of evidence of microbiota in or on the cornea; even in some cases of keratitis, no microbes are found at the site of "infection" (Srinivasan, Mascarenhas et al. 2008).

The conjunctiva is not often sampled unless disease is present. Additionally, it can be difficult to sample the conjunctiva without contamination from the surrounding eyelids. The microbiome analysis technique is so sensitive that a single microbe can be detected; which can lead to background noise that is difficult to separate. Thus, results from microbiome analysis could result from contamination in the samples. The fact that we have found primarily skin flora in these studies offers the biggest clue that this may be the case. However, several animal studies have found culturable bacteria in the conjunctiva, showing it is possible to culture bacteria when they are present. Further, studies of contact lens wearers did reveal culturabe from the 1990s have samples cultured from patients with and without disease.

While my data continue to support the idea that a stable microbiome consisting of a significant number of live microbes does not exist at the ocular surface, it remains possible that microbial debris plays important roles in maintaining ocular health. Indeed, studies of gut host-microbe interactions have shown that microbial ligands, not the live microbes from which they are derived, modulate normal immune tone. While the presence of live microbes could be beneficial in the gut for other reasons, it is less likely at the ocular surface where the consequences of infection and subsequent scarring are dire. Thus, I propose that rather than a microbiome, the ocular surface harbors a "necrobiome" that plays important roles in maintaining ocular surface homeostasis, perhaps including barrier function against microbes. Testing that hypothesis will require further investigation beyond the scope of this dissertation.

References

Abe, A. and H. Nagano (2000). "Functional analysis of the type III secretion system in enteropathogenic Escherichia coli O157:H45." Microbiology and immunology **44**(10): 857-861.

Alarcon, I., L. Kwan, C. Yu, D. J. Evans and S. M. Fleiszig (2009). "Role of the corneal epithelial basement membrane in ocular defense against Pseudomonas aeruginosa." Infect Immun **77**(8): 3264-3271.

Alarcon, I., C. Tam, J. J. Mun, J. LeDue, D. J. Evans and S. M. Fleiszig (2011). "Factors impacting corneal epithelial barrier function against Pseudomonas aeruginosa traversal." Invest Ophthalmol Vis Sci **52**(3): 1368-1377.

Allentoft, M. E., M. Collins, D. Harker, J. Haile, C. L. Oskam, M. L. Hale, P. F. Campos, J. A. Samaniego, M. T. Gilbert, E. Willerslev, G. Zhang, R. P. Scofield, R. N. Holdaway and M. Bunce (2012). "The half-life of DNA in bone: measuring decay kinetics in 158 dated fossils." Proc Biol Sci **279**(1748): 4724-4733.

Aoki, R., K. Fukuda, M. Ogawa, T. Ikeno, H. Kondo, A. Tawara and H. Taniguchi (2013). "Identification of causative pathogens in eyes with bacterial conjunctivitis by bacterial cell count and microbiota analysis." Ophthalmology **120**(4): 668-676.

Augustin, D. K., S. R. Heimer, C. Tam, W. Y. Li, J. M. Le Due, D. J. Evans and S. M. Fleiszig (2011). "Role of defensins in corneal epithelial barrier function against Pseudomonas aeruginosa traversal." Infect Immun **79**(2): 595-605.

Bloemberg, G. V., G. A. O'Toole, B. J. Lugtenberg and R. Kolter (1997). "Green fluorescent protein as a marker for Pseudomonas spp." Appl Environ Microbiol **63**(11): 4543-4551.

Brint, J. M. and D. E. Ohman (1995). "Synthesis of multiple exoproducts in Pseudomonas aeruginosa is under the control of RhlR-RhlI, another set of regulators in strain PAO1 with homology to the autoinducer-responsive LuxR-LuxI family." J Bacteriol **177**(24): 7155-7163.

Broekhuyse, R. M. (1974). "Tear lactoferrin: a bacteriostatic and complexing protein." Invest Ophthalmol **13**(7): 550-554.

Bucior, I., K. Mostov and J. N. Engel (2010). "Pseudomonas aeruginosa-mediated damage requires distinct receptors at the apical and basolateral surfaces of the polarized epithelium." Infect Immun **78**(3): 939-953.

Clarke, T. B., N. Francella, A. Huegel and J. N. Weiser (2011). "Invasive bacterial pathogens exploit TLR-mediated downregulation of tight junction components to facilitate translocation across the epithelium." Cell Host Microbe **9**(5): 404-414.

Coburn, B., I. Sekirov and B. B. Finlay (2007). "Type III secretion systems and disease." Clin Microbiol Rev **20**(4): 535-549.

Coburn, J. and D. W. Frank (1999). "Macrophages and epithelial cells respond differently to the Pseudomonas aeruginosa type III secretion system." Infect Immun **67**(6): 3151-3154.

Collazo, C. M. and J. E. Galan (1996). "Requirement for exported proteins in secretion through the invasion-associated type III system of Salmonella typhimurium." Infection and Immunity **64**(9): 3524-3531.

Collier, S. A., M. P. Gronostaj, A. K. MacGurn, J. R. Cope, K. L. Awsumb, J. S. Yoder and M. J. Beach (2014). "Estimated burden of keratitis--United States, 2010." MMWR. Morbidity and mortality weekly report **63**(45): 1027-1030.

Colmer, J. A. and A. N. Hamood (2001). "Molecular analysis of the Pseudomonas aeruginosa regulatory genes ptxR and ptxS." Can J Microbiol **47**(9): 820-828.

Cowell, B. A., D. Y. Chen, D. W. Frank, A. J. Vallis and S. M. Fleiszig (2000). "ExoT of cytotoxic Pseudomonas aeruginosa prevents uptake by corneal epithelial cells." Infect Immun **68**(1): 403-406.

Cowell, B. A., S. S. Twining, J. A. Hobden, M. S. Kwong and S. M. Fleiszig (2003). "Mutation of lasA and lasB reduces Pseudomonas aeruginosa invasion of epithelial cells." Microbiology **149**(Pt 8): 2291-2299.

Creech, J. L., L. T. Do, I. Fatt and C. J. Radke (1998). "In vivo tear-film thickness determination and implications for tear-film stability." Curr Eye Res **17**(11): 1058-1066.
Dart, J. K., F. Stapleton and D. Minassian (1991). "Contact lenses and other risk factors in microbial keratitis." Lancet **338**(8768): 650-653.
Dong, Y., Z. X. Yang, K. Dong, L. Tang, Y. Zheng and G. B. Hu (2013). "[Effects of nitrogen application rate on faba bean fusarium wilt and rhizospheric microbial metabolic functional diversity]." Ying Yong Sheng Tai Xue Bao **24**(4): 1101-1108.
Eiden, S. B. (2011). "Choosing the right solution can impact patient compliance with the lens care regimen, ocular health and patient satisfaction with their contact lenses." Review of Contact Lenses.
Engelsberg, K. and F. Ghosh (2011). "Human retinal development in an in situ whole eye culture system." Dev Neurosci **33**(2): 110-117.
Evans, D. J. and S. M. Fleiszig (2013). "Why does the healthy cornea resist Pseudomonas aeruginosa infection?" Am J Ophthalmol **155**(6): 961-970 e962.
Finck-Barbancon, V., J. Goranson, L. Zhu, T. Sawa, J. P. Wiener-Kronish, S. M. Fleiszig, C. Wu, L. Mende-Mueller and D. W. Frank (1997). "ExoU expression by Pseudomonas aeruginosa correlates with acute cytotoxicity and epithelial injury." Mol Microbiol **25**(3): 547-557.
Finlay, B. B. and P. Cossart (1997). "Exploitation of mammalian host cell functions by bacterial pathogens." Science **276**(5313): 718-725.
Fleiszig, S. M. and N. Efron (1992). "Microbial flora in eyes of current and former contact lens wearers." J Clin Microbiol **30**(5): 1156-1161.
Fleiszig, S. M., D. J. Evans, N. Do, V. Vallas, S. Shin and K. E. Mostov (1997). "Epithelial cell polarity affects susceptibility to Pseudomonas aeruginosa invasion and cytotoxicity." Infect Immun **65**(7): 2861-2867.
Fleiszig, S. M., J. P. Wiener-Kronish, H. Miyazaki, V. Vallas, K. E. Mostov, D. Kanada, T. Sawa, T. S. Yen and D. W. Frank (1997). "Pseudomonas aeruginosa-mediated cytotoxicity and invasion correlate with distinct genotypes at the loci encoding exoenzyme S." Infect Immun **65**(2): 579-586.
Foulks, G. N. (2007). "The correlation between the tear film lipid layer and dry eye disease." Surv Ophthalmol **52**(4): 369-374.
Frank, D. W. (1997). "The exoenzyme S regulon of Pseudomonas aeruginosa." Mol Microbiol **26**(4): 621-629.
Frithz-Lindsten, E., Y. Du, R. Rosqvist and A. Forsberg (1997). "Intracellular targeting of exoenzyme S of Pseudomonas aeruginosa via type III-dependent translocation induces phagocytosis resistance, cytotoxicity and disruption of actin microfilaments." Mol Microbiol **25**(6): 1125-1139.
Galloway, D. R. (1991). "Pseudomonas aeruginosa elastase and elastolysis revisited: recent developments." Mol Microbiol **5**(10): 2315-2321.
Ganz, T. and R. I. Lehrer (1995). "Defensins." Pharmacol Ther **66**(2): 191-205.
Gipson, I. K. (2004). "Distribution of mucins at the ocular surface." Exp Eye Res **78**(3): 379-388.
Gipson, I. K., M. Yankauckas, S. J. Spurr-Michaud, A. S. Tisdale and W. Rinehart (1992). "Characteristics of a glycoprotein in the ocular surface glycocalyx." Invest Ophthalmol Vis Sci **33**(1): 218-227.
Golovkine, G., E. Faudry, S. Bouillot, R. Voulhoux, I. Attree and P. Huber (2014). "VE-cadherin cleavage by LasB protease from Pseudomonas aeruginosa facilitates type III secretion system toxicity in endothelial cells." PLoS Pathog **10**(3): e1003939.
Gulsen, D. and A. Chauhan (2004). "Ophthalmic drug delivery through contact lenses." Invest Ophthalmol Vis Sci **45**(7): 2342-2347.
Hauser, A. R., S. Fleiszig, P. J. Kang, K. Mostov and J. N. Engel (1998). "Defects in type III secretion correlate with internalization of Pseudomonas aeruginosa by epithelial cells." Infection and Immunity **66**(4): 1413-1420.
Hauser, A. R., P. J. Kang and J. N. Engel (1998). "PepA, a secreted protein of Pseudomonas aeruginosa, is necessary for cytotoxicity and virulence." Mol Microbiol **27**(4): 807-818.

Hazlett, L. D., D. D. Rosen and R. S. Berk (1977). "Pseudomonas eye infections in cyclophosphamide-treated mice." Investigative ophthalmology & visual science **16**(7): 649-652.
Hirano, S. S., A. O. Charkowski, A. Collmer, D. K. Willis and C. D. Upper (1999). "Role of the Hrp type III protein secretion system in growth of Pseudomonas syringae pv. syringae B728a on host plants in the field." Proceedings of the National Academy of Sciences of the United States of America **96**(17): 9851-9856.
Hobden, J. A. (2002). "Pseudomonas aeruginosa proteases and corneal virulence." DNA Cell Biol **21**(5-6): 391-396.
Hoge, R., A. Pelzer, F. Rosenau and S. Wilhelm (2010). "Weapons of a pathogen: proteases and their role in virulence of Pseudomonas aeruginosa."
Holly, F. J. (1980). "Tear film physiology." Am J Optom Physiol Opt **57**(4): 252-257.
Hsu, K. H., R. C. Fentzke and A. Chauhan (2013). "Feasibility of corneal drug delivery of cysteamine using vitamin E modified silicone hydrogel contact lenses." Eur J Pharm Biopharm **85**(3 Pt A): 531-540.
Iyer, S. and B. Lonnerdal (1993). "Lactoferrin, lactoferrin receptors and iron metabolism." Eur J Clin Nutr **47**(4): 232-241.
Jackson, T. L., S. J. Eykyn, E. M. Graham and M. R. Stanford (2003). "Endogenous bacterial endophthalmitis: a 17-year prospective series and review of 267 reported cases." Surv Ophthalmol **48**(4): 403-423.
Jain, M. R. (1988). "Drug delivery through soft contact lenses." Br J Ophthalmol **72**(2): 150-154.
Jones, L., D. Jones and M. Houlford (1997). "Clinical comparison of three polyhexanide-preserved multi-purpose contact lens solutions." Cont Lens Anterior Eye **20**(1): 23-30.
Kessler, E., M. Safrin, J. K. Gustin and D. E. Ohman (1998). "Elastase and the LasA protease of Pseudomonas aeruginosa are secreted with their propeptides." J Biol Chem **273**(46): 30225-30231.
Kok, J. H., E. P. Boets, J. A. van Best and A. Kijlstra (1992). "Fluorophotometric assessment of tear turnover under rigid contact lenses." Cornea **11**(6): 515-517.
Kuang, Z., Y. Hao, B. E. Walling, J. L. Jeffries, D. E. Ohman and G. W. Lau (2011). "Pseudomonas aeruginosa elastase provides an escape from phagocytosis by degrading the pulmonary surfactant protein-A." PLoS One **6**(11): e27091.
Lab, T. C. T. C. E. M. (2015). "Lab Diagnostic Testing: Bacteria." University of Pittsburgh Schools of the Health Sciences, from http://eyemicrobiology.upmc.com/Bacteria.htm.
Leduc, D., N. Beaufort, S. de Bentzmann, J. C. Rousselle, A. Namane, M. Chignard and D. Pidard (2007). "The Pseudomonas aeruginosa LasB metalloproteinase regulates the human urokinase-type plasminogen activator receptor through domain-specific endoproteolysis." Infect Immun **75**(8): 3848-3858.
Lee, E. J., D. J. Evans and S. M. Fleiszig (2003). "Role of Pseudomonas aeruginosa ExsA in penetration through corneal epithelium in a novel in vivo model." Invest Ophthalmol Vis Sci **44**(12): 5220-5227.
Liu, H., C. Begley, M. Chen, A. Bradley, J. Bonanno, N. A. McNamara, J. D. Nelson and T. Simpson (2009). "A link between tear instability and hyperosmolarity in dry eye." Invest Ophthalmol Vis Sci **50**(8): 3671-3679.
Maeda, H. and K. Morihara (1995). "Serralysin and related bacterial proteinases." Methods Enzymol **248**: 395-413.
Maltseva, I. A., S. M. Fleiszig, D. J. Evans, S. Kerr, S. S. Sidhu, N. A. McNamara and C. Basbaum (2007). "Exposure of human corneal epithelial cells to contact lenses in vitro suppresses the upregulation of human beta-defensin-2 in response to antigens of Pseudomonas aeruginosa." Experimental Eye Research **85**(1): 142-153.
Maresso, A. W., M. R. Baldwin and J. T. Barbieri (2004). "Ezrin/radixin/moesin proteins are high affinity targets for ADP-ribosylation by Pseudomonas aeruginosa ExoS." J Biol Chem **279**(37): 38402-38408.
Marquart, M. E., A. R. Caballero, M. Chomnawang, B. A. Thibodeaux, S. S. Twining and R. J. O'Callaghan (2005). "Identification of a novel secreted protease from Pseudomonas aeruginosa that causes corneal erosions." Invest Ophthalmol Vis Sci **46**(10): 3761-3768.

Masters, S. C., K. J. Pederson, L. Zhang, J. T. Barbieri and H. Fu (1999). "Interaction of 14-3-3 with a nonphosphorylated protein ligand, exoenzyme S of Pseudomonas aeruginosa." Biochemistry **38**(16): 5216-5221.
McClellan, B. H., C. R. Whitney, L. P. Newman and M. R. Allansmith (1973). "Immunoglobulins in tears." Am J Ophthalmol **76**(1): 89-101.
McNamara, N. A., R. Van, O. S. Tuchin and S. M. Fleiszig (1999). "Ocular surface epithelia express mRNA for human beta defensin-2." Experimental Eye Research **69**(5): 483-490.
McNatt, J., S. D. Allen, L. A. Wilson and V. R. Dowell, Jr. (1978). "Anaerobic flora of the normal human conjunctival sac." Arch Ophthalmol **96**(8): 1448-1450.
Moreno, N. P., R. D. Moreno and L. B. Sousa (2014). "Aerobic bacterial microbiota of the conjunctiva in diabetic patients with normal and altered glycated hemoglobin levels in two regions in Brazil." Arq Bras Oftalmol **77**(6): 351-354.
Mun, J. J., C. Tam, D. Kowbel, S. Hawgood, M. J. Barnett, D. J. Evans and S. M. Fleiszig (2009). "Clearance of Pseudomonas aeruginosa from a healthy ocular surface involves surfactant protein D and is compromised by bacterial elastase in a murine null-infection model." Infect Immun **77**(6): 2392-2398.
Musch, D. C., A. Sugar and R. F. Meyer (1983). "Demographic and predisposing factors in corneal ulceration." Arch Ophthalmol **101**(10): 1545-1548.
Muthappan, V., A. Y. Lee, T. L. Lamprecht, L. Akileswaran, S. M. Dintzis, C. Lee, V. Magrini, E. R. Mardis, J. Shendure and R. N. Van Gelder (2011). "Biome representational in silico karyotyping." Genome Res **21**(4): 626-633.
Nichols, J. J. and P. E. King-Smith (2004). "The impact of hydrogel lens settling on the thickness of the tears and contact lens." Invest Ophthalmol Vis Sci **45**(8): 2549-2554.
Niederkorn, J. Y., H. J. Kaplan, J. W. Streilein and S. Karger (Firm) (2007). Immune response and the eye in memoriam J. Wayne Streilein. Chemical immunology and allergy vol 92. Basel ; New York, Karger,**:** 1 online resource (xix, 336 p.
Niederkorn, J. Y., J. S. Peeler and J. Mellon (1989). "Phagocytosis of particulate antigens by corneal epithelial cells stimulates interleukin-1 secretion and migration of Langerhans cells into the central cornea." Reg Immunol **2**(2): 83-90.
Olson, J. C., J. E. Fraylick, E. M. McGuffie, K. M. Dolan, T. L. Yahr, D. W. Frank and T. S. Vincent (1999). "Interruption of multiple cellular processes in HT-29 epithelial cells by Pseudomonas aeruginosa exoenzyme S." Infect Immun **67**(6): 2847-2854.
OVS (2014). Microbes in the Eye: Uncharted? Optometry and Vision Science, American Academy of Optometry. **91:** e197.
Peng, C. C., M. T. Burke, B. E. Carbia, C. Plummer and A. Chauhan (2012). "Extended drug delivery by contact lenses for glaucoma therapy." J Control Release **162**(1): 152-158.
Polse, K. A. (1979). "Tear flow under hydrogel contact lenses." Invest Ophthalmol Vis Sci **18**(4): 409-413.
Preston, M. J., S. M. Fleiszig, T. S. Zaidi, J. B. Goldberg, V. D. Shortridge, M. L. Vasil and G. B. Pier (1995). "Rapid and sensitive method for evaluating Pseudomonas aeruginosa virulence factors during corneal infections in mice." Infect Immun **63**(9): 3497-3501.
Ramachandran, L., S. Sharma, P. R. Sankaridurg, C. M. Vajdic, J. A. Chuck, B. A. Holden, D. F. Sweeney and G. N. Rao (1995). "Examination of the conjunctival microbiota after 8 hours of eye closure." CLAO J **21**(3): 195-199.
Ramirez, J. C., S. M. Fleiszig, A. B. Sullivan, C. Tam, R. Borazjani and D. J. Evans (2012). "Traversal of multilayered corneal epithelia by cytotoxic Pseudomonas aeruginosa requires the phospholipase domain of exoU." Invest Ophthalmol Vis Sci **53**(1): 448-453.
Rietsch, A., M. C. Wolfgang and J. J. Mekalanos (2004). "Effect of metabolic imbalance on expression of type III secretion genes in Pseudomonas aeruginosa." Infect Immun **72**(3): 1383-1390.
Sack, R. A., B. Jones, A. Antignani, R. Libow and H. Harvey (1987). "Specificity and biological activity of the protein deposited on the hydrogel surface. Relationship of polymer structure to biofilm formation." Invest Ophthalmol Vis Sci **28**(5): 842-849.

Sandkvist, M. (2001). "Biology of type II secretion." Mol Microbiol **40**(2): 271-283.
Sandkvist, M. (2001). "Type II secretion and pathogenesis." Infect Immun **69**(6): 3523-3535.
Saulnier, J. M., F. M. Curtil, M. C. Duclos and J. M. Wallach (1989). "Elastolytic activity of Pseudomonas aeruginosa elastase." Biochim Biophys Acta **995**(3): 285-290.
Sawa, T., T. L. Yahr, M. Ohara, K. Kurahashi, M. A. Gropper, J. P. Wiener-Kronish and D. W. Frank (1999). "Active and passive immunization with the Pseudomonas V antigen protects against type III intoxication and lung injury." Nature medicine **5**(4): 392-398.
Schabereiter-Gurtner, C., S. Maca, S. Rolleke, K. Nigl, J. Lukas, A. Hirschl, W. Lubitz and T. Barisani-Asenbauer (2001). "16S rDNA-based identification of bacteria from conjunctival swabs by PCR and DGGE fingerprinting." Invest Ophthalmol Vis Sci **42**(6): 1164-1171.
Schneider, J. J., A. Unholzer, M. Schaller, M. Schafer-Korting and H. C. Korting (2005). "Human defensins." J Mol Med (Berl) **83**(8): 587-595.
Shaikh-Lesko, R. (2014). Visualizing the Ocular Microbiome. The Scientist.
Sorensen, M. (1939). "The proteins of Whey." Carlsberg Laboratory **23**(55).
Soscia, C., A. Hachani, A. Bernadac, A. Filloux and S. Bleves (2007). "Cross talk between type III secretion and flagellar assembly systems in Pseudomonas aeruginosa." J Bacteriol **189**(8): 3124-3132.
Srinivasan, M., J. Mascarenhas and C. N. Prashanth (2008). "Distinguishing infective versus noninfective keratitis." Indian J Ophthalmol **56**(3): 203-207.
Stapleton, F., M. D. Willcox, N. Sansey and B. A. Holden (1997). "Ocular microbiota and polymorphonuclear leucocyte recruitment during overnight contact lens wear." Aust N Z J Ophthalmol **25 Suppl 1**: S33-35.
Sullivan, A. B., K. P. Tam, M. M. Metruccio, D. J. Evans and S. M. Fleiszig (2015). "The importance of the Pseudomonas aeruginosa type III secretion system in epithelium traversal depends upon conditions of host susceptibility." Infect Immun **83**(4): 1629-1640.
Sun, J., A. W. Maresso, J. J. Kim and J. T. Barbieri (2004). "How bacterial ADP-ribosylating toxins recognize substrates." Nat Struct Mol Biol **11**(9): 868-876.
Tam, C., J. LeDue, J. J. Mun, P. Herzmark, E. A. Robey, D. J. Evans and S. M. Fleiszig (2011). "3D quantitative imaging of unprocessed live tissue reveals epithelial defense against bacterial adhesion and subsequent traversal requires MyD88." PLoS One **6**(8): e24008.
Tam, C., J. J. Mun, D. J. Evans and S. M. Fleiszig (2010). "The impact of inoculation parameters on the pathogenesis of contact lens-related infectious keratitis." Investigative ophthalmology & visual science **51**(6): 3100-3106.
Tam, C., J. J. Mun, D. J. Evans and S. M. Fleiszig (2012). "Cytokeratins mediate epithelial innate defense through their antimicrobial properties." J Clin Invest **122**(10): 3665-3677.
Twining, S. S. (2003-2015). PA103 produces a Unique lasB protease under T3SS inducing conditions.
Twining, S. S., S. E. Kirschner, L. A. Mahnke and D. W. Frank (1993). "Effect of Pseudomonas aeruginosa elastase, alkaline protease, and exotoxin A on corneal proteinases and proteins." Invest Ophthalmol Vis Sci **34**(9): 2699-2712.
Vaishnava, S., M. Yamamoto, K. M. Severson, K. A. Ruhn, X. Yu, O. Koren, R. Ley, E. K. Wakeland and L. V. Hooper (2011). "The antibacterial lectin RegIIIgamma promotes the spatial segregation of microbiota and host in the intestine." Science **334**(6053): 255-258.
Valyi-Nagy, T., S. Deshmane, A. Dillner and N. W. Fraser (1991). "Induction of cellular transcription factors in trigeminal ganglia of mice by corneal scarification, herpes simplex virus type 1 infection, and explantation of trigeminal ganglia." J Virol **65**(8): 4142-4152.
Vance, R. E., A. Rietsch and J. J. Mekalanos (2005). "Role of the type III secreted exoenzymes S, T, and Y in systemic spread of Pseudomonas aeruginosa PAO1 in vivo." Infect Immun **73**(3): 1706-1713.
Vance, R. E., A. Rietsch and J. J. Mekalanos (2005). "Role of the type III secreted exoenzymes S, T, and Y in systemic spread of Pseudomonas aeruginosa PAO1 in vivo." Infection and Immunity **73**(3): 1706-1713.
Wichterle, O., D. Lim and M. Dreifus (1961). "[On the problem of contact lenses]." Cesk Oftalmol **17**: 70-75.

Wikipedia. (2015). "Edge Detection." from http://en.wikipedia.org/wiki/Edge_detection.
Willcox, M. D. (2013). "Characterization of the normal microbiota of the ocular surface." Exp Eye Res **117**: 99-105.
Willcox, M. D., K. N. Power, F. Stapleton, C. Leitch, N. Harmis and D. F. Sweeney (1997). "Potential sources of bacteria that are isolated from contact lenses during wear." Optom Vis Sci **74**(12): 1030-1038.
Wu, W. and S. Jin (2005). "PtrB of Pseudomonas aeruginosa suppresses the type III secretion system under the stress of DNA damage." Journal of Bacteriology **187**(17): 6058-6068.
Xinming, L., C. Yingde, A. W. Lloyd, S. V. Mikhalovsky, S. R. Sandeman, C. A. Howel and L. Liewen (2008). "Polymeric hydrogels for novel contact lens-based ophthalmic drug delivery systems: a review." Cont Lens Anterior Eye **31**(2): 57-64.
Yahr, T. L., L. M. Mende-Mueller, M. B. Friese and D. W. Frank (1997). "Identification of type III secreted products of the Pseudomonas aeruginosa exoenzyme S regulon." Journal of Bacteriology **179**(22): 7165-7168.
Zegans, M. E. and R. N. Van Gelder (2014). "Considerations in understanding the ocular surface microbiome." Am J Ophthalmol **158**(3): 420-422.
Zhou, Y., M. J. Holland, P. Makalo, H. Joof, C. H. Roberts, D. C. Mabey, R. L. Bailey, M. J. Burton, G. M. Weinstock and S. E. Burr (2014). "The conjunctival microbiome in health and trachomatous disease: a case control study." Genome Med **6**(11): 99.

Appendix:

PA14 In-vivo Controls

Appendix: PA14 In-vivo Controls

Figure A1. Inoculation time: 24hrs after infection

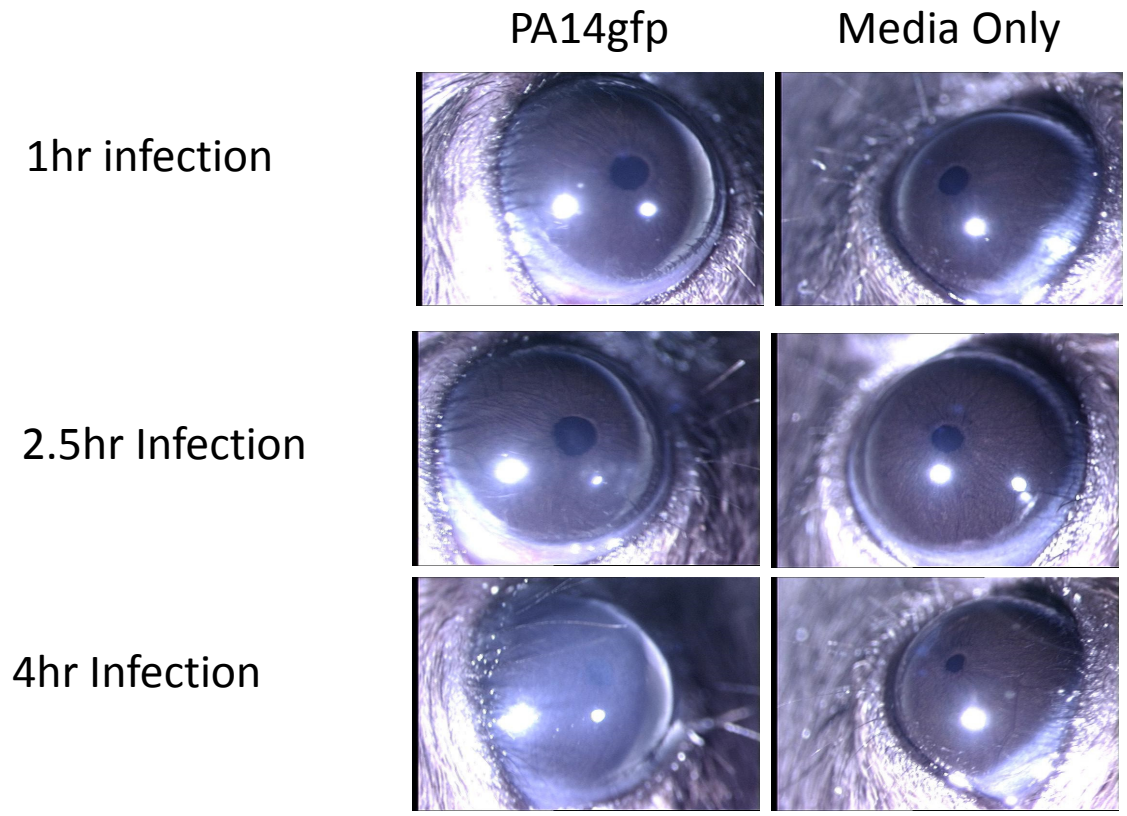

C57 b/6 mice were inoculated with PA14gfp bacteria, 10^11 CFU/mL, for 1h, 2.5h, and 4h under general anesthesia. After 24h, no opacity was observed in the 1h-inoculated eyes. The 2.5h-inoculated eyes showed slight opacity covering approximately 30% of the eye. Opacity in the 4h-inoculated eyes covered 100% of the eye and was significantly thicker than that in the 2.5h-inoculated eyes.

Figure A2. Inoculation time: 48h after infection

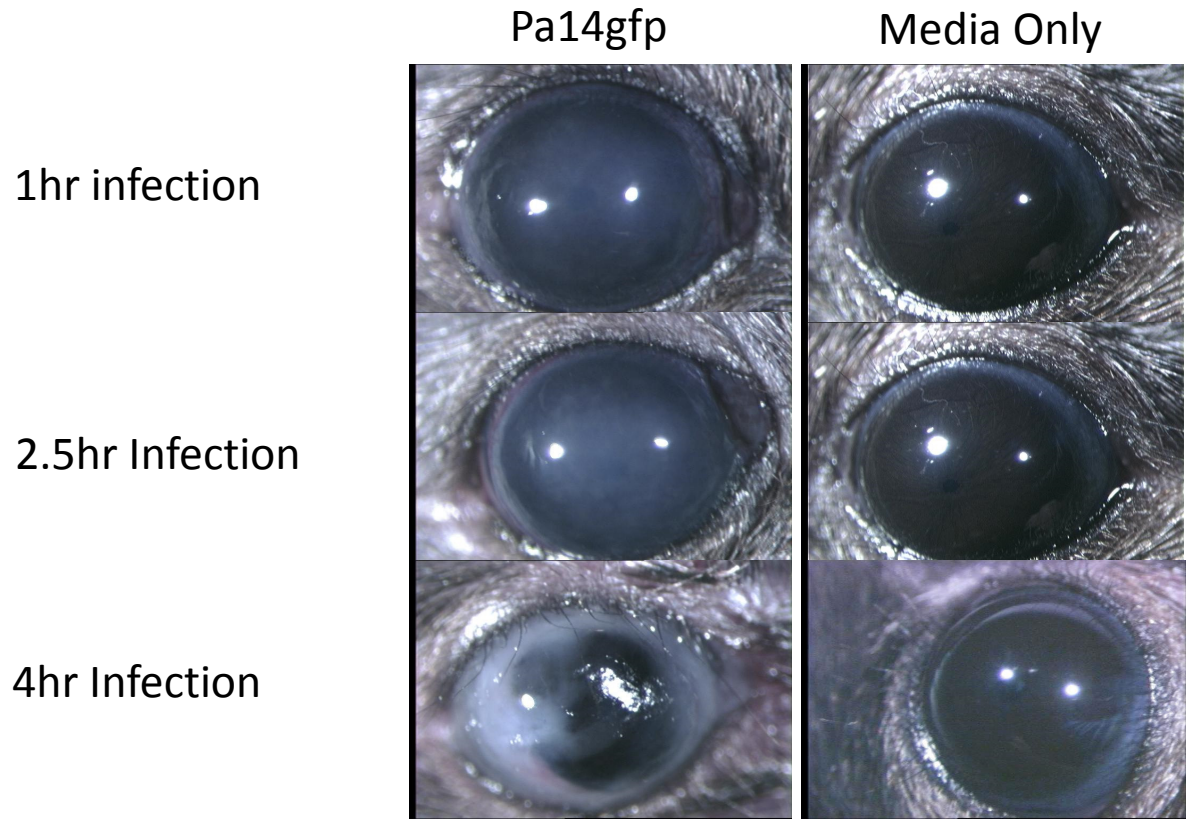

After 48h, opacity was observed covering 100% of both the 1h- and 2.5h-inoculated eyes. The opacity of the 2.5-inoculated eyes was significantly greater than that of the 1h-inoculated eyes. The pupil was no longer visible in in the 2.5h-inoculated eyes but was still visible in the 1h-inoculated eyes. The 4h-inoculated eyes had progressed beyond general opacity. A clear zone in the center of the eye was observed where the opacity had spread beyond the limbal region of the cornea. The surface of the cornea was no longer smooth in the 4h-inoculated eyes, and a discharge was found in these eyes.

Figure A3. Inoculation time 48h, with variable bacterial inocula

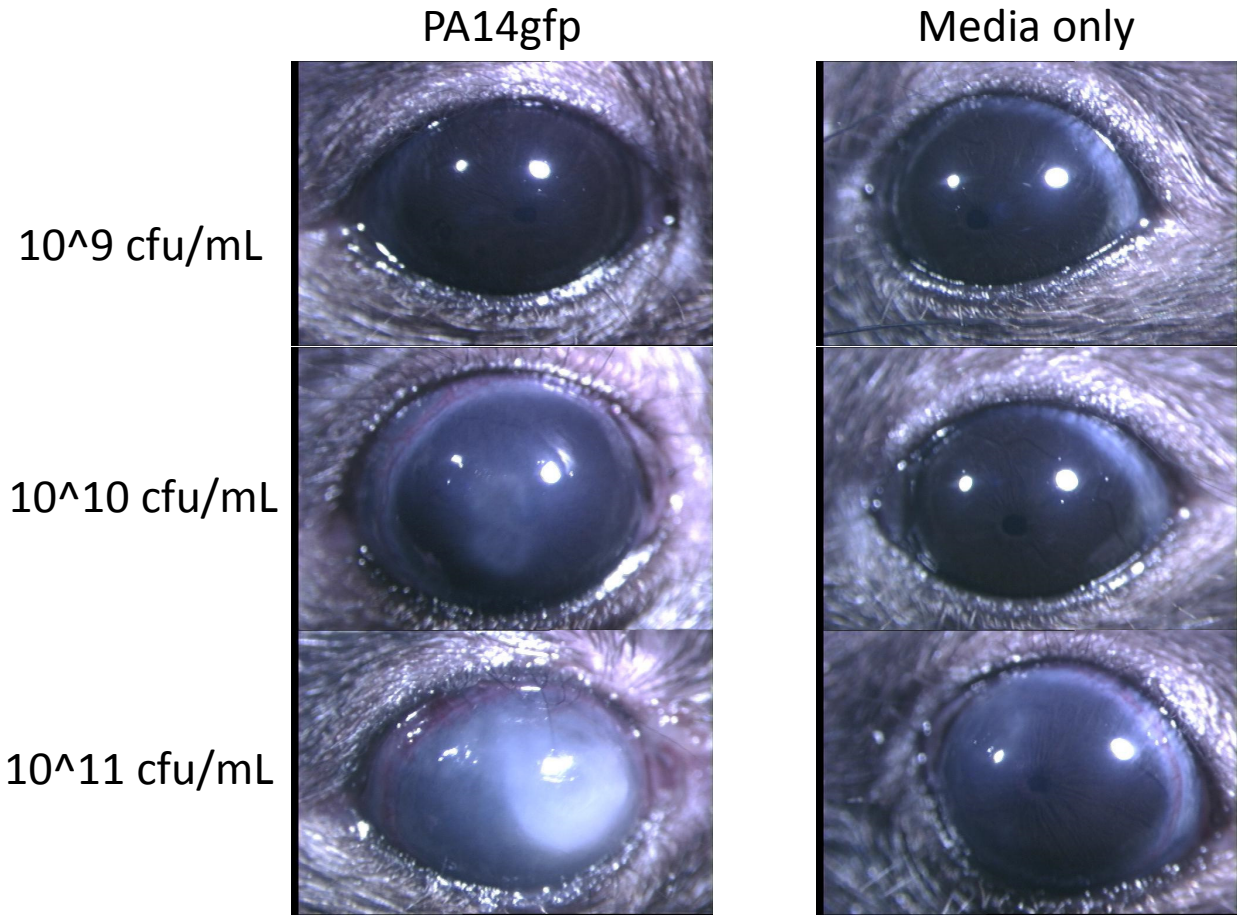

Three inocula were tested to determine the minimum amount of inoculum needed to cause disease in the in-vivo infection model. All eyes were inoculated for 4h and observed for 48h to determine eye disease. The eyes treated with 10^9 cfu/mL did not show any eye disease after 48h. Those treated with 10^10 cfu/mL had a slight opacity covering 100% of the corneal surface. Denser opacity and surface irregularities were observed in the center of the cornea. The eyes treated with 10^11 cfu/mL had severe eye disease. Opacity extended beyond the corneal limbus, and surface irregularities in the central corneal had begun to lose their opacity as the corneal epithelium was being destroyed. In the contralateral eye, occasionally a transfer of bacteria was observed from the inoculated eye to the control eye (1 of 3 subjects). This phenomenon was not observed in any of the other inocula.